The Role of Peroxisomes in Pulmonary Fibrosis

Inaugural dissertation submitted to the Faculty of Medicine in partial fulfillment of the requirements for the PhD-Degree of the Faculties of Veterinary Medicine and Medicine of the Justus Liebig University Giessen

by

Boateng, Eistine

of

Accra, Ghana

Giessen, 2018

From the Institute for Anatomy and Cell Biology,

Division of Medical Cell Biology

Director/Chairperson: Prof. Dr. Eveline Baumgart-Vogt

of the Faculty of Medicine of Justus Liebig University Giessen

First Supervisor and Committee member: Prof. Dr. Eveline Baumgart-Vogt

Second Supervisor and Committee member: Prof. Dr. Martin Diener

Declaration

"I declare that I have completed this dissertation single-handedly without the unauthorized help of a second party and only with the assistance acknowledged therein. I have appropriately acknowledged and referenced all text passages that are derived literally from or are based on the content of published or unpublished work of others, and all information that relates to verbal communications. I have abided by the principles of good scientific conduct laid down in the charter of the Justus Liebig University of Giessen in carrying out the investigations described in the dissertation."

Giessen, July 19, 2018 Eistine Boateng

List of Abbreviations

AA, Arachidonic acid

AECs, Alveolar epithelial cells

ALK, Activin receptor-like kinase

AP1, Activator protein-1

AT, 3-amino-1, 2, 4-triazole

BSA, Bovine serum albumin

CAT, Catalase

cDNA, Complementary deoxyribonucleic acid

CTGF, Connective tissue growth factor

DHA, Docosahexaenoic acid

DMEM, Dulbecco's Modified Eagle Medium

DMSO, Dimethyl sulfoxide

DRP, dynamin-related Protein

ECM, Extracellular matrix

EPA, Eicosapentaenoic acid

ER, Endoplasmic reticulum

FAK, Focal adhesion kinase

GAPDH, Glyceraldehyde-3-phosphate dehydrogenase

HRCT, High resolution computer tomography

IF, Immunofluorescence

IFN-γ, Interferon gamma

IL, Interleukin

IPF, Idiopathic pulmonary fibrosis

LTBP, latent TGF-β binding protein

MAPK, Mitogen activated protein kinase

MMPs, Matrix Metalloproteinases

NADPH, Nicotinamide adenine dinucleotide phosphate

NF-κB, Nuclear factor kappa-light-chain-enhancer of activated B cells

NOX, NADPH oxidase

NSIP, Non-specific interstitial pneumonia

N-WASP, Neuronal Wiskott-Aldrich syndrome protein

PAI-1, plasminogen activator inhibitor-1

PBS, Phosphate-buffered saline

PDGF, Platelet-derived growth factor

PEX, Gene encoding a peroxin (peroxisome biogenesis protein)

PI3K, Phosphatidylinositol-3-kinase

PPAR, Peroxisome proliferator-activated receptors

PPRE, PPAR response element

PTS, Peroxisomal Targeting Signal

PUFA, Polyunsaturated fatty acids

ROS, Reactive oxygen species

siRNA, Small interfering RNA

TGF-β, Transforming growth factor β

TMEPAI, Trans Membrane Prostate Androgen-Induced gene/protein

TNF-α, Tumor necrosis factor alpha

UIP, Usual interstitial pneumonia

VLCFA, Very long chain fatty acid

WB, Western blotting

α-SMA, α-smooth muscle actin

List of Figures

List of Tables

Table of Contents

1. Introduction

1.1. General concept and epidemiological perspectives of idiopathic pulmonary fibrosis

Injury responses in tissues trigger multiple signaling pathways that may result in normal or aberrant pathologic repair, leading to overproduction of extracellular matrix (ECM) and connective tissue remodeling [1]. This pathobiological response causes persistent scar formation that disrupts tissue parenchyma, impairs organ functions, causes organ failure and ultimately, organ death [2]. In the lung this mechanism leads to pulmonary fibrosis which was characterized as diffuse fibrosing alveolitis, diffuse interstitial fibrosis and idiopathic pulmonary fibrosis (IPF) [3], among which the latter was documented to be common.

Idiopathic pulmonary fibrosis is a severe restrictive interstitial lung disease with patient median survival of 2.5-3.5 years [4]. The disease is almost absent in individuals below age 50 albeit reported in 0.2% of people beyond 75 years [5]. Idiopathic pulmonary fibrosis is predominant in males [6] and despite discrepancies in the availability of data, the prevalence and incidence are estimated to range from 0.5 to 27.9/100,000 and 0.2 to 8.8/100,000 respectively [7]. Recent data also reported that 5000 people are diagnosed with IPF in the United Kingdom each year [8]. Interestingly, the prevalence of IPF is comparatively lower in south Europe than in northern parts of the continent [9] and speculations implicate environmental and ethnic factors [10]. Despite the above statistics, it is worth noting that the mortality and incidence of IPF are continually increasing [7].

Idiopathic pulmonary fibrosis is suggested to be related to risk factors such as environmental pollutants, genetic predisposition, cigarette smoking, chronic aspiration [11], exposure to radiotherapy and some chemotherapeutic drugs [12, 13], and latent viral infections such as Epstein-Barr virus and herpes virus [14, 15]. Symptoms and clinical manifestations identified in IPF are nonproductive coughs, progressive exertional dyspnea with scalene muscle hypertrophy, fine respiratory crackles and finger clubbing [6, 16]. In principle, acute exacerbations with no known triggering factors are suggested to be indications of the progression of the disease in patients [17].

There are limited treatment regimens for IPF and novel therapeutic medications available for the management of the disease, that are nintedanib [18] and pirfenidone [19], only slow IPF progression but do not reduce mortality, making lung transplantation the only means of

patient's survival [20]. Conversely, median survival of IPF patients after lung transplantation is 4.5 years [21] expressing how devastating the disease is.

1.2. Idiopathic pulmonary fibrosis: development and molecular overview

This section elucidates the pathogenesis of IPF and the role of molecules involved in the progression of the disease. Cellular mechanisms, ECM production and histopathological features of IPF have been sequentially explained to give a general perspective of the disease.

1.2.1. Lung injury

Gas exchange in the lungs occurs at the alveolar capillary unit, which is composed of capillary endothelial cells, type I alveolar epithelial cells [22] and common basement membranes separated by a thin interstitium. The common basement membrane is a specialized form of thin extracellular matrix composed mainly of collagen IV and laminin, and primarily resides cells which are either separated or connected to their interstitial matrices [23].

Various acute or chronic stimuli cause injurious damages to tissues, hence activate the initiation of an orderly complex replacement of cells during repair. Tissue repair processes can be either regenerative, where the same cell types replace damaged ones, or result in a scar, a characteristic restoration of parenchymal tissues with connective tissues [24]. Injury to the alveolar capillary unit results in platelet activation and degranulation, followed by the release of cytokines and lipid mediators that stimulate various responses from leukocytes, endothelial cells, fibroblasts/myofibroblasts and epithelial cells [25, 26]. Pulmonary fibrosis occurs during loss of type I epithelial and endothelial cells, injury and apoptosis of type II alveolar epithelial cells, disruption of the basement membrane, proliferation of type I alveolar epithelial and endothelial cells in the extracellular matrix, and recruitment and proliferation of fibroblasts and myofibroblasts [27-29].

1.2.2. Response to inflammation and reactive oxygen species

Following tissue and cellular injuries, inflammation ensures the removal of noxious stimuli and damaged tissues in order for the repair process to begin. This molecular mechanism can become chronic and may lead to the destruction of normal tissue [30].

During chronic inflammation, reactive oxygen species (ROS) are released to the site of inflammation and this may cause cellular and tissue damages [31]. Excess amounts of ROS are toxic to the body, though lower levels of ROS serve as signaling molecules that mediate migration, proliferation and circadian rhythm of cells [32].

In response to oxidative and nitrosative stress, cells in the lungs release cytokines/chemokines and inflammatory mediators to induce the recruitment of neutrophils, activate nuclear factor-κB (NF-κB) and activator protein-1 (AP-1), which may contribute to an increased uncontrolled inflammatory response and tissue damage [33, 34]. This molecular event is suggested to trigger the pathogenesis of IPF and other lung diseases [30], thus associates ROS to fibrosis [35]. Other cellular responses implicated in fibrosis include depletion of antioxidant defenses, genetic predisposition, endoplasmic reticulum (ER) stress in the alveolar epithelium, stimulation of p53-dependent DNA damage response and ROS activation of latent TGF-β [36]. Advances in this field have emphasized the vicious role of TGF-β in fibrosis [37] and treatments targeted at arresting inflammation have also proven ineffective [38].

1.2.3. General signaling pathways used by TGF-β family

TGF-βs constitute a subfamily of cytokines, expressed in three isoforms in mammalian tissues [39]. Among the three ligands; TGF-β1, TGF-β2 and TGF-β3, TGF-β1 is ubiquitously expressed and functions in numerous biological pathways essential for normal physiology and some disease conditions [39, 40]. TGF-β is generally synthesized as a dimer by a wide variety of cells in a form known as TGF-β pro-protein [41]. The dimer is initially cleaved in the Golgi apparatus and further released as inactive homodimeric TGF-β bound to extracellular proteins, together with a glycoprotein known as latent TGF-β binding protein (LTBP) [42, 43]. Four LTBPs have been discovered, however, LTBP-3 has a specific binding selectivity to TGF-β1 ligand [44].

TGF-β potentially initiates cytoplasmic signaling after activation. The activation process is enhanced by retinoic acid, fibroblast growth factor-2 [45], endotoxin, bleomycin, proteolytic cleavage by plasmin, matrix metalloproteinases 2 and 9 [46, 47], thrombospondin-1 [48] and integrin [49]. The active TGF-β molecule is composed of a dimer stabilized by hydrophobic interactions and intersubunit disulphide bridge [50].

Three cell surface proteins namely, TGF-β receptor I, II and III are known for TGF-β signaling [51, 52]. The molecular structural composition of the receptors include: an N-

terminal extracellular ligand-binding domain, a transmembrane region and an intracellular C-terminal serine/threonine kinase domain [53]. Seven mammalian TGF-β receptor I are known and named as ALK1-ALK7 (activin receptor-like kinase 1-7). The TGF-β1 ligand specifically induces ALK-5 during signal transduction [54]. The signaling functions of TGF-β receptor proteins are as follows: 1) TGF-β III modulates the binding of the TGF-β 2 molecule to the TGF-β receptor II, 2) TGF-β II induces TGF-β I to mediate intracellular signaling, and 3) the TGF-β receptor I phosphorylates Smad proteins for further signaling cascades and gene regulation [55, 56]. To explain this mechanism briefly, during cell signaling, activated TGF-β molecules bind to TGF-β receptor II dimers, resulting in the autophosphorylation of the receptor as well as further interaction and kinase phosphorylation of the glycine and serine-rich domains of the TGF-β receptor I [57]. Two TGF-β receptors I and two TGF-β receptors II eventually dimerize [58]. Additionally, the phosphorylation of the TGF-β receptor I triggers profound conformational changes in the receptor [59]. The downstream effects of TGF-β signaling are partly conserved in numerous cells [60] and are initiated through Smad and non-Smad pathways to regulate transcription, translation, biogenesis of microRNA, protein synthesis, and posttranslational modifications [61, 62].

Earlier publications have shown that the Smad proteins are the only cytoplasmic transcription factors directly activated after TGF-β ligands that bind to their transmembrane receptors, thus classifying this phenomenon as the canonical signaling pathway [53]. During canonical signaling, the phosphorylated TGF-β receptor I interacts with the basic patch of the MH2 domain of Smad 2 and 3 proteins [60] to phosphorylate their serine residues at the C-terminus of the respective proteins. Phosphorylated Smad 2 and 3 interact with each other, resulting in a weaker communication between the Smad proteins and TGF-β receptor I, which leads to their release into the cytoplasm [60] to form a heterooligomeric complex with Smad 4 [63]. The complex is translocated into the nucleus for DNA binding and modulation of gene expression [64]. The non-Smad signaling of TGF-β includes the Ras-Erk-MAPK pathway, p42/p44 MAPK, c-Src, phosphoinositide 3-kinase-Akt-mTOR pathway, protein phosphatase 2A (PP2A)/p70s6K, JNK MAPK and small GTPases Rho, Rac, and Cdc42 [62, 65-69].

TGF-β exerts a negative feedback on its own expression [70]. This occurs when Smad activation is controlled via a feedback loop regulated by TMEPAI (Trans Membrane Prostate Androgen-Induced gene/protein), a target gene of TGF-β signaling [71]. Transcription factors associated with TGF-β are AP-1, ETS (E26 Transformation Specific family), basic helix-

loop-helix proteins, C/EBPβ, FoxH1, FoxO1, FoxO3 and FoxO4 [72-75]. Additionally, p300 and CREB-binding proteins are classified coactivators of Smad [76, 77].

1.2.4. The role of TGF-β1 in fibrosis associated signaling pathways

The pathogenesis of IPF involves multiple cellular responses and signaling pathways, however, the role of TGF-β1 has been emphasized in fibrosis diseases of various organs due to higher expressions of TGF-β1 mRNA and protein abundance in patients and experimental mouse models [78-82]. Consequently, overexpression of TGF-β1 has also resulted in fibrosis [83, 84] and the opposite has been observed after the administration of TGF-β1 binding proteins and anti-TGF-β antibody [85, 86].

TGF-β1 remains a major molecule that promotes fibrosis through the activation of fibroblasts, induction of epithelial/endothelial mesenchymal transition, apoptosis of epithelial and endothelial cells, and regulation of extracellular matrix turnover [87]. Additionally, TGF-β1 and integrin signaling are known to modulate the differentiation of myofibroblasts [88] and the persistence of myofibroblast accumulation is reported to enhance the progression of fibrosis [89]. In fibrosis conditions, TGF-β1 induces the expression of higher levels of α-smooth muscle actin (α-SMA) to capacitate cells with tremendous contractile abilities [90, 91]. It is reported in lung fibroblasts that TGF-β1 causes the phosphorylation of the Y256 of the Neuronal Wiskott-Aldrich syndrome protein (N-WASP) by focal adhesion kinase (FAK). Moreover, with the support of actin-related protein (Arp2/3) complex signaling, N-WASP regulates α-SMA formation during myofibroblast differentiation and maturation [92]. Additionally, excessive proliferation of myofibroblasts results in the production of dysregulated amounts of ECM proteins such as collagen and fibronectin [93]. Rho-like GTPase, mitogen activated protein kinase (MAPK) and phosphatidylinositol-3-kinase (PI3K) pathways are collectively non-canonical pathways of TGF-β signaling, linked to pro-fibrotic cellular responses [65, 69, 84, 94]. For example, Rho-GTPase and ROCK are reported to regulate TGF-β-induced transdifferentiation of fibroblast to myofribroblasts [95].

Another concept in the fibrogenic process is the cellular generation of ROS by TGF-β1 in pulmonary fibrosis [96]. ROS are produced by mitochondria, peroxisomes and cytochrome P-450 as byproducts of normal cellular metabolism [97-99]. TGF-β1 increases mitochondrial ROS in many cells for the modulation of epithelia/mesenchymal transition [100], and expression of genes involved in fibrosis and myofibroblast differentiation [101]. There are

also exogenous sources of oxidants usually derived from cigarette smoking [102], ozone exposure [103], hyperoxia [104], ionizing radiation [105] and heavy metal ions[106].

ROS alter the functions of molecules by interacting and destroying cell components such as lipids, proteins and DNA [107]. The imbalance caused as a result of increased accumulation of ROS and depletion of antioxidants introduces oxidative stress [108], a cellular process reported in lung diseases such as idiopathic pulmonary fibrosis (IPF), chronic obstructive pulmonary diseases and acute respiratory distress syndrome [109].

It has also been shown that glutathione is suppressed in cystic fibrosis [110, 111] and sarcoidosis [112]. Interestingly, TGF-β1 is known to decrease the expression level and activity of catalase, glutathione peroxidase and glutaredoxin [113-115] in airway smooth muscle cells and interstitial lung diseases. In IPF patients, the expression of extracellular superoxide dismutase is altered without any known mechanism to that effect [116]. Additionally, TGF-β1 suppresses extracellular superoxide dismutase in mouse lung fibroblasts and the overexpression of the enzyme in mouse lungs inhibits the activation of latent TGF-β [117]. Conversely, catalase, a key antioxidant in peroxisomes [118], is demonstrated to be fairly resistive to degradation due to NADPH binding, that prevents and reverses the formation of compound II (an inactive form of catalase) [119]. Due to the depletion of the cellular antioxidant system during ROS, non-enzymatic antioxidants such as vitamins C and E [120], carotenoids [121], and glutathione [122] have been suggested as alternatives and could metabolize ROS.

It is important to explain the various ROS generated since TGF is generally known to enhance ROS production. The principal step in ROS generation is the reduction of O_2 to $\cdot O_2^-$[32]. Following $\cdot O_2^-$ production, $^{\bullet}OH^-$ and H_2O_2 are subsequently generated [123]. Additionally, $^{\bullet}OH^-$ is produced from H_2O_2 in a reaction catalyzed by iron ions, which is called Fenton reaction [124]. In ROS metabolism, the ROS molecules are noted to interact with nitric oxide ($NO^{\bullet}$) and peroxynitrite ($ONOO^-$) [125]. The most detrimental amongst the reactive species described are $^{\bullet}OH^-$, $ONOO^-$ as well as HOCl [126-128]. At the cellular level, H_2O_2 is produced by oxidases [108, 129]. Mitochondrially produced superoxide is dismutated by SOD2 which is converted further to H_2O_2. Hydrogen peroxide is also maintained at a balance by the actions of catalase and in general, intracellular glutathione peroxidases [108].

The NADPH family of oxidases is also associated with ROS imbalances in cells. Primarily is NOX4, known to be expressed in human lung fibroblasts [130], which stimulates

myofibroblast differentiation and progresses pulmonary fibrosis [131]. In smooth muscle cells, the induction of NOX4 mRNA is known to occur as a result of response to TGF-β1 stimulation [132]. It is further suggested that active TGF-β1 stimulates the increase in mitochondrial ROS production, induces NOXs and decreases antioxidants, leading to redox imbalance, fibroblast activation and fibrosis development [87].

Apart from ROS induction by TGF-β1, other molecules influence the pathophysiology of fibrosis. For instance, hyaluronan, a linear glycosaminoglycan of the extracellular matrix, is involved in myofibroblast differentiation [133] and also regulates TGF-β1 signaling and response in fibroblasts [134, 135]. With regards to the former, hyaluronan and CD44 interact with the epidermal growth factor receptor (EGFR) to support the proliferation and differentiation of fibroblasts [136, 137]. The molecular interactions are as follows: hyaluronan first binds to CD44 to enhance the interaction of CD44 with EGFR for the initiation of signal transduction via the mitogen-activated protein kinase (MAPK/ERK) pathway and Ca^{2+}/calmodulin kinase II (CaMKII) [138].

Besides the adverse roles of TGF-β1 in fibrosis, earlier and emerging evidence have suggested that fibroblast growth factor [139] and prostaglandin E_2 [140] reverse myofibroblast differentiation, expressing the need to explore this avenue for interventions against fibrosis. That notwithstanding, targeting one molecular process in pulmonary fibrosis might not be enough to resolve the disease since other cellular processes such as pro-inflammatory mediators are remarkably connected to the pathogenesis of IPF.

1.2.5. Pro-inflammatory mediators in pulmonary fibrosis

Inflammatory mediators are key candidates proposed to induce the initiation and progression of pulmonary fibrosis [141]. For example, cytokines such as macrophage inflammatory protein-1α (MIP-1α/CCL3) [142], MCP-1/CCL2 [143] and IL-8 are found in elevated amounts in IPF patients, and are implicated in chemotaxis and activation of neutrophils, monocytes and lymphocytes. Similarly, proangiogenic and antiangiogenic cytokines are also recorded at elevated levels in patients with IPF [144]. In the international literature it was demonstrated that IGF-1, TNF-α, FGF, VEGF, IL-1β, PDGF, and EGF [145, 146] play different roles in the regulation of fibrosis and tissue repair.

High levels of TNF-α have been reported in patients with idiopathic or systemic sclerosis-associated pulmonary fibrosis [147, 148]. In addition, overexpression of TNF-α in the lungs

of mice enhanced the development of pulmonary fibrosis [149]. Although elevated amounts of TNF-α have been found in patients and pulmonary fibrosis models, inhibition of the molecule with antibodies have been suggested to progress cardiac and interstitial lung disease [150, 151].

IL-1β was indicated to cause acute lung injury and also play a critical role in the development of pulmonary fibrosis [152]. Increased expression of TNF-α was observed in IL-1β-induced fibrosis, suggesting a mechanistic role of the two molecules in the pathogenesis of the disease [153]. Similarly, IL-1β also elevates neutrophil attraction of CXC chemokines, platelet-derived growth factor (PDGF) and TGF-β1, leading to possible initiation of fibrosis following inflammation [152, 154].

Moreover, IL17-A increased in patients with IPF [155] and is associated with the progression of pulmonary fibrosis [155]. Indeed, the expression of IL17-A is linked with persistent neutrophilia [155] which is proposed to indicate early mortality in patients with IPF when abundant in bronchoalveolar lavage fluids [156]. In addition to alteration of neutrophils, some data have also shown the localization of macrophages in pseudo-alveoli and $CD3^+$ T-helper cells in the interstitium of lungs expressing IL-17 [157], implying the presence of autoimmune reactivity [158] or a possible role of IL-17 in IPF [159]. However, IL-17 is functionally needed for the mediation of inflammation and destruction of extracellular fungi and bacteria [160].

Th2 cytokines such as IL-4, IL-5 and IL-13 were also measured in high quantities in alveolar macrophages from IPF patients [161]. IL-13 receptors are upregulated in lung biopsies of patients with UIP (usual interstitial pneumonia) and IL-4Rα was found in elevated amounts in lung biopsies of NSIP (non-specific interstitial pneumonia) patients [162]. Conversely, Th1 cytokines such as IFN-γ and IL-12 were reported to be protective and as such inhibit pulmonary fibrosis progression [163]. Apart from the roles cytokines play in the pathogenesis of fibrosis, relevant to the disease are the cellular involvements in the progression of the process.

1.2.6. Cells involved in the pathogenesis of fibrosis

Apoptosis and necrosis of cells occur in the alveolar of patients suffering from IPF [164, 165]. In principle, in the pathogenesis of IPF much has to be still revealed, however, the roles of epithelial cells and fibroblasts have been primarily studied in relation to the disease progression [166]. Moreover, in sites of excess deposition of matrix proteins, called fibrotic

foci, fibroblasts and myofibroblasts are accumulated [4] during fibrogenesis. The source of collagen producing fibroblasts in the interstitium of the lungs and fibrotic foci [167] has been debated over the years [168]. Suggestions have been made, implicating epithelial/mesenchymal transition [169] though these assertions remain to be empirically confirmed [157].

The lungs of IPF patients exhibit elevated levels of connective tissue growth factor (CTGF) mRNA and protein in the AECs (Alveolar epithelial cells), whereas tissues from normal lungs have sparse CTGF-expressing AECs [170], proposing the involvement of AECs in pulmonary fibrosis. Supporting this notion, the alveolar epithelium of patients with IPF was reported to possess an increased expressions of CXCL12 [171, 172] and CCL2 [173]. These proteins are known ligands for CXCR4 [171, 174] and CCR2 [175] chemokine receptors present in the surface of fibrocytes, suggesting an interplay between the two cell types in the pathogenesis of IPF.

Furthermore, the sources of cytokines in the lungs are epithelial, mesenchymal and inflammatory cells, such as macrophages, B-lymphocytes, T-lymphocytes, neutrophils, eosinophils and platelets [176]. Interferon-γ activated macrophages secrete TNF-α, IL-6, IL-1β, and inducible nitric oxide. T-lymphocytes were suggested to play bifunctional roles in fibrosis, alleviating fibrosis and also promoting the progression of the disease by producing Th-1 or Th-2 cytokines [176]. B-Lymphocytes produce autoantibodies against periplakin, a protein localized to desmosomes and intermediate filaments, in epithelial cells of IPF patients and this has been shown to worsen the physiological condition of the disease [177]. Conversely, B-cells elicit protective roles in fibrosis in transgenic mice overexpressing anti-inflammatory cytokines and IL-9 [178, 179].

1.2.7. Composition of the extracellular matrix (ECM) in the lung

The ECM is a connecting framework of fibres and ground substances synthesized and released by cells via exocytosis [180]. An example is the basement membrane, which is a specialized type of ECM produced by epithelial, endothelial and stromal cells [181]. Moreover, stromal cells are as well known to produce components of the interstitial matrix. The ECM consists of four different components: structural proteins of fibres, ground substances with glycosaminoglycans, proteoglycans and adhesion proteins in between the distinct epithelial cell types [182]. The epithelial (AECI and AECII) and endothelial cells of

the lung alveolar wall are also separated by a thin interstitial space [183]. It is known that two thirds of the dry weight of ECM is composed of Collagen fibres (type I, III, and V in the airway wall) and elastin [184]. The basement membrane in the lung is made up of collagen IV and it is documented that collagens I and II basically provide the structural integrity of the organ [185, 186]. The other fraction of lung ECM comprise of glycoproteins (fibronectin, tenascin, laminin) and ground substance components, including heparin sulfate and hyaluronan and entactin [185]. Collectively, the collagen fibres in the ECM give tensile strength [187], among which collagen type III fibers are malleable and easily broken down and collagen type I fibres exhibit thick cross-linked fibrils [188, 189]. Fibronectin regulates the morphology, motility and differentiation of cells in the lungs, as well as enhances the adhesion of various cells to the ECM.

The ECM of the lung provides mechanical tensile, strength and elasticity, and maintains interstitial fluid dynamics [190]. Other key functions of the ECM include: 1. Provision of low resistance to optimum gas exchange. 2. Influence of cellular processes through the binding of growth factors, cytokines and chemokines. 3. Promotion of cell-surface receptor interactions to regulate cell morphology, cell to cell interaction, cell signaling, differentiation, proliferation, polarization and migration [146, 191]. and 4. Modulation of wound healing [192]. The broad scope of functions of the ECM makes it important for the mediation of almost all cellular behaviors. This makes the regulation of ECM production, degradation and remodeling multi-mechanistic [193]. The disruption of any of these biological processes will result in abnormal behavior of cells leading to failure of organ homeostasis as observed in tissue fibrosis [194]. Furthermore, some proteins as well as proteoglycans and glycosaminoglycans in ECM contribute to stiffness and also regulate cell behavior [195]. Interestingly, matrix stiffness of the lung induces mechanical stimuli to influence cell function for the progression of fibrosis [195, 196].

1.2.8. Major collagen secreting cells in fibrosis

As discussed earlier, fibroblasts are the main collagen I and extracellular matrix secreting cells in IPF [4, 197]. The major cell types that are responsible for collagen production during the pathogenesis of the disease are essential possible targets to develop therapeutic interventions. The lung parenchyma and circulation of IPF patients harbor an important cell type known as fibroblast precursor [171, 198]. The contributions of fibroblast precursors in IPF cannot be underemphasized since they are activated into fibroblasts or quiet cells in the

stroma differentiate to myofibroblasts, produce collagen type I and also release cytokines to induce collagen deposition [174, 199]. Increase in circulating fibroblast precursors have been described during exacerbations in patients with IPF [198].

In addition to increased matrix secretion, progression of lung fibrosis also depends on changes in the phenotype of fibroblasts, which render them resistant to apoptosis and induce their migration [200, 201]. At the molecular level, resistance to apoptosis of fibroblasts is enhanced by increased levels of survivin [202] or SPARC [203], elevation of STAT-3 signaling [204], declined release of prostaglandin E2 due to decreased induction of cyclooxygenase 2 (COX-2) [205] and reduced forkhead box O3a (FoxO3a) [206].

1.2.9. Pathological features and diagnosis of IPF

Controversies related to the diagnosis of IPF through surgical biopsies and high resolution computer tomography (HRCT) influenced the use of classical clinical disease patterns associated with Usual Interstitial Pneumonia (UIP) as sufficient evidence for IPF diagnosis [207, 208]. The lungs of patients with UIP are characterized with a timely and heterogeneous distribution of interstitium, a patchwork appearance due to alternating areas of scarred and normal lung tissues, distortion in normal lung architecture with honeycomb structures and thick scars at the alveolar region, and accumulation of myofibroblasts [209, 210]. The scarred tissues persist in subpleural/paraseptal regions of the lungs [211, 212]. The honeycomb structure comprises enlarged airspaces with bronchiolar epithelium and in many cases, filled with mucous, neutrophils and macrophages [209]. Though extensive fibroblastic foci have been related to poor prognosis in IPF patients, it is interesting to note that not all cases tend to be true [213].

The features described above are also used in the diagnosis of IPF coupled with the aid of two main diagnostic tools, namely high resolution computer tomography (HRCT) and histopathological studies. The classical characteristic features of UIP on HRCT used in the diagnosis of IPF include: subpleural abnormalities mostly at the base of the lung, reticular abnormalities, honeycombs with or without traction bronchiectasis and the absence of unrelated features of UIP [208, 214, 215].

1.3. Treatment and management of IPF

Management of IPF was once based on arresting inflammation until opinions shifted to abnormal repair of alveolar epithelial injury [216]. In recent times, pirfenidone has been extensively used and it is suggested to regulate the proliferation of fibroblasts, inhibit the synthesis of collagen, interrupt the production of TGF-β and TNF-α, and stimulate anti-inflammatory and anti-oxidative responses [217, 218]. Additionally, another compound, Nintedanib, was generated to inhibit the progression of IPF. Nonetheless, nintedanib unfortunately decreased respiratory function by blocking signaling pathways of vascular endothelial growth factor receptors, platelet-derived growth factor receptors and fibroblast growth factor receptors in addition to what it was intended to function against [219, 220].

Oxidative stress is a common biological mechanism in IPF and N-Acetylcysteine, a compound with antioxidative properties, has also been tried in the management of IPF. Additionally, it was observed that more than 90% of patients suffering from IPF presented with gastrooesophageal reflux disease [221], wherefore antacid drugs were used, however, were invariably reported to reduce the forced vital capacity of patients [222]. Furthermore, other non-pharmacologic approaches like long-term oxygen therapy [208], lung transplantation [223], and pulmonary rehabilitation [224] have helped in the management of patients with IPF.

Among all the interventions available, the use of Pirfenidone and Nintedanib has shown promising signs by reducing the progression of IPF. Nonetheless, these compounds do not cure the disease and the development of IPF is progressed in some patients irrespective of treatments with these drugs [225]. The growing concerns to find putative therapeutic interventions for IPF and to prolong the lifespan of patients have resulted in numerous studies which are investigating the use of some known compounds for experimental and clinical trial. As a result, activators of peroxisome proliferator-activated receptors (PPARs) were suggested and studied in IPF.

1.4. PPARs and their potential roles in fibrosis resolution

Peroxisome proliferator-activated receptors (PPAR) belong to the superfamily of nuclear hormone receptors [226, 227] that are ligand-activated to regulate gene expression for the modulation of multiple cellular functions. The three isotypes of PPARs in lower vertebrates and mammals are PPAR-α, PPAR-β/δ and PPAR-γ [228]. PPAR-γ has three isoforms namely: γ1, γ2 and γ3 [229, 230]. Each PPAR exhibits its own specific and distinct tissue and cell type distribution and also possess some ligand specificity [231, 232]. The receptors are known to be activated by different fatty acids, eicosanoids and many xenobiotics [233]. PPARs function as transcription factors [234] to regulate genes involved in the metabolism of glucose and lipids, adipogenesis, homeostasis, inflammation, immune response, insulin sensitivity, cell growth and differentiation [227, 234-240].

The PPAR family members share similarities in their structural and functional features. They possess an N-terminal domain containing a ligand-independent activation function 1 [241] for PPAR phosphorylation, a DNA binding domain [242], a co-factor binding domain and a ligand-binding domain. There also exists a ligand-dependent activation function 2 at the ligand binding domain of the receptors [232].

After ligand binding, PPARs form heterodimeric complexes with another ligand-activated nuclear receptor known as retinoid X receptor (RXR) [243]. Ligand-binding to PPARs results in changes in receptor conformation, release of co-repressors and recruitment of co-activators [232, 234]. This complex binds to a PPAR response element (PPRE) in the promoter of target genes [242, 244]. Transcription starts after the dissociation of related proteins, such as nuclear receptor corepressors (NCoR), histone deacetylases (HDAC), and G-protein pathway suppressor 2 (GPS2) [245, 246], and recruitment of coactivators, including PPAR coactivator (PGC-1), histone acetyltransferase p300, CREB binding protein (CBP) and steroid receptor coactivator (SRC)-1 [243].

The anti-fibrotic potentials of natural and synthetic ligands of PPARs have been studied in different organ systems. For instance, PPAR-α activation was reported to reduce fibrosis in a thioacetamide model of liver cirrhosis [247], attenuate cardiac and vascular fibrosis [248] and lung fibrosis [249]. PPAR-β/δ was suggested to support the anti-fibrotic potential of PPAR-γ [250]. Moreover, a wide spectrum of research data on the anti-fibrotic effects of PPAR-γ in the lung has been published using diverse experimental approaches to elucidate its essential molecular properties [251-254] though many of them are stimulating anti-inflammatory effects and fibrosis prevention.

1.4.1. Molecular mechanisms of PPARs in fibrosis

Ligand stimulation of PPAR-α is known to exert therapeutic effects in fibrotic disease conditions through its interference with some cellular signaling pathways. For example, oleoylethanolamide activates PPAR-α to inhibit Smad 2/3 phosphorylation in TGF-β1 stimulated hepatic stellate cells [255]. PPAR-α interacts and inhibits AP-1 and NF-κB thus blocks the transcription of pro-inflammatory cytokines in cystic fibrosis [256]. In the heart, inhibition of HMG-CoA reductase in combination with a Western diet was reported to increase the levels of PPAR-α and PPAR-γ which further induced the reduction of cardiac fibrosis in ApoE-/- mice [257]. Interestingly, a remarkable reduction in tubulointerstitial fibrosis was noted when PPAR-α was overexpressed in the proximal tubule of a PPAR-α transgenic mouse model [258].

The molecular effects of PPAR-β/δ in fibrotic diseases are clearly related to inflammation and prevention of oxidative stress. Activated PPAR-β increases the phosphorylation of phosphoinositide-3 kinase/protein kinase-C alpha/beta mixed lineage kinase-3 pathway, leading to the activation of p38 and c-Jun N-terminal kinases [259]. This mechanism stimulates the proliferation of hepatic stellate cells, thus modulate fibrosis and inflammatory responses in conditions of uncontrolled hepatic repair. PPAR-β is also known to induce the expression of some TGF-β-repressed and TGF-β-activated genes [260]. TGF-β stimulates corepressor genes, for instance NCOR2, which complements the recruitment of SMRT and various corepressors to the PPRE-bound PPAR-β complex hence blocks the transcription of downstream genes. In cardiac fibrosis, activated TRPV1 upregulates PPAR-β to protect the heart from oxidative stress-induced fibrosis in mice [261]. Also, PPAR-β potentially prevents CTGF/MMP9-induced fibrotic changes in the heart of patients and mice by upregulating STAT3 expression in hyperglycemic environment [262]. No reports are available yet on the function of this receptor in pulmonary fibrosis.

The involvement of PPAR-γ in fibrotic disease processes has been well delineated. It was reported that PPAR-γ is controlled by TGF-β1 partly through Smad3 signaling [263]. The study, which was done in primary murine lung fibroblasts, suggested that TGF-β1 downregulates PPAR-γ transcription whereas in lung fibroblasts deficient in Smad3, the effect was reduced. Further, TGF-β1 stimulates the activation of the PPAR-γ gene promoter and induces the phosphorylation of PPAR-γ in primary lung fibroblasts. However, TGFβ-induced Akt phosphorylation is inhibited by activated PPAR-γ through post-translational and post-transcriptional mechanisms which are independent of MAPK-p38 and PTEN, and dependent

on TGFβ-induced phosphorylation of FAK [264]. In mouse embryonic fibroblasts lacking PPAR-γ, constitutive up-regulation of collagen I and Smad activation were observed and this was partly due to autocrine TGF-β stimulation [265]. The study highlighted that constitutive phosphorylation of Smad2/3 leads to ligand-independent interaction of Smad3 with its general DNA recognition site and p300. This suggests that PPAR-γ may play a crucial role in controlling Smad-dependent Type I collagen gene expression. In cardiac fibrosis, ligand activated PPAR-γ interacts with TGF-β1/Smad2/3 and JNK signaling pathways to reduce the production of ECM and suppression of angiotensin II-induced production of PAI-1 (plasminogen activator inhibitor-1) in rat cardiac fibroblasts, proposing a potential beneficial effect in cardiac fibrosis [266].

The link between microRNAs and PPAR-γ in fibrotic diseases explains different mechanisms of actions with regards to the type of tissue and the type of microRNA studied. An example is tubulointerstitial fibrosis in renal tissues of diabetic rats and diabetic nephropathy. Inhibition of PPAR-γ by miR-27a and further activation of TGF-β/Smad3 signaling promote the expression of connective tissue growth factor (CTGF), fibronectin and collagen I [267]. Conversely, in fibroblasts isolated from keloid patients, troglitazone-activated PPAR-γ induced the expression of miR-92b which further inhibited the expression of Axl (AXL Receptor Tyrosine Kinase) and TGF-β1 [268]. Additionally, it was reported that activated PPAR-γ upregulated IκBα [269]. This protein negatively modulates NF-kB-dependent inflammation in cystic fibrosis-associated liver disease in mice.

Overall, PPARs have shown to interfere with important signaling pathways involved in the pathophysiology of fibrosis and metabolic diseases. Moreover, PPAR-α induced the proliferation of peroxisomes and also exhibited anti-fibrotic effects in primary human lung fibroblasts [270], hence the need to investigate further into peroxisomal functions in fibrosis resolution.

1.5. Peroxisomes

Peroxisomes are single membrane bound ubiquitous organelles with a fine granular electron-lucent matrix containing metabolic enzymes and diameters ranging from 0.1–1 μm [271]. Though frequently spherical in hepatocytes, peroxisomes can be elongated especially in mice or found also in reticular forms [272]. Peroxisomes are present in all eukaryotic cells (ubiquitous organelles) and were initially reported in microbodies [273]. Peroxisomes possess several oxidases and catalase for hydrogen peroxide production and decomposition leading to

the suggestion of the peroxisome concept [274]. The organelle responds to cellular and environment changes by regulating its size, morphology, number and function [275]. The morphology of peroxisomes also depends on the presence of inducing stimuli such as hepatectomy [276], growth factors and polyunsaturated fatty acids [277]. Additionally, peroxisomes are also influenced by the conditions in other subcellular compartments, such as lipid droplets [278], domains of the plasma membrane and mitochondrial processes [279]. There are 32 peroxin proteins associated with peroxisomal biogenesis which are proteins diversely found in the cytoplasm, the peroxisomal membrane and the matrix of the organelle [280]. The expression of some peroxins and peroxisomal enzymes is stimulated by Fatty acid-responsive transcription factors [281]. It is also known that the metabolic functions of peroxisomes are altered by changes in its specific protein composition [282].

Over the past years, reports have indicated peroxisomal gene regulation by PPARs especially PPAR-α. Genes of the peroxisomal compartments regulated by PPAR-α include: 1) Peroxisomal β-oxidation (ABCD2, ABCD3, ACAA1A, ACOX1, MFP2) and 2) cholesterol and bile acids metabolism (ABDC1) [283]. PPAR-β was also shown to regulate peroxisomes in osteoblasts [284].

1.5.1. Peroxisomal disorders

Peroxisomal biogenesis proteins were named peroxins that are encoded by PEX genes whose mutations result in peroxisomal biogenesis disorders, the diseases of the Zellweger syndrome spectrum (Zellweger syndrome, neonatal adrenoleukodystrophy and infantile Refsum's disease). The most severe form is Zellweger syndrome also called cerebrohepatorenal syndrome, a devastating disease leading to liver fibrosis/cirrhosis and early death of children [285]. In addition to peroxisomal biogenesis disorders, the second group of the inherited peroxisomal diseases are the peroxisomal single enzyme deficiencies [286]. Mutation in ABCD1 gene encoding a transport protein for very long chain fatty acid CoA-derivatives results in X-linked adrenoleukodystrophy [287], a disease leading to the accumulation of VLCFAs, neurodegeneration and adrenal deficiency. Peroxisomes are involved in the last step of bile acids synthesis via their β-oxidation pathways [288] and disruption to this organelle is known to result in cholestasis, hepatomegaly and rise in serum enzymes [289]. Deficiencies in peroxisomal functions result in secondary proliferation of pleomorphic mitochondria and respiratory chain defects in activity (complex I and III) [290].

1.5.2. The biogenesis of peroxisomes and organ distribution

Compiling evidence have shown that the regulation of peroxisome biogenesis modulates peroxisomal function [291]. Possible mechanisms by which peroxisomes could come into existence, namely: de novo generation of peroxisomal vesicles from the endoplasmic reticulum [292, 293] and, fusion [294] or fission of pre-existing peroxisomes [295].

Peroxisomal fission begins with tubulation, a mechanism facilitated by activated PEX11β [296, 297] and the enrichment of dynamin-related Protein (DRP)-interacting proteins in its membrane. The peroxisomal membrane further undergoes constriction and a recruited dynamin-related protein enhances the fission mechanism for the formation of new peroxisomes in mammalian cells. Reports have also shown that DRP-interacting proteins and DRPs mediate the proliferation of mitochondria as well [279, 298]. After fission, peroxisomes are distributed in mammalian cells along the microtubules [299]. It is noteworthy that peroxisomes also proliferate at a rate compared to that of the cell cycle [295].

Vesicular transport of proteins and membranes from the endosplasmic reticulum to matured peroxisomes was suggested to result in a coordinated membrane expansion and fission of the organelle [295]. However, there are clear differences between these vesicles and those involved in de novo formation of peroxisomes since the latter do not fuse with matured peroxisomes [294].

Peroxisomes are heterogenously distributed in different organs of the body. For instance, in the lungs, the distribution and abundance of peroxisomal proteins depend on the type of cell and developmental stage of the organ [300]. Also in the mouse heart, the four chambers have different peroxisomal genes expression and protein abundance [301].

1.5.3. Import of membrane proteins

A majority of membrane proteins of peroxisomes are synthesized in the cytosol and are post-translationally embedded into the peroxisomal membrane either by direct targeting of the protein to peroxisomes via the recognition of a membrane PTS (Peroxisomal Targeting Signal) in the cytosol or are invariably targeted through the endoplasmic reticulum [302]. The former often occurs in mammalian cells where a shuttling receptor, PEX19, forms a cargo complex with the membrane proteins in the cytosol and coordinates the recognition of a membrane PTS [303, 304]. This complex further progress to another peroxisomal membrane-

bound protein called PEX16 for the insertion of cargo proteins into the membrane of peroxisomes [303, 304].

1.5.4. Import of matrix proteins

The import of matrix proteins from the cytosol to peroxisomes is coordinated by PEX5 and PEX7 receptors which recognize peroxisomal targeting signals 1 and 2 (PTS1 and PTS2) at different termini of the matrix proteins [271]. Membrane proteins imported into peroxisomes start with the docking of the cargo-bound import receptors (PEX5 or PEX7) on the peroxisomal membrane, translocation of the cargo into the peroxisomal matrix [305] and final release and recycling. The receptors are released back into the cytosol.

Supporting data from some studies have revealed that the mechanisms involved in PTS1-dependent translocation of proteins into the peroxisomal matrix are as follows: 1) Cytosolic soluble import receptor PEX5 binds to the cargo. 2) The complex formed by the cargo and import receptor resides on peroxisomes by docking on a complex of peroxins (example PEX13 and PEX14) on the membrane. 3) PEX5 forms a channel with the peroxisomal membrane for the translocation of the cargo into the matrix and is released and recycled by exportomers [306, 307] or degraded by proteasomes [308] when the receptor recycling machinery is compromised. Reference to this mechanism, it is striking that there were no pores described on the peroxisomal membrane [309] though it is known that small metabolites are able to permeate the organelle [310].

1.5.5. α- and β-oxidation

Peroxisomes and mitochondria cooperate in β-oxidation, detoxification of ROS [311, 312] and anti-viral signaling and defense [313]. Very-long chain fatty acids undergo β-oxidation preferably in peroxisomes [314]. Peroxisomes function in the α-oxidation of branched-chain fatty acids [315], a unique metabolic function absent in mitochondrion. The metabolism of dicarboxylic acids degradation, products of ω-oxidation, occurs via peroxisomal β-oxidation [316].

Before transport into the organelle and β-oxidation, saturated unbranched and 2-methyl-branched fatty acids are activated to thiol-CoA derivatives and undergo a stepwise process catalyzed by various acyl-CoA oxidases (ACOX 1-3), multifunctional enzymes (L-bifunctional protein and D-bifunctional protein) and thiolases in mammals [317].

The β-oxidation mechanisms in peroxisomes as well as in mitochondria involves four successive processes which include dehydrogenation of fatty acyl-CoA (done in peroxisomes by ACOXs and in mitochondria by acyl-CoA dehydrogenases), hydration to form 3-L-hydroxyacyl-CoA, dehydrogenation of 3-L-hydroxyacyl-CoA, leading to the formation of 3-ketoacyl CoA and thiolytic cleavage of the terminal acetyl-CoA group, giving rise to a new acyl-CoA molecule.

Peroxisomal fatty acid oxidation results in the shortening of very long-chain fatty acids, and long-chain fatty acids up to chain length (> C8), which are further oxidized in the mitochondrion. Moreover, signaling and bioactive lipids are degraded in peroxisomes, for example, pro-inflammatory prostaglandins and leukotrienes. Furthermore, the β-oxidation in peroxisomes leads to modification of polyunsaturated fatty acids and bile acids [317-319]. Finally, β-oxidation precursors of ether phospholipids (plamalogens) and cholesterol are synthesized in this organelle.

1.5.6. Antioxidative and ROS metabolism in peroxisomes

Peroxisomes are a rich source of catalase, superoxide dismutase 1, and glutathione peroxidase, which degrade reactive oxygen species [320]. In contrast, peroxisomal oxidases during metabolism of specific substrates such as xanthine or urate (xanthine and urate oxidase) or D-amino acids, α-hydroxy acids or other substrates (example polyamines) reduce O_2 [99]. The $^{\bullet}O^{-}_{2}$ produced by xanthine oxidase is converted by superoxide dismutase (CuZnSOD or SOD1) into O_2 and H_2O_2 in peroxisomes [321]. In response to the accumulation of H_2O_2 in cells, catalase, glutathione peroxidase and peroxiredoxin I or V (PMP20) scavenge the reactive oxygen species into H_2O and O_2 [322, 323]. Due to the various oxidases present in peroxisomes, the organelle also functions in amino acid catabolism and polyamine oxidation [317].

1.5.7. Peroxisomes in fibrosis

In Zellweger patients, β-oxidation is compromised, leading to the accumulation of toxic C(27) bile acid intermediates, a condition suggested to cause liver disorders and fibrosis [324]. Our recent paper supported this claim by reporting that profibrotic response to TGF-β1 in primary human lung fibroblasts downregulated peroxisomal proteins, example PEX13 (peroxisomal protein) which resulted in the activation of proinflammatory mediators and the Smad signaling pathway, leading to the progression of fibrosis [270]. However, PPAR-α activation induced the proliferation of peroxisomes as well as inhibited profibrotic responses.

1.6. Aims of the study

The scientific basis of the study relates to our earlier publication which reported that in vitro treatment of primary human lung fibroblasts with PPAR-α induced peroxisome proliferation and exhibited anti-fibrotic responses [270]. Additionally, it was later reported from our working group that PPAR-β activation induced the proliferation of peroxisomes and also increased catalase in primary osteoblasts [284]. The pathogenesis of IPF is influenced by cytokines, ROS accumulation and other pathophysiological mechanisms that can be modulated when peroxisomes are proliferated. This study investigated the functional molecular role of peroxisomes using control and IPF primary human lung fibroblasts as well as lung tissues from humans and a bleomycin-induced fibrosis mouse model. As a result, the aims of this study were as follows:

1. To characterize markers of fibrosis in lung tissues and the relative abundance of different PPARs in basal and TGFβ1 stimulated control and IPF primary human lung fibroblasts.
2. To assess the differences between control and IPF primary human lung fibroblast with regards to the expression of collagen degrading enzymes and their proliferative capacities.
3. To investigate the anti-fibrotic properties of activated PPARs.
4. To assess the role of peroxisome biogenesis in fibrosis after PPAR activation in TGF-β1 stimulated control and IPF primary human lung fibroblasts.
5. To determine the effects of activated PPARs on migration and invasion of lung fibroblasts.
6. To explore the anti-fibrotic potential of dual PPAR agonist in primary human lung fibroblasts.
7. To elucidate the functional molecular role of catalase and peroxisomes in pulmonary fibrosis.

2. Materials and methods

2.1. Materials

The instruments, chemicals, reagents, enzymes, drugs and consumables used for this study and their suppliers are outlined in the tables that follow.

2.1.1. Instruments and general materials

Table I shows the instruments and materials used for the experiments.

Instrument	Supplier
Biocell A10 water system	Milli Q-Millipore, Schwalbach, Germany
Biofuge Fresco	Heraeus, Hanau, Germany
Bio-Rad electrophoresis apparatus (Sub Cell GT) system	Bio-Rad, Heidelberg, Germany
Cary 50 Bio-UV-visible spectrophotometer	Varian, Darmstadt, Germany
Dish washing machine (G 78 83 CD)	Miele, Gütersloh, Germany
Hera cell 240 incubator	Heraeus, Hanau, Germany
Hera safe, clean bench KS-12	Heraeus, Hanau, Germany
Ice machine, Scotsman AF-100	Scotsman Ice Systems, Vernon Hills, IL,USA
iCycler PCR machine MyiQ2 optical module	Bio-Rad, Heidelberg, Germany
Leica DMRD fluorescence microscope	Leica, Bensheim, Germany
Leica DC 480 camera	Leica, Bensheim, Germany
Leica TP1020 embedding machine	Leica, Nussloch, Germany
Leica SM 2000R rotation microtome	Leica, Nussloch, Germany
Leica TCS SP2 confocal laser scanning microscope (CLSM)	Leica, Nussloch, Germany

Magnetic stirrer, MR3001	Heidolph Instruments GmbH & Co.KG, Schwalbach,Germany
Microtome stretching water bathType 1003	Vieth Enno, Wiesmoor, Germany
Microwave oven MB-392445	LG, Willich, Germany
Mini Trans-Blot® Cell	Bio-Rad
Mini-Protean 3 cell system	Bio-Rad, Heidelberg, Germany
Multifuge 3SR centrifuge	Heraeus, Hanau, Germany
NanoDrop™ 8000	ThermoFisher
Oven HERAEUS T 5050 EKP	Heraeus, Hanau, Germany
Paraffin tissue floating bath	Medax
pH meter E163649	IKA, Weilheim, Germany
Pipette tips	Eppendorf AG, Hamburg, Germany
Pipettes	Eppendorf, Hamburg, Germany
Potter-Elvehjem homogenizer	B.Braun, Melsungen, Germany
Power supply - 200, 300 and 3000 Xi	Bio-Rad, Heidelberg, Germany
Pressure/ Vacuum Autoclave FVA/3	Fedegari, Albuzzano, Italy
Sorvall Evolution RC centrifuge	Kendro, NC, USA
Smartspec™ 3000 spectrophotometer	Bio-Rad, Heidelberg, Germany
Thermo plate	Medax, Kiel, Germany
Thermo mixer HBT 130	HLC, BioTech, Bovenden, Germany
Trans-Blot SD semi dry transfer cell	Bio-Rad, Heidelberg, Germany
Trimmer TM60	Reichert, Wolfratshausen, Germany
TRIO-Thermoblock	Biometra, Göttingen, Germany
Ultra-balance LA120S	Sartorius, Göttingen, Germany

Ultra Turrax T25 basic homogenizer	Junke & Kunkel, Staufen, Germany
Vortex M10	VWR International, Darmstadt, Germany
Water bath shaker GFL 1083	GFL, Burgwedel, Germany
General Material	**Supplier**
BioMax MR-films	Kodak, Stuttgart, Germany
Cover slips	Menzel-Gläser, Braunschweig, Germany
Culture dish (35 mm)	BD Biosciences, Heidelberg, Germany
Culture dish (60 mm)	BD Biosciences, Heidelberg, Germany
Dimethyl sulfoxide (DMSO)	Invitrogen Life Technologies GmbH, Karlsruhe, Germany
DMEM, low glucose, GlutaMAX™ supplement	Sigma, Steinheim, Germany
Eppendorf tubes	Eppendorf AG, Hamburg, Germany
Falcon tubes	Becton Dickinson, Heidelberg, Germany
Fetal bovine serum	Thermo Fisher Scientific, Schwerte, Germany
Filter tips	Braun, Melsungen, Germany
Microscope slides	R. Langenbrinck, Emmendingen, Germany
Microtome blade A35	Feather, Köln, Germany
Multi-well cell culture plates (12-wells)	BD Biosciences, Heidelberg, Germany
Multi-well cell culture plates (24-wells)	BD Biosciences, Heidelberg, Germany
Multi-well cell culture plates (6-wells)	BD Biosciences, Heidelberg, Germany
Nalgene syringe filter (0.2µm)	Thermo Fisher Scientific, Schwerte, Germany
Nitrile gloves	Kimberly-Clark Professional, Koblenz-Rheinhafen, Germany
Paraffin	Paraplast Plus, MO, USA

Pasteur pipettes	VWR International GmbH, Darmstadt, Germany
Penicillin-Streptomycin	PAN Biotech, Aidenbach, Germany
Phosphate-buffer saline (PBS)	PAA laboratories GmbH, Pasching, Austria
Plastic pipettes, for cell culture (sterile)	Becton Dickinson GmbH, Heidelberg, Germany
PVDF membranes	Millipore, Schwalbach, Germany
Tissue culture plate (96-wells)	Sarstedt, USA
Syringe filters 0.22 microns	Millipore GmbH, Schwalbach, Germany

Table I. Instruments and general materials

2.1.2. Drugs, siRNA and Chemicals

Table II displays the suppliers of drugs and siRNAs used for treatment and transfection of cells, and chemicals for the experiments.

Drug substances and compounds used for Treatments	**Supplier**
Arachidonic acid, docosahexaenoic acid, eicosapentaenoic acid	Cayman Chemical, Ann Arbor, USA
3-Amino-1,2,4-triazole	Merck, Darmstadt, Germany
Dual PPAR-β and -γ agonist (V6)	Vitas-M, Champaign, USA
GSK0660 (PPAR-β antagonist)	Trocris bioscience, Wiesbaden-Nordenstadt, Germany
GW0742 (PPAR-β agonist)	Sigma-Aldrich, Steinheim, Germany
GW6471 (PPAR-α antagonist)	Sigma-Aldrich, Steinheim, Germany
GW9662 (PPAR-γ antagonist)	Trocris bioscience, Wiesbaden-Nordenstadt, Germany
Hydrogen peroxide solution	Merck, Darmstadt, Germany

MMP inhibitor (4-Aminobenzoyl-Gly-Pro-D-Leu-D-Ala hydroxamic acid)	Sigma-Aldrich, Steinheim, Germany
rhTGF-β1	R&D, Minneapolis, USA
Rosiglitazone	Sigma-Aldrich, Steinheim, Germany
Troglitazone	Trocris bioscience, Wiesbaden-Nordenstadt, Germany
WY14643 (PPAR-α agonist)	Trocris bioscience, Wiesbaden-Nordenstadt, Germany
SiRNA and reagent	**Supplier**
Allstars negative siRNA	Qiagen, Hilden, Germany
ScreenFect A	InCella, Berlin, Germany
siMMP1	Ambion, Darmstadt, Germany
Catalase siRNA	GE Dharmacon, Lafayette, USA
Chemical	**Supplier**
AccuGENE™ water	Lonza, Basel, Switzerland
Acrylamide	Roth, Karlsruhe, Germany
Agarose	Roche, Grenzach-Wyhlen, Germany
Bradford reagent	Sigma, Steinheim, Germany
Bromophenol blue	Riedel-de Haën, Seelze, Germany
Clarity ^{TM} western ECL substrate	Bio-Rad, Heidelberg, Germany
3,3´-Diaminobenzidine-tetrahydochloride (DAB)	Sigma, Steinheim, Germany
Deoxynucleotide Mix (dNTP)	5 Prime, Hilden, Germany
di-sodium hydrogen phosphate (Na_2HPO4)	Merck, Darmstadt, Germany

Dithiothreitol	Bio-Rad, Heidelberg, Germany
Dual luciferase reporter assay kit	Promega, Mannheim, Germany
Ethanol	Merck, Darmstadt, Germany
Ethylene diamine tetra acetic acid (EDTA)	Fluka, Neu-Ulm, Germany
Gibco´s 0.25% Trypsin/EDTA	Invitrogen Life Technologies GmbH, Karlsruhe, Germany
Glutaraldehyde	Serva, Heidelberg, Germany
Glycerol	Sigma, Steinheim, Germany
Glycine	USB Europe GmbH, Staufen, Germany
High-Capacity cDNA Reverse Transcription Kit	Thermo Fisher Scientific, Schwerte, Germany
HEPES/4-(2-hydroxyethyl)-1-piperazineethanesulfonic acid	Roth, Karlsruhe, Germany
Hoechst	Molecular Probes/Invitrogen
Milk powder	Roth, Karlsruhe, Germany
Mowiol 4-88	Polysciences, Eppelheim, Germany
N-Propyl-gallate	Sigma, Steinheim, Germany
Paraformaldehyde (PFA)	Sigma, Steinheim, Germany
Paraformaldehyde (PFA)	Merck, Darmstadt, Germany
Penicillin/Streptomycin	PAN Biotech, Aidenbach, Germany
Ponceau S	Serva, Heidelberg, Germany
Potassium chloride (KCl)	Merck, Darmstadt, Germany
Potassium dihydrogen phosphate (KH_2PO_4)	Merck, Darmstadt, Germany

Protease inhibitor mix M	Serva, Heidelberg, Germany
READYMATIC® Fixer and replenisher	Carestream Health, Stuttgart, Germany
READYMATIC® Developer and replenisher	Carestream Health, Stuttgart, Germany
RNAzol® RT	Sigma, Steinheim, Germany
Sodium chloride	Merck, Darmstadt, Germany
Sodium dodecyl sulfate (SDS)	Sigma, Steinheim, Germany
Sucrose	Merck, Darmstadt, Germany
Tetramethylethylenediamine (TEMED)	Roth, Karlsruhe, Germany
Trishydroxymethylaminomethane (Tris)	Roth, Karlsruhe, Germany
Triton X-100	Sigma, Steinheim, Germany
Tween 20	Merck, Darmstadt, Germany
Xylene	Merck, Darmstadt, Germany

Table II. Drugs, siRNA and chemicals

2.1.3. Materials for assays

The following table shows a summary of the kits used for the respective assays done in the study. **Table III**

Material	**Supplier**
BrdU cell proliferation assay kit	Millipore GmbH, Schwalbach, Germany
Catalase assay kit	Abnova, Heidelberg, Germany
Dual luc reporter assay kit	Promega, Mannheim, Germany
Hydrogen peroxide assay kit	Cayman Chemical, Ann Arbor, USA
Human TGF-β1 immunoassay kit	R&D systems, Minneapolis, USA

Matrigel (for invasion assay)	Becton Dickinson, Franklin Lakes, USA
Pierce LDH Cytotoxicity Assay kit	Thermo Scientific, Rockford, USA
PPAR reporter luciferase kit	Qiagen Cignal PPAR Reporter, Hilden, Germany
Sircol collagen assay kit	Biocolor, Newtownabbey, UK

Table III. Materials for assays

2.1.4. Luciferase reporter plasmids and overexpression vector

The reporter and overexpression plasmids in **Table IV** below were transfected into cells to study promoter activities and downstream targets.

Plasmid	Company/Institution
Catalase overexpression plasmid	Prof. Marc Fransen (Université catholique de Louvain, Belgium), Louvain-la-Neuve, Belgium
COL1A2-luc	Dr. Eunsum Jung (BioSpectrum Life Science Institute, Korea), Gyeonggi-do, Korea
pRL-SV40 Vector	Promega, Mannheim, Germany

Table IV. Luciferase reporter plasmids and overexpression vector

2.1.5. Buffers and solutions

Table V shows the buffers and solutions, including their compositions.

Buffer/solution	Composition
Buffer/solution composition for Western Blotting	
10X Electrophoresis buffer	2 M glycin, 250 mM Tris and 1% SDS
10X TBS	0.1 M NaCl and 0.1 M Tris, pH 8.0
20X Transfer buffer	Bis-Tris-HCl buffered (pH 6.4) polyacrylamide gel, NuPAGE transfer buffer (Invitrogen, Heidelberg, Germany)
5% Blocking buffer	5% fat free milk powder in 1X TBST solution

Cell lysis buffer (IPB)	50 mM Tris, 150 mM NaCl, 1% Triton X-100 (pH 7.4), with 1% protease inhibitor mix M prior to use
Tissue homogenization buffer (HMB)	50 ml 0.25 M sucrose and 5 mM MOPS (pH 7.4) + 500 µl 100 mM EDTA + 50 µl 100% ethanol + 5 µl 2 M DTT + 50 µl 1 M aminocaproic acid and 100 µl cocktail of protease inhibitors
Resolving gel (10%)	5 ml buffer A + 1.67 ml dH_2O + 3.34 ml 30% acrylamide + 7.5 µl TEMED + 65 µl 10% APS
Resolving gel (Buffer A)	1.5 M Tris-HCl, pH 8.8 + 0.4% SDS
Sample buffer (10X)	3.55 ml dH_2O + 1.25 ml 0.5M Tris-HCl (pH 6.8) + 2.5 ml 50% (w/v) glycerol + 2.0 ml 10% (w/v) SDS + 0.05% bromophenol blue. 50 µl of 1M Dithiothreitol added to 200 µl of 10X Sample buffer before use.
12% Stacking gel (for 4 SDS-PAGE gels)	1.25 ml 30% acrylamide + 3.75 ml dH_2O + 5 ml buffer B + 15 µl TEMED + 130 µl 10% APS
Stacking gel (Buffer B)	0.5 M Tris-HCl, pH 6.8 + 0.4% SDS
Stripping buffer	10% SDS + 0.5M Tris + 500 ml dH_2O, pH 6.8. 50 ml of buffer/membrane + 350µl β-mercaptoethanol + in water-bath at 60°C for 15 min
Transfer Buffer	Bis-Tris-HCl buffered (pH 6.4) polyacrylamide gel; NuPAGE transfer buffer, Invitrogen, Heidelberg, Germany
Solutions for immunofluorescence (cells and lungs)	
10X PBS	50 mM KH_2PO_4, 131 mM K_2HPO_4, 1.5 M NaCl, pH 7.4
Anti-fading agent	2.5% N-propylgallate in 50 % glycerol + 1 X PBS
Blocking buffer for cells	1% PBSA + 0,05% Tween 20
Blocking buffer for tissues	4% BSA in 1X PBS, 0.05% Tween 20

Citrate buffer	1 mM $C_6H_8O_7.H_20$ (Buffer A) and 50 mM $C_6H_5Na_3O_7.2H_20$ (Buffer B). 0.15 mM buffer A + 8.5 mM buffer B, pH 6
Dilution buffer	1% PBSA + 0,05% Tween 20
Fixative solution	4% PFA in 1X PBS
Glycine + Triton X-100 solution	0.2% Triton X-100 in 1% glycine
Glycine solution	1% glycine in 1X PBS
Mounting medium	1 part of anti-fading agent in 3 parts of Mowiol 4-88
Mowiol 4-88 solution	16.7 % Mowiol 4-88 (w/v) in 80 ml of 1X PBS (stir overnight) followed by the addition of 40 ml of glycerol (stir overnight; centrifuge at 15,000 U/min for 1 h and store supernatant at -20°C)
Trypsin	0.1% trypsin in 1X PBS
Washing buffer	1X PBS

Table V. Buffers and solutions

2.1.6. Medium for cell culture

The composition of medium used to culture cells is shown in **Table VI** below.

Component	Supplier
10% Fetal bovine serum	PAA Laboratories, Cölbe, Germany
1% Penicillin / Streptomycin	PAN Biotech, Aidenbach, Germany
1% Puromycin	PAN Biotech, Aidenbach, Germany
DMEM, 4.5g/L D-glucose, GlutaMAX™ supplement	Thermo Fisher Scientific, Paisley, UK

Table VI. Medium composition for cell culture

2.1.7. Freezing solution

Cells were preserved in a freezing solution prepared with the components illustrated in **Table VII.**

Component	Percentage
Culture medium	70%
Dimethyl sulfoxide (DMSO)	10%
Fetal bovine serum	20%

Table VII. Composition of freezing solution

2.1.8. Primary and secondary antibodies

A summary of the antibodies used in the study are outlined in Table **VIII.** All antibodies have been well characterized and previously used for experiments in the lab.

Primary antibody against antigen	Host	Dilution IF (Cells)	Dilution IF (Tissues)	Dilution (WB)	Supplier
α- Smooth muscle actin (α-SMA)	Mouse, monoclonal	1:2000	1:2000	1:2000	Sigma, Cat. No.: A-2547, Darmstadt, Germany
Beta-actin (β-actin)	Mouse, monoclonal	-	-	1:2000	Sigma, Cat. No.: A-5316, Darmstadt, Germany
Catalase	Rabbit, polyclonal	1:50	1:50	1:200	Proteintech, Cat No.: 21260-1-AP, Rosemont, USA
Collagen I (H-197)	Rabbit, polyclonal	-	1:50	-	Santa cruz, Cat. No.: sc-28657, Heidelberg, Germany

Collagen I	Rabbit, polyclonal	1:50	1:50	1:200	Proteintech, Cat. No.: 14695-1-AP, Rosemont, USA
PEX 3p	Rat, monoclonal	1:300	-	-	Gift from Dr. Claudia Colasante (Post-doc in the lab)
Glutathione peroxidase (GPx-1/2)	Mouse, polyclonal	-	-	1:50	Santa Cruz, Cat. No.: 74498, Heidelberg, Germany
Glyceraldehyde-3-phosphate dehydrogenase (GAPDH), rabbit	Mouse, polyclonal	-	-	1:10,000	HyTest, Cat. No: 5G4, Turku, Finland,
Matrix metalloproteinase-1 (MMP1)	Rabbit, polyclonal	-	-	1:200	Proteintech, Cat. No.: 10371-2-AP, Rosemont, USA
Peroxin 13 (PEX13p), mouse	Rabbit, polyclonal	-	-	1:1,000	Gift from Denis I. Crane; School of Biomol. Biophys. Sci., Griffith Univ., Nathan, Brisbane, Australia.
Peroxin 14 (PEX14p), mouse	Rabbit, polyclonal	1:1,000	-	-	Gift from Denis I. Crane; School of Biomol. Biophys. Sci., Griffith Univ., Nathan, Brisbane, Australia.

Peroxisome proliferator-activated receptor alpha (PPAR-α)	Rabbit, polyclonal	-	-	1:100	Santa Cruz, Cat No.: sc1985, Heidelberg, Germany
Peroxisome proliferator-activated receptor beta (PPAR-β)	Rabbit, polyclonal	-	1:250	1:1000	Abiocode, Cat No.: R2295-1, Agoura Hills, USA
Peroxisome proliferator-activated receptor gamma (PPAR-γ)	Rabbit, polyclonal	-	-	1:100	Santa Cruz, Cat No.: sc-7196, Heidelberg, Germany
TGF-β1 receptor	Rabbit, polyclonal	-	-	1:500	Abcam, Cat. No.:31013, Cambridge, UK
Secondary antibody	**Host**	**Experimental type**	**Dilution**	**Supplier**	
Anti-mouse IgG-peroxidase	Goat	WB	1:10,000	Sigma, Cat. No.: A9044, Darmstadt, Germany	
Anti-Mouse-IgG Alexa Fluor 555	Donkey	IF/IHC	1:1000	Molecular Probes/Invitrogen, Cat. No: A31570	
Anti-rabbit IgG-peroxidase	Goat	WB	1:7,000	Sigma, Cat. No.: A0545, Darmstadt, Germany	
Anti-Rabbit-IgG Alexa Fluor 488	Donkey	IF/IHC	1:1000	Molecular Probes/Invitrogen, Cat. No: A21206	

Table VIII. Primary and secondary antibodies

2.1.9. Primers

Primers used for qRT-PCR are illustrated in **Table IX** below.

Table IX. Primers used for qRT-PCR

Primer	Sense primer (5'- 3')	Antisense primer (5'- 3')	Product length (bp)
HPRT1	CCTGGCGTCGTGATTAGTGAT	AGACGTTCAGTCCTGTCCATAA	131
ACTA2	CCGGGACTAAGACGGGAATC	TTACAGAGCCCAGAGCCATT	98
COL1A1	GCCAAGACGAAGACATCCC	GTTGTCGCAGACGCAGAT	107
COL1A2	GAAGGAAAGAGAGGCCCTAATG	TCCAGGAAGACCACGAGAA	96
MMP1	CTGAGAAAGAAGACAAAGGCAAG	TCATCACCTTCAGGGTTTCAG	134
MMP2	GCTGGCCTAGTGATGATGTTAG	CAGGTATTGCATGTGCTAGGT	125
MMP3	CTCGTTGCTGCTCATGAAATTG	TCAGGTCTGTGAGTGAGTGATA	100
MMP7	TCTCTGGACGGCAGCTAT	TGAGATAGTCCTGAGCCTGTT	134
MMP8	GAATCCTTGCTCATGCCTTTC	GTTGTAATTTGCGGAGGTGTT	98
MMP9	TTTGGTGTCGCGGAGCA	AAATGGGCGTCTCCCTGAAT	104

MMP10	CAGCGGACAAATACTGGAGAT	CTTAGGCTCAACTCCTGGAAAG	98
MMP11	TTGACCCTGTGAAGGTGAAG	AAGCCATGGTCAGAGGAAAG	104
MMP12	TTCCTTAGGTCTTGGCCATTC	CACGTATGTCATCAGCAGAGAG	104
MMP13	GTTTGCAGAGCGCTACCT	CCTCTAAGCCGAAGAAAGACTG	125
MMP14	GCCGACTAAGCAGAAGAAAGA	TGTCGGCTTGGAGTTAAAGG	93
MMP16	TCACATTCAGCACTGGAAGAC	CCGCAGACTGTAGCACATAAA	97
MMP17	CACCAAGTGGAACAAGAGGA	CTTGAGGGCGTAGTACATGAG	106
MMP19	GGGACTATGTGTGGACTGTATC	ATTGTGTTCGAGGCGAGTAG	117
PPARA	TCATCACGGACACGCTTTC	CATTCGATGTTCAATGCTCCAC	106
PPARD	GGGACAGTGTTGTACAGTGTTT	TCGTTGGTGCATCTGTCTTC	90
PPARG	GCAAACCCCTATTCCATGCT	AGGAATCGCTTTCTGGGTCA	72
PEX13	CCATGTAGTTGCCAGAGCAG	CATCAAGGCTAGCCAGAAGC	140
PEX14	CTGCCTTTGGCTTTGATCTC	CGTGGTGTCACGGTAGTCAA	140
ACOX1	ATTTCCTTCAGGGGAGCATC	GCCAAGTGTCACATCCTGAA	137

ACAA1	AGCTTCTCTCGGCAGTCA	CAGCACATTTCCGACACAGA	89
AGPS	AGGGGGATCGTGAGAAGGT	CCAAAGCCAAGTCTCGAATG	147
GNPAT	GTGCAGAAAAACGCCTTAGC	GGCTGGTTTTCCTATTGGTG	150
CAT	AGCAAACCGCACGCTAT	TCAGGACATCAGCTTTCTGC	97
GPX1	CATCAGGAGAACGCCAAGAA	GCACTTCTCGAAGAGCATGA	99
PRDX1	CCTAAGAAACAAGGAGGACTGG	GAGATGCCTTCATCAGCCTTTA	107
PRDX2	CAGACGCTTGTCTGAGGATTAC	TTAACAGTGATCTGGCGAAGG	108
PRDX3	TCGCACTCTTGTCAGACTTAAC	TGGACTTGGCTTGATCTTAGTG	94
PRDX4	TTACCCATTTGGCCTGGATTA	CCTTTGAGATCTGATGGGTCAA	99
PRDX5	GATTCGCTGGTGTCCATCTT	ACATTCAGGGCCTTCACTATG	86
PRDX6	CCAACCATCCCTGAAGAAGAA	GGTGTGTAGCGGAGGTATTT	95

2.2. Methods

Sample preparation and experimental procedures in this study are outlined as follows.

2.2.1. Preparation of experimental samples

The study was done with primary human lung fibroblasts isolated from human lung tissue biopsies of patients arranged for lobectomy and pneumonectomy. Additionally, paraffin embedded human donor lung samples were obtained from the central tissue bank of the University of Giessen Lung Center (UGLC) as well as human lung tissues from non-transplanted healthy donors and IPF which were further fixed in 4% depolymerized PFA in PBS for 24 h at 4°C before paraffin embedding. Cells were obtained from patients diagnosed with IPF and control patients who had no related lung fibrosis diseases. Lung tissue was acquired from patients who had agreed by written consented for their biopsies to be used for research purposes. All patients' tissue samples were provided by the Giessen DZL-biobank (Deutsches Zentrum für Lungenforschung), UGMLC (University of Giessen and Marburg Lung Center) and bleomycin-induced fibrosis mouse model from Prof. Dr. Norbert Weissmann.

2.2.2. Preparation and culture of human fibroblasts

Cryotubes containing frozen fibroblasts obtained for the study were put in Nalgene cryobox filled with isopropanol, kept in -80 °C freezer overnight and finally in liquid nitrogen for longer storage.

Before experiments, frozen primary human lung fibroblasts were thawed and cultured in Dulbecco's Modified Eagle Medium (DMEM) supplemented with the components in **Table VI** that is, 10% fetal bovine serum and 1% penicillin/streptomycin (with the exception of puromycin). Cryotubes containing the cells were brought to room temperature and transferred into 15 ml Falcon tubes. Five ml of culture medium was added and further centrifuged at 200 x g for 5 min. Cell pellets were resuspended in 2 ml of medium and pipetted into a cell culture dish (**Table I**) containing 10 ml culture medium, and placed in an incubator conditioned at 37 °C and 5% CO_2.

Medium was aspirated and cells washed with 5 ml 1X PBS when they reached 80% confluency. Cells were trypsinized with 0.25% Trypsin/EDTA for 2 min, re-suspended in culture medium, centrifuged at 500 x g, counted and seeded ($8x10^4$ cells/well or $4x10^4$ cells/well) for experiments. The rest of the suspended cells were cultured for later use. All

cells used for this study were from passages 2-10 and used for experiments at 80% confluency.

2.2.3. Lentivirus production and concentration

This procedure was carried out at the Institute of Molecular Neurooncology and Neuropathology, Justus Liebig University. The production of pGIPZ-shCatalase and pGIPZ-non silencing control lentiviruses were done as described by Filatova and colleagues [325]. The human embryonic kidney cell line, HEK293T, was used as the producer line. Calcium phosphate was used in the transfection of second generation packaging and envelope plasmids (psPAX2 and pCI-VSVG), together with lentiviral plasmids, into HEK293T cells. Supernatant containing the lentiviruses was collected over 2 days after transfection and further concentrated by centrifugation at 20,000 x g for 4 h. The virus titer was determined using fluorescence-based titration in human GBM line G55TL.

2.2.4. Generation of the catalase knockdown cell line

Control and IPF primary human lung fibroblasts were cultured in high-glucose DMEM (Gibco) containing 10% FBS (Merck). To generate a catalase knockdown, the cells were transduced at MOI 50 with pGIPZ-shCAT (GE Dharmacon) and afterwards selected with puromycin. The control lines were generated using non-silencing control lentivirus.

2.2.5. Treatment of ligands, compounds and recombinant TGF-β1

Treatments of control and IPF primary human lung fibroblasts as well as catalase knockout cell lines were done after seeding and culturing $8x10^4$ cells/well or $4x10^4$ cells/well in 12-well and 24-well plates respectively. Cells were cultured for 24 h in an incubator set at 37 °C and 5% CO_2. Primary human lung fibroblasts were serum-starved and consequently stimulated with 5 ng/ml rhTGF-β1 for 24 h. The following treatments were done with stock solutions of drugs diluted in dimethyl sulfoxide (DMSO), sterile H_2O and 98% ethanol, reference according to the experimental plan.

PPAR agonists were added for treatment after stimulating control and IPF primary human lung fibroblasts with rhTGF-β1 for 24 h. WY14643 (PPAR-α agonist) were used at 100 μM, and GW0742 (PPAR-β agonists), Rosiglitazone (PPAR-γ agonist) and Troglitazone (PPAR-γ agonist) were all used at a concentration of 10 μM.

The antagonists of PPAR-α (GW6471), PPAR-β (GSK0660) and PPAR-γ (GW9662) were treated at concentrations of 10 μM, 10 nM and 10 μM respectively. The receptors were inhibited for 24 h and 48 h following TGF-β1 stimulation of primary human lung fibroblasts.
Cells were challenged with the MMP1 inhibitor 4-aminobenzoyl-Gly-Pro-D-Leu-D-Ala hydroxamic acid at 20 μM. The dual PPAR-β and PPAR-γ agonist, STK 648389, was used at 25 μM, 50 μM and 100 μM following TGF-β1 treatments of primary human lung fibroblasts for 24 h. Aminotriazole was used at 10 mM, and hydrogen peroxide (H_2O_2) at 50 μM, 300 μM, 500 μM, 1 mM, 5 mM and 10 mM corresponding to the treatment plans.
Arachidonic acid, docosahexaenoic acid and eicosapentaenoic acid were all treated at 25 μM without or following TGF-β1 treatments of primary human lung fibroblasts for 24 h.

2.2.6. Transfection of cells with plasmids and siRNA

Knockdown of the MMP1 and catalase genes were done with siRNA (see **Table II**) using the ScreenFectA transfection reagent (InCella). Primary human lung fibroblasts were simultaneously seeded and transfected with InCella reagent according to the manufacturer's instructions.
Solutions for the transfection of cells were prepared as follows: Two separate 1.5 ml Eppendorf tubes were labeled, one for dilution buffer and transfection reagent, and the other for dilution buffer and siMMP1 or catalase siRNA. Two ul of ScreenFectA transfection reagent was added to 40 μl of dilution buffer in 1.5 ml Eppendorf tube, and further incubated at room temperature for 5 min. Forty ul of dilution buffer and 30 nmol siMMP1 or catalase siRNA were respectively added to another tube, and kept at room temperature for 5 min. The contents of the two tubes were thoroughly mixed and incubated at room temperature for 20 min. Cells were seeded in 24-well plates and the solution containing siMMP1 or catalase siRNA was added in a dropwise manner. The same procedure was concurrently followed for scramble siRNA transfection.
Each well contained in total 420 ml of cell suspension, culture medium, transfection reagent, dilution buffer and siMMP1 or catalase siRNA. Plates were gently swirled and placed in an incubator set at 37°C and 5% CO_2 for 48-72 h. Cells were challenged with 5 ng/ml rhTGF-β1 and drugs according to the experimental treatment process.
Transfection of COL1A2-luc and pRL-SV40 plasmids also followed similar routine as written above however, 1 μl of transfection reagent and 3 μg of plasmid DNAs were used. Treatments of cells were done after 24 h of transfection. One μg of catalase overexpression plasmid was transfected into cells following a similar routine.

2.2.7. Protein isolation, sample preparation and Western blotting

Treated, non-treated and/or siRNA transfected primary human lung fibroblasts were washed with phosphate buffered saline (1X PBS) and 100 µl of cell lysis buffer (IPB) (**Table V**) was added to the cell-containing wells. Plates were placed on ice and the cells were scraped off with a rubber policeman. The content of each well was collected into labeled 1.5 ml Eppendorf tubes and vortexed three times after every 10 min. The tubes were centrifuged (Biofuge Fresco, Heraeus, Germany) at 3,000 x g for 15 min at 4 °C. The supernatants were carefully pipetted into separately labelled tubes and stored in -80 °C Freezer until use.

Bleomycin-induced lung tissues from mice were snap-frozen directly after explantation and stored in liquid nitrogen until use. Lung tissues were thawed and 2 g of each sample weighed for the homogenization process. Two milliliters of freshly prepared homogenization buffer containing 1% protease inhibitor mix M (SERVA, Germany) was added to 2 g lung tissues and further homogenized with a Potter-Elvehjem homogenizer at 1,000 rpm (1 stroke, 60s). lung homogenates were centrifuged (Biofuge Fresco, Heraeus, Germany) at 2,500 x g for 3 min at 4°C and the supernatants collected for protein analysis.

Extracted protein concentrations were later measured with Bradford reagent. Two µl of protein solutions were added to 498 µl of distilled water. Five hundred µl of Bradford reagent was added to each tube and vortexed briefly. The solutions, which included a blank (no protein), were transferred into labelled electroporation cuvettes and the colour change was measured with a spectrophotometer at a wavelength of 570 nm. Readings for samples were made in duplicates in reference to a standard curve. Dilution for desired protein concentrations of all samples was later calculated.

Sample buffer (10X) (**Table V**) was added to the appropriate volumes according to the calculated protein concentrations in labeled 1.5 ml Eppendorf tubes at a ratio of 3:1 respectively. The proteins were denatured by heating the Eppendorf tubes at 95 °C for 4-5min in a Thermostat Block. Tubes were chilled on ice for 5 min and centrifuges for 5 sec. The denatured proteins and 10 µl of dual color precision plus protein Standard were loaded into identified wells, run and separated in 10% SDS-polyacrylamide resolving gels (**Table V**) using 1X electrophoresis buffer and Bio-Rad gel electrophoresis apparatus at a voltage of 110 on a PowerPac 200. A sandwich was made using blotting papers, ethanol-activated polyvinylidene membrane (PVDF) and the gel-containing proteins in 1X transfer buffer (**Table V**). A semi-dry Trans-blot apparatus was used to transfer proteins from the gel to the polyvinylidene membrane (PVDF) at 120 mA for 3 h.

Membranes were blocked in 5% non-fat milk powder in TBST for 1 h at room temperature and then incubated with primary antibodies at 4 °C overnight. Membranes were further washed in TBST 3X for 10 min and then incubated with horse radish peroxidase-linked secondary antibodies for 1 h at room temperature. A chemiluminescent substrate mixture, Clarity ™ Western ECL, was prepared at a ratio of 1:1 and incubated with membranes for 5 min and the bands visualized by the chemiluminescence and exposure on CL-X Posure™ films (**Table I)**. The exposed films were first developed with READYMATIC® developer and replenisher and further fixed with READYMATIC® fixer and replenisher.

2.2.8. Immunofluorescence on cells

Control and IPF primary human lung fibroblasts were seeded on coverslips ($4x10^4$ cells/well) in 24-well plates and treatment routines were followed according to the experimental plans. After treatments, medium was removed from wells and washed with 1X PBS. All procedures were done at room temperature. Cells were immediately fixed with 4% paraformaldehyde and 2% sucrose in PBS buffer, pH 7.4 for 20 min at RT, and washed three times with 1X PBS at 10 min interval. Fibroblasts were incubated with 1% glycine in 1X PBS for 10 min followed by 0.2% Triton X-100 in 1% glycine for another 10 min. Cells were further blocked with 1% BSA in PBS/0.05% Tween 20 for 1 h to avoid non-specific binding of antibodies. All processes were done at room temperature.

Blocked cells were incubated with primary antibodies of interest according to the concentrations stated in **Table X** and kept at 4 °C overnight in a moist chamber. The next morning, cells on coverslips were washed three times with 1X PBS at 10 min intervals. Secondary antibodies were diluted in 1X PBS and the cells on the coverslips incubated for 1 h at room temperature. Coverslips were further washed three times with 1X PBS and incubated with 1 μM Hoechst 33342 (1:1000 in PBS) at room temperature for 5 min to counterstain nuclei. Coverslips with labelled cells were embedded in Mowiol 4-88 containing N-propyl gallate as anti-bleaching agent and left for polymerization in a dark enclosure overnight. Imaging of stained cells was done with a regular fluorescence microscope (**Table I**) and then processed with Adobe Photoshop version CS5.

2.2.9. Immunofluorescence on tissue sections

Paraffin-embedded lung tissue blocks from control and IPF patients were cut into 2-3 µm thick sections with a rotation microtome (**Table I**). Cut tissue sections on objective slides were placed in an oven set at 50 °C overnight to remove the paraffin. The sections were further deparaffinized with xylene and rehydrated in decreasing gradients of ethanol, each for 3 min at room temperature. Sections were further digested with 0.01% trypsin buffer/PBS at 37 °C for 10 min and thereafter placed in citrate buffer and microwaved at 900 W for 3-5 min. The lungs after antigen retrieval were subsequently blocked with 4% PBSA for 2 h at room temperature and incubated overnight with primary antibodies of interest (**Table VIII**) at room temperature. Unbound antibodies on the sections were intermittently washed away three times with 1X PBS and thereafter, the tissues incubated with appropriate secondary antibodies (**Table VIII**) at room temperature for 1 h. After antibody labelling the lung sections were washed three times at room temperature at 5 min intervals followed by counterstaining of nuclei with TOTO-3 iodide for 10 min, also at room temperature. The sections were finally washed three times with 1X PBS and mounted on Mowiol mixed with N-propyl gallate. Images were captured with a confocal laser scanning microscope (CLSM) (**Table I)** and processed with Adobe Photoshop version CS5.

2.2.10. DHE staining for ROS detection

Control and IPF primary human lung fibroblasts were seeded on coverslips. Cells were transfected with catalase overexpression plasmids and treated according to the experimental plan. For other experiments, cells were seeded and challenged with appropriate compounds. Fibroblasts were further incubated with 5 µM dihydroethidium (DHE) in fresh culture medium at 37 °C for 30 min. To detect ROS (mainly $^{\cdot}O_2^-$) cells were washed with 1X PBS and fixed in PFA for 20 min at RT. Following fixation, cells were washed, counterstained with Hoechst 33342 for 10 min and further washed with 1X PBS. Coverslips were mounted on objective slides, images analyzed with a regular fluorescence microscope (**Table I)** and processed with Adobe Photoshop version CS5.

2.2.11. Hydrogen peroxide assay

Hydrogen peroxide released into the mediums by treated and non-treated cells was assessed using an assay kit from Cayman Chemical, following the protocol provided. Media from treated cells and controls were collected. Eighty µl of media and standards were added to separate wells in a 96-well plate. Ten µl of assay buffer and 10 µl of catalase solution were

pipetted into each labelled wells. Ten µl of enzyme reaction solution was added to each well and the fluorescence intensity of each well measured at 570nm. The concentrations of H_2O_2 were determined as follows:

H_2O_2 conc. (µM) = [corrected sample fluorescence - (y-intercept)/Slope x Dilution].

Corrected sample fluorescence represents the values obtained after subtracting average fluorescence of blank from sample readings as well as standards. All experiments were done in triplicates.

2.2.12. Catalase assay

Cells were treated, homogenized in 1X PBS and centrifuged at 14,000 rpm for 10 min. Catalase activity was determined using an assay kit purchased from Abnova, following the instructions given by the manufacturer. Ten µl of samples, controls and positive controls were pipetted into labelled wells of a flat-bottom 96-well plate. Five µl of 50 µM H_2O_2 substrate was added to each well to initiate the catalase reaction. Plates were gently tapped and incubated at RT for 30 min. Standards of 400 µM, 240 µM, 120 µM and 0 of H_2O_2 were prepared and 10 µl of each transferred into different wells. Ninety µl of reaction assay buffer was added to the standards. Hundred µl of detection reagent, comprising assay buffer, dye reagent and HRP enzyme, was added to samples, controls and standard wells. The plate was incubated for 10 min and immediately read at a wavelength of 570 nm. Catalase activity was determined using a formular outlined in the protocol given by the manufacturer as illustrated: Catalase (U/L) = [$R_{sample\ blank}$ - R_{sample}/Slope (μM^{-1}) x 30 min] x n, where $R_{sample\ blank}$ and R_{sample} represent the optical density readings of the sample blank and samples respectively. The slope was calculated from a generated standard curve and 30 min represents the time taken for the catalase reaction. The letter 'n' is the dilution factor used for the samples. All experiments were performed in triplicates.

2.2.13. Isolation of total RNA, cDNA synthesis and qRT-PCR

Total RNA was isolated from cultured control and IPF primary human lung fibroblasts after or without experimental treatments using RNAzol (**Table II**). Treatment medium was gently aspirated and 500 µl of RNAzol was added to each well. The contents were homogenized by pipetting and releasing for a few times. The homogenates were collected into labeled 1.5 ml Eppendorf tubes and 200 µl of RNase-free water was added to each tube, shook vigorously and allowed to stand for 15 min at room temperature. The tubes were centrifuged at 12,000 x g for 15 min and the supernatant carefully collected into freshly labeled 1.5 ml Eppendorf

tubes. Equal volumes of 100% isopropanol were added to the contents of the tubes and allowed to stand for 10 min at room temperature. The tubes were centrifuged at 12,000 x g for 10 min and the pellets formed in the tubes were washed twice with 500 µl of 75% ethanol (v/v) by centrifuging at 8,000 x g for 3 min, each at room temperature. Excess ethanol in the tubes was carefully removed and the pellets solubilized with RNase-free water. Tubes were vortexed for 2-5 min at room temperature and chilled on ice for measurement of total RNA concentration using a Nanodrop spectrophotometer. Tubes containing total RNAs were either stored at -80 °C for further use or the RNAs were directly reverse transcribed into cDNAs.

Synthesis of cDNA from isolated total RNA was done with the High Capacity cDNA Reverse Transcription Kit in accordance to the manufacturer's protocol. One µg of RNA was calculated using the RNA concentrations obtained from Nanodrop spectrophotometer measurements. The synthesis of cDNA included the following components and volumes: 2 µl 10X RT random primers, 0.8 µl of 25X dNTP Mix (100 mM), 2 µl 10X RT buffer, 1 µl RNase inhibitor, 1 µl MultiScribe reverse transcriptase and 3.2 µl nuclease-free water. The volume of the calculated RNA was added to the reaction mixture and the total volumes of the tubes rounded up to 20 µl using nuclease-free water. The tubes were subjected to the following cycles of temperatures and time periods in a Trio-Thermoblock: 25 °C for 10 min, 37 °C for 120 min and 85 °C for 5 min. Synthesized cDNAs were either stored at -20°C or used for qRT-PCR.

The regulation of the genes with the primers outlined in **Table IX** were investigated using SYBR™ Green PCR mix, nuclease-free water and diluted synthesized cDNAs, and the iCycler iQ5™ Real-Time PCR Detection System with the following protocol settings: initial cycle at 95 °C for 3 min, 42 cycles at 95 °C for 15 s, annealing temperature of 60 °C for 30 s, and primer extension at 72 °C for 30 s as well as 91 cycles at 50 °C - 95 °C for 10s. The cycle thresholds (Ct) above the baseline for the genes of interest were normalized with the reference gene, HPRT1, and the values for gene expression were calculated using the ΔΔCt method with the following formula: $2^{-\Delta\Delta Ct}$ (where ΔCt = Ct of target gene − Ct of reference gene).

2.2.14. Sircol collagen assay

Fibroblasts were treated in 24-well plates and the media collected for performance of the Sircol collagen assays following the instructions given by manufacturer. Two hundred µl of cold Isolation and Concentration Reagent was added to each 1.5 ml tube containing 1 ml of medium collected after experiments. The contents were thoroughly mixed by gentle inversion and placed in a tube rack in a container half-filled with ice-water mix. The setup was stored

at 4 °C overnight and then centrifuged at 15,000 x g for 10 min on the following day. The supernatant was discarded and the invisible pellets at the bottom of the tubes were mixed with 1 ml Sircol Dye Reagent. Collagen standards were also calculated from 0-50 µg, volumes pipetted and further mixed with 1 ml of Sircol Dye Reagent as well. The samples and standards were inserted into a mechanical shaker for 30 min at room temperature. The contents were further centrifuged at 15,000 x g for 10 min and the supernatant drained to expose the visible pellets. The pellets were washed with 750 µl ice-cold Acid-salt Wash Reagent 2X by centrifuging at 15,000 x g for 10 min. The fluid content of the tubes was drained followed by the addition of 250 µl of Alkali Reagent, and the tubes were vortexed to dissolve the pellets. Two hundred µl of the mixed solutions were pipetted into appropriate wells in a 96 micro well plate. The plate was read at a wavelength of 570 nm. A line of best fit was drawn with the figures obtained from measured standards and the collagen concentrations of samples extrapolated from the standard line using GraphPad prism 6.

2.2.15. Dual luciferase reporter gene assay

Plasmid transfected fibroblasts were washed with 1X PBS after treatment. One volume of Cell Lysis Reagent (Promega) was diluted in 4 volumes of sterile water and added to each well, swirled and scraped with a rubber policeman. Cell lysates were collected into 1.5 ml Eppendorf tubes, vortexed briefly and centrifuged at 13,000 x g for 30 s at room temperature. The renilla and firefly luciferase activities in each sample were measured using substrates provided by the manufacturer (**Table III**).

2.2.16. BrdU cell proliferation assay

Control and IPF primary human lung fibroblasts were seeded at $2x10^5$ cell/ml in 100 µl/well of cell culture media in 96-well tissue culture plates. Cells in some identified wells were challenged with 5 ng/ml TGF-β1 for 24 h followed by BrdU addition for 24 h. Media were aspirated from wells and 200 µl of fixing solution was added to each well for 30 min. Fixing solution was aspirated and the plate blotted dry. Wells were washed with 50 X Wash Buffer and 100 µl anti-BrdU monoclonal diluted antibody added to each well for 1 h. Wells were further washed and incubated with goat anti-mouse IgG (1:2000) at room temperature for 30 min. Plates were washed and incubated with 100 µl of TMB Peroxidase Substrate for 30 min at room temperature. Hundred µl of Stopping Solution was added to each well and the colour change measured with spectrophotometer microplate reader at 450 nm.

2.2.17. Invasion and migration assays

Primary human lung fibroblasts from IPF patients were cultured in 6-well plates and treated with PPAR-β and PPAR-γ ligands for 24 h and 48 h. Cells were trypsinized after treatment and re-suspended in DMEM (without FBS) and further in 1 mg/ml Matrigel (Beckton Dickinson). Hundred µl of suspended cells were pipetted onto the top insert of a modified Boyden chamber. Samples were incubated for 1 h at 37 °C. Six hundred µl of DMEM with 10 % FBS and 100 µl of DMEM with 1% FBS were added to the bottom of the chamber to create an FBS-gradient to stimulate cell migration. The inserts were incubated for 18-24 h at 37 °C, 5% CO_2. The medium in the lower compartment of the chamber was replaced with 600 µl 70% ethanol and incubated for 10 min at room temperature. The cells were re-hydrated by replacing the ethanol in the lower compartment with 600 µl 1X PBS for 10 min at room temperature, followed by another replacement with 600 µl of 2 µg/ml DAPI solution in PBS, for another 10 min at room temperature. The cells in the lower compartment of the chamber were washed with 1X PBS for 10 min at room temperature. Images of the upper and the lower compartments of the chamber were captured with a 5X objective of a fluorescence lamp. The PBS and medium in both parts of the chambers were aspirated. Filters were separated from the plastic parts of the chambers, placed on a glass slide with drops of mounting medium, and the slides incubated for 30 min at 37 °C overnight. Images of the filters were taken using 5x objective of a fluorescence lamp in a systematic fashion and the images analyzed for cell counts using ImageJ.

Migration was analyzed after treating primary human lung fibroblasts from IPF patients with PPAR-β and PPAR-γ ligands for 24 h and 48 h as well as control. A 20 µl pipette tip was used to scratch a line at the bottom of each well in the 24-well plate and the closure of the space monitored and quantified from 0-48 h with a 5X objective of a fluorescence lamp and pictures taken as well.

2.2.18. Human TGF-β1 Immunoassay

Control and IPF primary human lung fibroblasts were seeded at $8x10^4$ cell/ml in 24-well cell culture plates. Cells were serum-starved for 24 h and cell culture media collected for centrifugation. Cell culture supernatants were separated from the pellets and 100 µl of each sample activated with 1 N HCL for 10 minutes. Samples were neutralized with 1.2 N NaOH/0.5 HEPES. Fifty µl Assay Diluent RD1-21 was added to microplate provided by the manufacturer (R &D systems, quantikine ELISA) followed by the addition of 50 µl of activated samples, controls and standards into labeled wells. The microplate was incubated at

room temperature for 2 h and contents aspirated. Microplates were thoroughly washed with a Wash Buffer and further blotted to remove all liquids in the wells. Hundred µl of TGF-β1 Conjugate were added to each well and the plate incubated at room temperature for 2 h. Washing step was repeated as already described and 100 µl of Substrate Solution added to each well. Microplates were protected from light and incubated for 30 min at RT. Hundred µl of Stop Solution was added to each well and the colour change read at 450 nm with a microplate reader.

2.3. Statistical analyses

Graphical and image representation of data were obtained from at least three individual experiments. Analyses of data were done with ImageJ and GraphPad prism 6, and values expressed as means +/- standard error of the mean (SEM). In case differences between 2 groups were of interest, the F-test was first applied to compare their variances. When the variances were non-equal (significantly different), the Mann-Whitney U test was further used to calculate *p*-values between groups; when the variances were equal (not significantly different) the unpaired student's t-test was used to calculate p-values between groups. When differences between more than two groups were of interest, one-way and two-way ANOVA were used to check whether groups were different and the post-hoc Tukey´s multiple comparisons test was used to calculate p-values between individual groups. All probability (*p*) values are indicated in the figures as * $p \leq 0.05$, ** $p \leq 0.01$, *** $p \leq 0.001$ and **** $p \leq 0.0001$. In complex figures where multiple groups were compared with each other, significances are indicated on the top of the lines drawn between groups and those with no significant differences remained unmarked.

3. Results

One manuscript with effects of TGF-β1 on peroxisomes has been published in the first year of my doctoral thesis with me as co-author [270]. A second manuscript has been prepared with me as first author with the major part of the results from this study for submission to a high-class journal (Eistine Boateng, Barbara Ahlemeyer, Vannuruswamy Garikapati, Natalia El-Merhie, Rocio Bonilla-Martinez, Omelyan Trompak, Michael Seimetz, Gani Oruqaj, Clemens Ruppert, Bernhard Spengler, Norbert Weissmann, Andreas Günther, Srikanth Karnati and Eveline Baumgart-Vogt. Peroxisome Proliferator-activated Receptor beta/delta and Catalase modulate collagen synthesis in Idiopathic Pulmonary Fibrosis.). Moreover, in the process of literature search and database screening for this thesis, a review article was published on the targeting of PPAR-γ in the therapy of IPF (Eistine Boateng, Natalia El-Merhie, Omelyan Trompak, Srinu Tumpara, Michael Seimetz, Adrian Pilatz, Eveline Baumgart-Vogt, Srikanth Karnati, 2016. Targeting PPARγ in Lung fibroblasts: Prospects of therapeutic treatment for IPF. PVRI Chronicle 3: 2).

3.1. Characterization of markers of fibrosis in human lung tissue as well as control and IPF primary human lung fibroblasts

To study the consistency of pathological markers already described in fibrosis of the lung, the basal levels of collagen and α-SMA were investigated in lung tissues from control and IPF patients as well as isolated primary human lung fibroblasts.

3.1.1. Human lung biopsies

Immunofluorescence analyses of Collagen I and α-SMA in control and IPF lung biopsy samples showed comparatively higher levels of the proteins in IPF tissues than in control subjects (Figure 1).

Figure 1

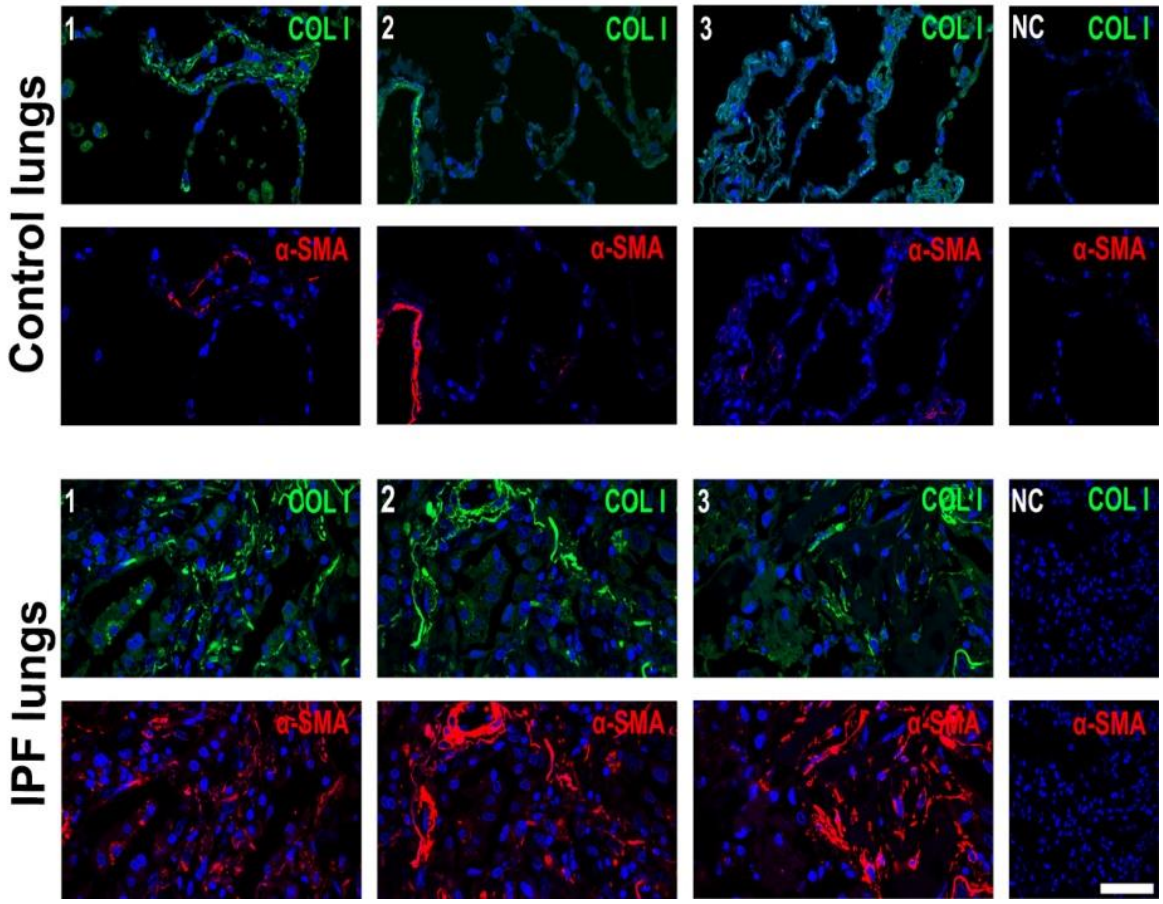

Figure 1. Relative abundance of collagen I and α-SMA in human lung biopsies.
Immunostainings for collagen I and α-SMA on formalin-fixed paraffin-embedded (FFPE) samples of 3 control and 3 IPF human lung biopsies (Scale bar: 10 μm). Data represent 3 experimental repeats.

3.1.2. Primary human lung fibroblasts

Control primary human lung fibroblasts had higher α-SMA, collagen I and TGFBR1 protein levels (Figure 2A) than IPF fibroblasts, nevertheless, extracellular collagen revealed no significant differences between the two cell groups (Figure 2B). Additionally, the levels of active TGF-β1 released by control primary human lung fibroblasts in culture media were comparatively higher than the amounts released by IPF primary human lung fibroblasts (Figure 2C).

Figure 2

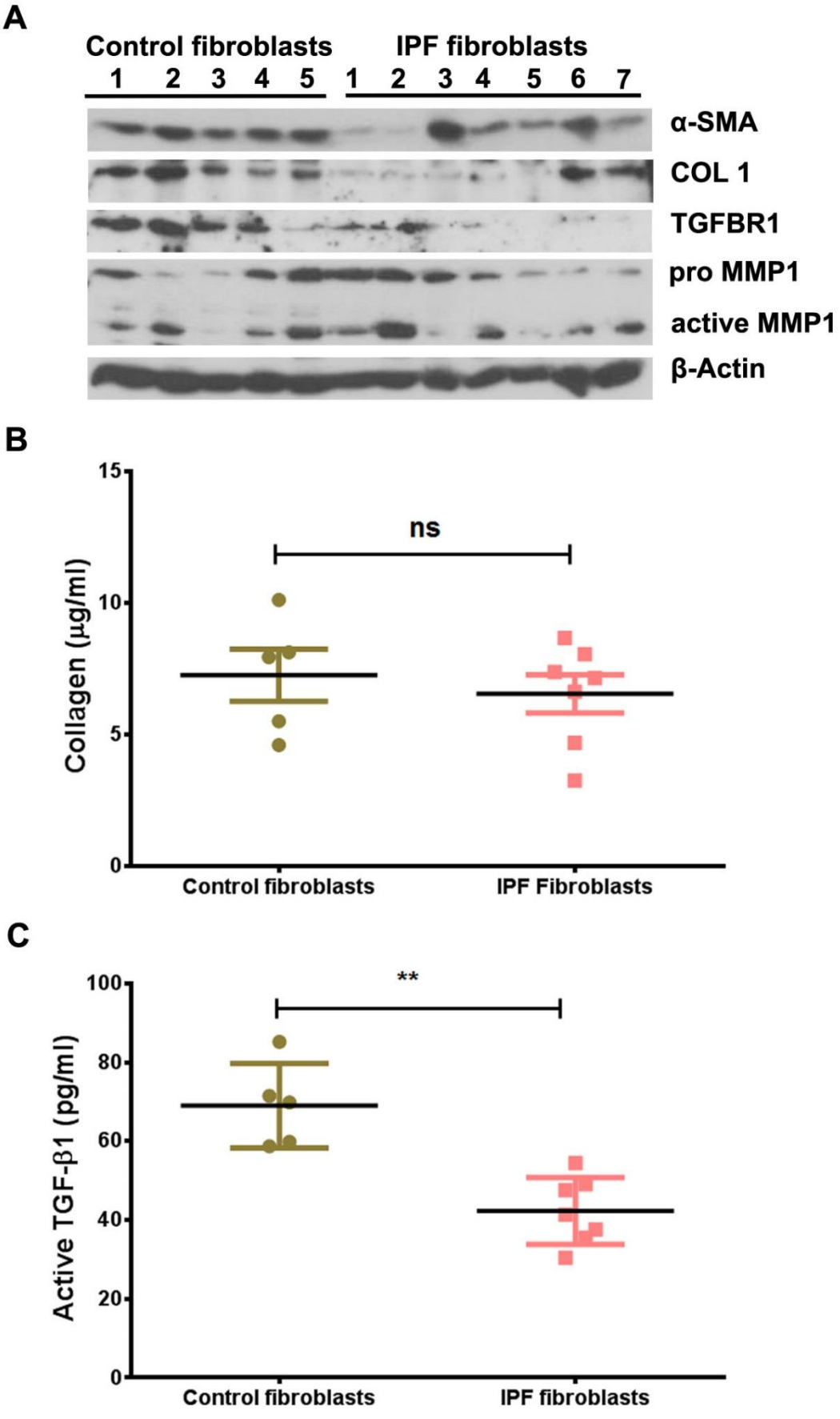
A
Control fibroblasts
IPF fibroblasts
1 2 3 4 5 1 2 3 4 5 6 7
α-SMA
COL 1
TGFBR1
pro MMP1
active MMP1
β-Actin
B
Collagen (µg/ml)
15
10
5
0
ns
Control fibroblasts
IPF Fibroblasts
C
Active TGF-β1 (pg/ml)
100
80
60
40
20
0
**
Control fibroblasts
IPF fibroblasts

Figure 2. Control primary human lung fibroblasts exhibited a higher fibrotic phenotype in culture.
(A) Immunoblotting for α-SMA, COL 1, TGFBR1, pro MMP1, active MMP1 and β-actin of 5 control and 7 IPF using homogenates of fibroblasts cultures, (n at least 3). (B) Quantification of collagen released into media by 5 control and 7 IPF primary human lung fibroblasts cultures. Mean values +/- SEM represent the collagen content in the media of cultured fibroblasts derived from control (n = 5) and IPF (n = 7) patients. Differences between the two groups were analyzed by the unpaired student´s t-test and were not significant (n.s., $p > 0.05$). (C) Immunoassay of active human TGF-β1 released into culture media by 5 controls and 7 IPF primary human lung fibroblast cultures. Mean values +/- SEM represent the active human TGF-β1 in the medium of cultured fibroblasts derived from control (n = 5) and IPF (n = 7) patients. Differences between the two groups were analyzed using the unpaired student´s t-test, $^{**}p \leq 0.01$.

3.2. Relative abundance of PPARs in human lung tissues and primary human fibroblasts and the effects of TGF-β1 on the nuclear receptors

To investigate PPAR involvement in fibrosis, all nuclear receptor proteins were first characterized in human lung tissues and isolated control and IPF primary human lung fibroblasts at basal conditions. Collectively, IPF lung samples showed increased PPAR-β/δ (Figure 3A), and IPF fibroblasts demonstrated higher levels and expressions of PPAR-α and PPAR-γ than control fibroblasts (Figure 3B and 3C). Since fibrosis is marked by elevated levels of TGF-β1 and for that matter, control and IPF primary human lung fibroblasts were challenged with recombinant human TGF-β1 to mimic the pathological condition of the disease in vitro. Interestingly, PPAR-β/δ was strongly induced after TGF-β1 stimulation in control and IPF primary human lung fibroblasts (Figure 3D), especially after 48 h, projecting a possible role of the receptor in pulmonary fibrosis. PPAR-α and PPAR-γ proteins were hardly affected under these conditions (only mildly).

3.3. TGF-β1 significantly proliferated primary human lung fibroblasts, and control fibroblasts expressed higher levels of some members of the MMP family

The proliferative abilities of the basal and TGF-β1 treated control and IPF primary human lung fibroblasts were assessed. Control primary human lung fibroblasts proliferated more than IPF fibroblasts (Figure 4A). Moreover, the proliferation of control primary human lung fibroblasts after TGF-β1 stimulation was higher compared to basal and TGF-β1 stimulated IPF primary human lung fibroblasts. Interestingly, TGF-β1 proliferated control and IPF primary human lung fibroblasts (Figure 4A). Control and IPF primary human lung fibroblasts were further characterized with regard to their expression of some selected MMPs (Matrix Metalloproteinases) since they are involved in the proteolytic degradation of collagen.

Interestingly MMP1, MMP2, MMP3, MMP8, MMP10 and MMP12 were significantly higher in control than in IPF primary human lung fibroblasts (Figure 4B, 4C, 4D, 4E, 4G and 4H). It was expected that lower expressions of MMPs might result in lower collagen degradation however; MMP1, MMP2, MMP3, MMP8, MMP10 and MMP12 might possibly not exhibit strong proteolytic degradation of collagen in primary human lung fibroblasts especially in controls.

Figure 3

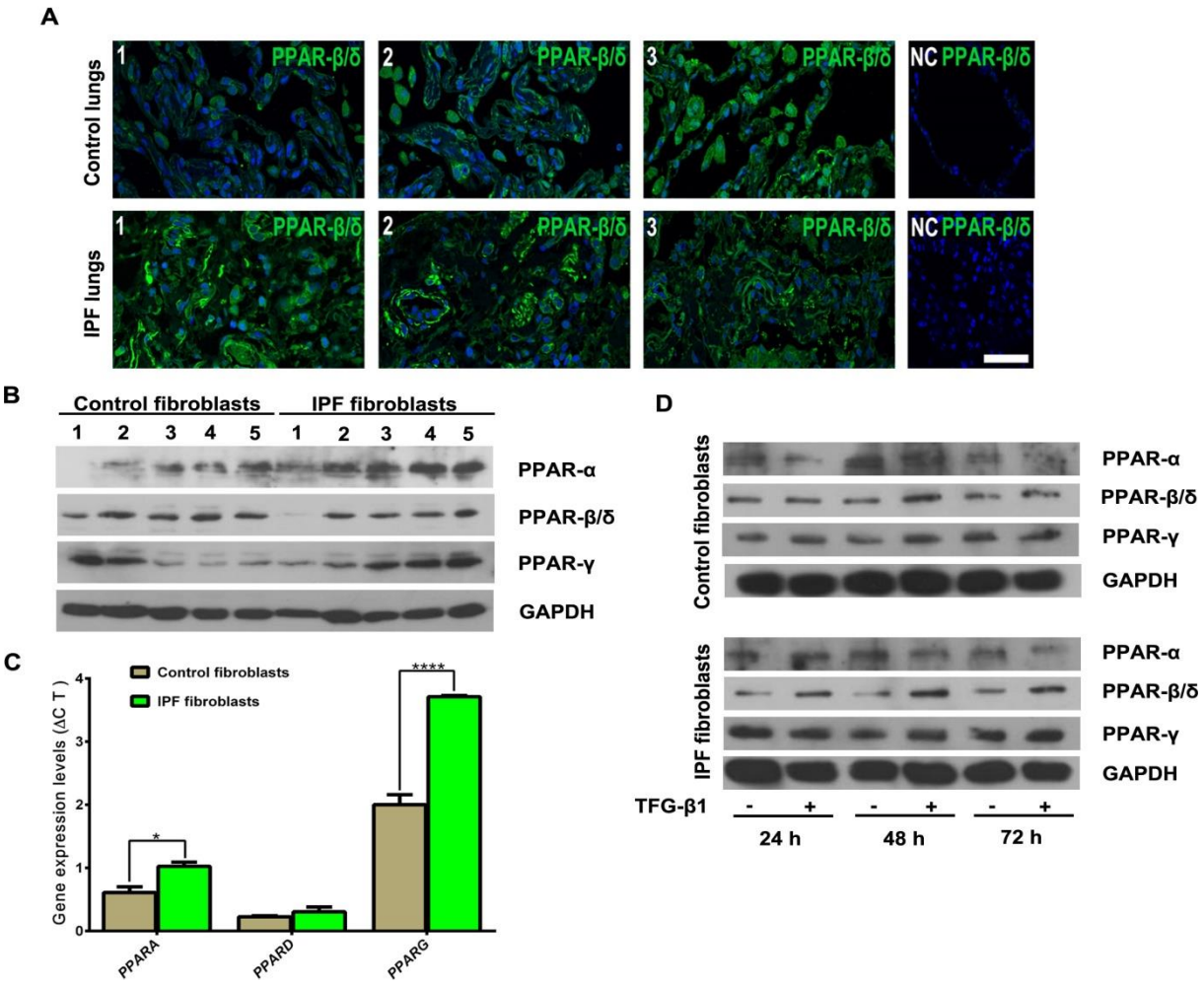

Figure 3. Relative abundance of PPARs in human lung tissues and primary human fibroblasts and the effects of TGF-β1 on the nuclear receptors.

(A) Immunostainings for PPAR-β/δ of FFPE samples of 3 control and 3 IPF human lung biopsies (Scale bar: 10 μm). NC- negative control. (B) and (C) Western blot of protein abundances and qRT-PCR of mRNA expressions of different PPARs in protein homogenates and total RNA of control and IPF primary human lung fibroblast cultures (n = 3). The unpaired student's t-test was used to analyse results of each gene in (C) and data are represented as +/- SEM with n as 3, * and **** are defined as $p \leq 0.05$ and $p \leq 0.0001$ respectively. (D) Western blots of homogenates of lung fibroblast cultures after 24 h, 48 h and 72 h of TGF-β1 (5 ng/ml) stimulation, depicting the increases of PPAR-β/δ, n = 3.

Figure 4

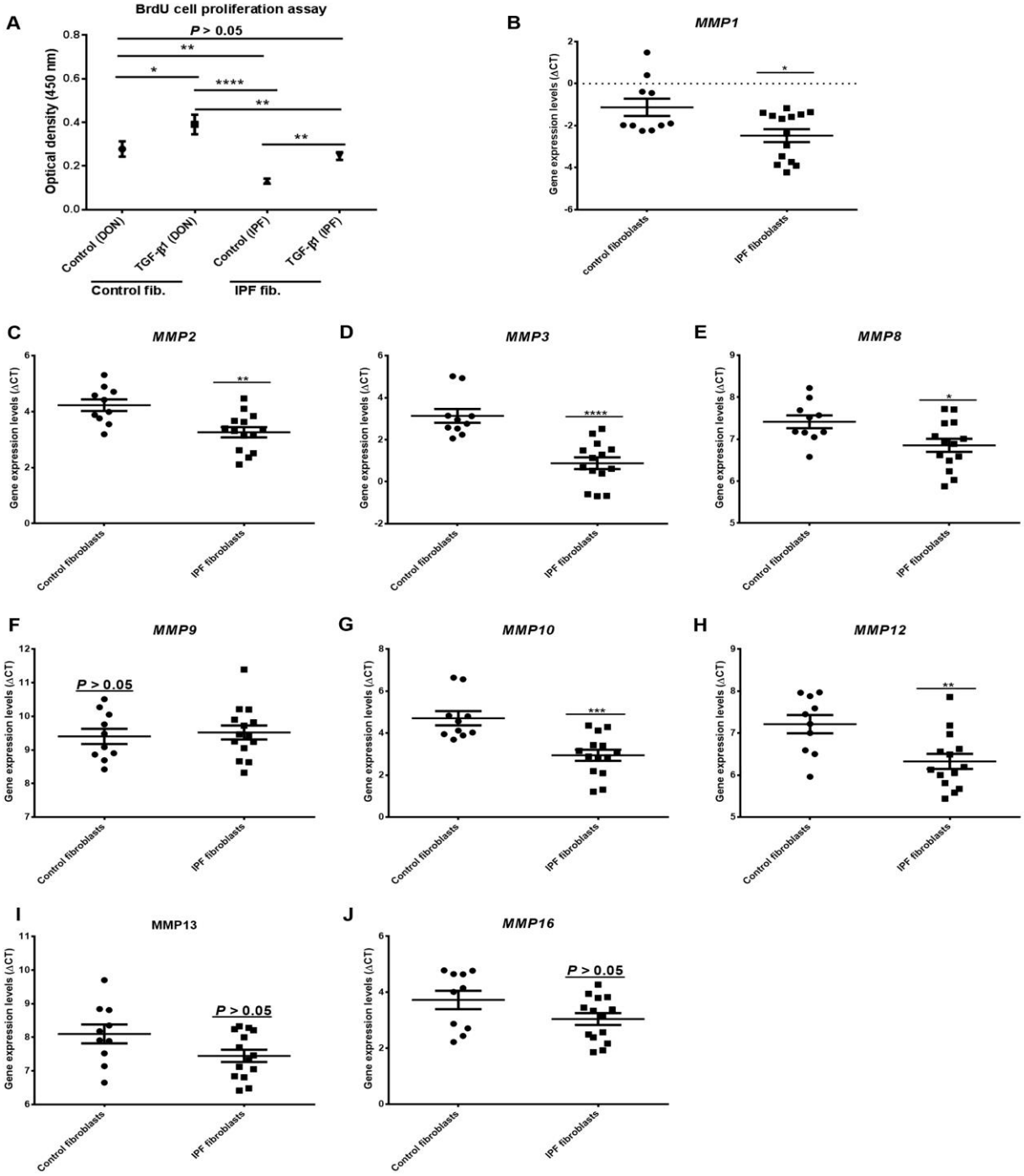

Figure 4. TGF-β1 significantly proliferated primary human lung fibroblasts, and control fibroblasts expressed higher levels of some members of the MMP family.

(A) TGF-β1 proliferated control and IPF primary human lung fibroblasts. BrdU cell proliferation assay. Groups were analyzed by two-way ANOVA, using the Tukey´s multiple comparisons test. Control fibroblasts (n = 5) and IPF fibroblasts (n = 7). (B) - (J) Gene expression profiles of selected MMPs in total RNA samples of control and IPF primary human lung fibroblasts. qRT-PCR, Ct values of genes were normalized with HPRT1. Unpaired student's t-test was used to analyse data samples of control (n = 5) and IPF (n = 7) fibroblast cultures. *, **, *** and **** are defined as $p \leq 0.05$, $p \leq 0.01$, $p \leq 0.001$ and $p \leq 0.0001$ respectively.

3.4. Activated PPAR-β/δ induces MMPs and also potentiates PPAR-α and PPAR-γ to exhibit anti-fibrotic responses

To investigate the possible reason why PPAR-β/δ is induced by TGF-β1 in our in vitro model of fibrosis, the receptor was activated with the specific exogenous ligand GW0742. Indeed, the data revealed a downregulation of α-SMA in TGF-β1 treated groups after ligand activation of PPAR-β/δ (Figure 5A). Further, to analyze whether any effect would be noted by the activation of other family members, the distinct PPARs were activated with WY14643 (PPAR-α), GW0742 (PPAR-β/δ) and rosiglitazone (PPAR-γ), as well as various combinations considering that the basal levels of PPAR-α and PPAR-γ were higher in IPF primary human lung fibroblasts. Remarkable lower abundance levels in α-SMA and collagen I were observed when PPAR-β/δ alone was activated (Figure 5B). Interestingly, PPAR-α and PPAR-γ also showed similar effects in primary human lung IPF fibroblast, however, not as strong as exhibited after PPAR-β/δ activation (Figure 5B). Combined activation of PPAR-α and PPAR-γ did not result in the downregulation of α-SMA and collagen I, but combined activation of PPAR-β/δ with either PPAR-α or PPAR-γ did (Figure 5B).

As a result, the molecular effects of activated PPARs on the modulation of collagen were analyzed in relations to MMPs (Matrix Metalloproteinases). Active MMP1 was drastically increased after PPAR-β/δ activation as well as its combined stimulation with PPAR-α or PPAR-γ (Figure 5C). Clearly, the essential receptor for the regulation of collagen I in TGF-β1 stimulated control and IPF primary human lung fibroblasts is PPAR-β/δ, and MMPs could be regulated after the activation of this receptor. In spite of this, the expressions of some selected MMPs were analyzed after ligand activation of PPAR-β/δ in TGF-β1 stimulated primary human lung fibroblasts. Interestingly, MMP1, MMP3 and MMP16 were strongly upregulated in both cell groups (Figure 5D), while MMP10 was upregulated in primary human lung IPF fibroblasts alone. Activation of PPAR-β/δ also increased the expression of MMP3 and MMP10 in IPF primary human lung fibroblasts, which are notably lower at the basal levels (Figure 4D and 4G).

Figure 5

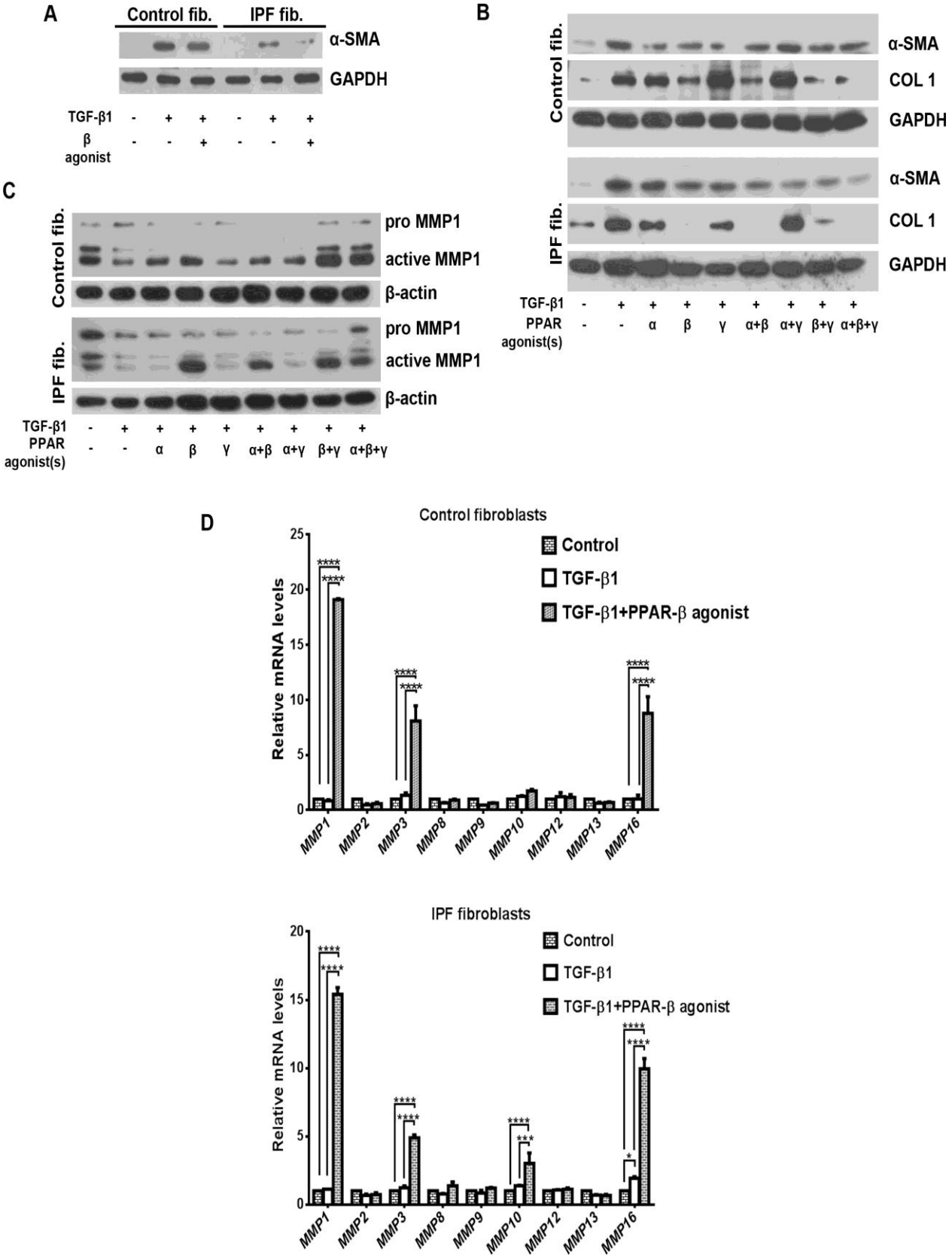
A
Control fib.
IPF fib.
α-SMA
GAPDH
TGF-β1
β agonist
B
Control fib.
IPF fib.
α-SMA
COL 1
GAPDH
TGF-β1
PPAR agonist(s)
C
Control fib.
IPF fib.
pro MMP1
active MMP1
β-actin
TGF-β1
PPAR agonist(s)
D
Control fibroblasts
IPF fibroblasts
Control
TGF-β1
TGF-β1+PPAR-β agonist
Relative mRNA levels
MMP1
MMP2
MMP3
MMP8
MMP9
MMP10
MMP12
MMP13
MMP16

Figure 5. Activated PPAR-β induces MMPs and also potentiates PPAR-α and PPAR-γ to exhibit anti-fibrotic responses.

(A) Activation of PPAR-β downregulates α-SMA in control and IPF primary human lung fibroblasts. Control and IPF primary human lung fibroblasts were seeded, and the cultures serum-starved after 80% confluency, and stimulated with TGF-β1 (5 ng/ml) for 24 h, followed by PPAR-β activation with GW0742 for another 24 h. Whole cell lysates were collected for Western blotting and protein detection. Data represent 3 experimental repeats (n = 3).

(B) PPAR-β activation regulates the degradation of collagen I. Control and IPF human lung fibroblast cultures were serum-starved, stimulated with TGF-β1 (5 ng/ml) for 24 h, followed by PPAR activation (α – WY14643, β – GW0742, γ – Rosiglitazone) for another 24 h. Whole cell lysates were collected for Western blotting and α-SMA, COL 1 and GAPDH protein detection. Data represent 3 experimental repeats (n = 3).

(C) PPAR-β upregulates MMP1 to degrade collagen I. Control and IPF primary human lung fibroblast cultures were serum-starved, stimulated with TGF-β1 (5 ng/ml) for 24 h, followed by PPAR activation with exogenous compounds for another 24 h. Whole cell lysates were collected for Western blotting to detect pro MMP1, active MMP1 and β-actin. Data represent 3 experimental repeats (n = 3).

(D) Ligand activation of PPAR-β upregulates some MMPs in control and IPF primary human lung fibroblasts. Control and IPF fibroblast cell cultures were treated with GW0742 for 24 h following TGF-β1 (5 ng/ml) stimulation for 24 h. Total RNAs were extracted for qRT-PCR analyses. Ct values of genes were normalized with HPRT1. Groups were analyzed by two-way ANOVA, using Tukey´s multiple comparisons test. *, *** and **** are defined as $p \leq 0.05$, $p \leq 0.001$ and $p \leq 0.0001$ respectively, n = 3.

3.5. Knockdown of MMP1 is compensated by other MMPs for the degradation of collagen I

The relative mRNA levels for MMP1 and MMP16 were strongly upregulated in control and IPF primary human lung fibroblasts (Figure 5D) after PPAR-β/δ activation. Since only a good MMP1 antibody was commercially available, MMP1 was silenced to ascertain whether it could play a significant role in fibrosis, relative to the other MMPs regulated via PPAR-β/δ activation. In contrast to what was expected, MMP1 knockdown decreased collagen I abundance and lead to strong compensatory regulation of MMP3, MMP10, MMP12 and MMP16 in control and IPF primary human lung fibroblasts (Figure 6B). Interestingly, though MMP3 was significantly reduced in IPF primary human lung fibroblasts compared to controls, the mRNA of the gene strongly compensated the deficiency of MMP1 in IPF primary human lung fibroblasts. Additionally, MMP7, MMP11, MMP13, MMP14 and MMP19 were also upregulated in control primary human lung fibroblasts (Figure 6B), showing heterogeneous responses from the cells after MMP1 knockdown. To prove these above-mentioned effects in control and IPF primary human lung fibroblasts and the

significance of MMPs in reversing fibrosis phenotype, a compound (4-Aminobenzoyl-Gly-Pro-D-Leu-D-Ala hydroxamic acid, Sigma-Aldrich) specific for the inhibition of multiple MMPs was used. Figure 6C (lane 6) and 6D depicted that MMPs are partly regulated by PPAR-β/δ for the modulation of fibrosis in control and IPF primary human lung fibroblasts.

3.6. The synergistic effects of PPAR-γ on PPAR-β/δ induced peroxisome biogenesis

PPAR-γ agonists have been frequently suggested as compounds for the treatment of fibrosis in the lungs and other organs. Also, activators of PPARs have been reported to induce the proliferation of peroxisomes. In order to delineate the molecular roles of peroxisomes in lung fibrosis, it was demonstrated that activated PPAR-β/δ and PPAR-γ increased peroxisome biogenesis and proliferation using PEX13p (Figure 7A) and PEX14p (Figure 7B). Combined activation of PPAR-β/δ and PPAR-γ also decreased α-SMA (Figure 7A and 7B), suggesting the reversal of the myofibroblastic phenotype in the events of peroxisome proliferation. Despite an earlier report from our group on the protective role of peroxisome proliferation prior to TGF-β1 treatment of pulmonary fibroblasts, nothing is known on the eventual positive specific stimulation of this compartment after TGF-β1 treatment. To explore this further, it was realized that there was a significant downregulation of catalase by TGF-β1 in comparison to most other mRNAs for peroxisomal markers in IPF primary human lung fibroblasts (Figure 7C). This observation set the precedent for further work.

Figure 6

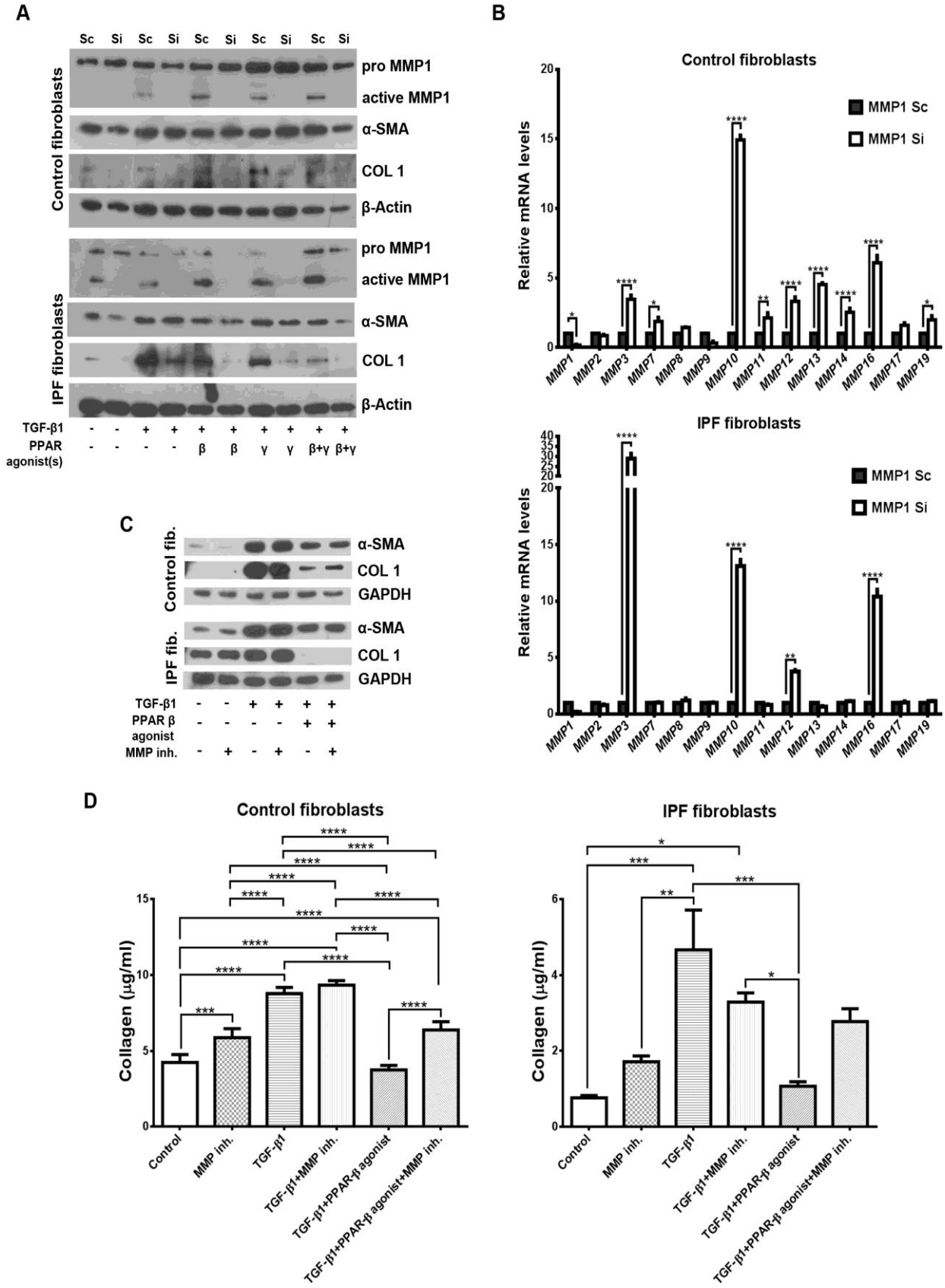
A
Sc Si Sc Si Sc Si Sc Si Sc Si
Control fibroblasts
pro MMP1
active MMP1
α-SMA
COL 1
β-Actin
IPF fibroblasts
pro MMP1
active MMP1
α-SMA
COL 1
β-Actin
TGF-β1 - - + + + + + + + +
PPAR agonist(s) - - - - β β γ γ β+γ β+γ
B
Control fibroblasts
Relative mRNA levels
MMP1 Sc
MMP1 Si
MMP1 MMP2 MMP3 MMP7 MMP8 MMP9 MMP10 MMP11 MMP12 MMP13 MMP14 MMP16 MMP17 MMP19
IPF fibroblasts
Relative mRNA levels
MMP1 Sc
MMP1 Si
MMP1 MMP2 MMP3 MMP7 MMP8 MMP9 MMP10 MMP11 MMP12 MMP13 MMP14 MMP16 MMP17 MMP19
C
Control fib.
α-SMA
COL 1
GAPDH
IPF fib.
α-SMA
COL 1
GAPDH
TGF-β1 - - + + + +
PPAR β agonist - - - - + +
MMP inh. - + - + - +
D
Control fibroblasts
Collagen (μg/ml)
Control
MMP inh.
TGF-β1
TGF-β1+MMP inh.
TGF-β1+PPAR-β agonist
TGF-β1+PPAR-β agonist+MMP inh.
IPF fibroblasts
Collagen (μg/ml)
Control
MMP inh.
TGF-β1
TGF-β1+MMP inh.
TGF-β1+PPAR-β agonist
TGF-β1+PPAR-β agonist+MMP inh.

Figure 6. Knockdown of MMP1 is compensated by other MMPs for the degradation of collagen I.
(A) and (B) Control and IPF primary human lung fibroblast cultures were stimulated with TGF-β1 (5 ng/ml) for 24 h after 72 h of transfections with MMP1 and scramble siRNAs. Cells were further treated with PPAR ligands (β – GW0742, γ – Rosiglitazone) for 24 h and protein homogenates isolated for Western blotting. Total RNAs from MMP Sc (scrambled) and MMP1 Si (siMMP1) transfected control and IPF primary human lung fibroblasts were isolated for qRT-PCR. Ct values of genes were normalized with HPRT1. Two-way ANOVA (Sidak's multiple comparisons test) was used to analyze data. *, ** and **** are defined as $p \leq 0.05$, $p \leq 0.01$ and $p \leq 0.0001$ respectively, n = 3. (C) and (D) MMPs are essential for the regulation of the fibrosis phenotype in control and IPF primary human lung fibroblasts. Control and IPF fibroblast cultures were treated with TGF-β1 (5 ng/ml) for 24 h. Cells were further treated with GW0742 and MMP inhibitor (MMP inh.) altogether for 24 h. Cell lysates were harvested for Western blotting and protein detection (n = 3), and media for Sircol collagen assays (n = 4). Groups for Sircol collagen assays were analyzed by two-way ANOVA, using Tukey´s multiple comparisons test. *, **, *** and **** are defined as $p \leq 0.05$, $p \leq 0.01$, $p \leq 0.001$ and $p \leq 0.0001$ respectively.

Figure 7

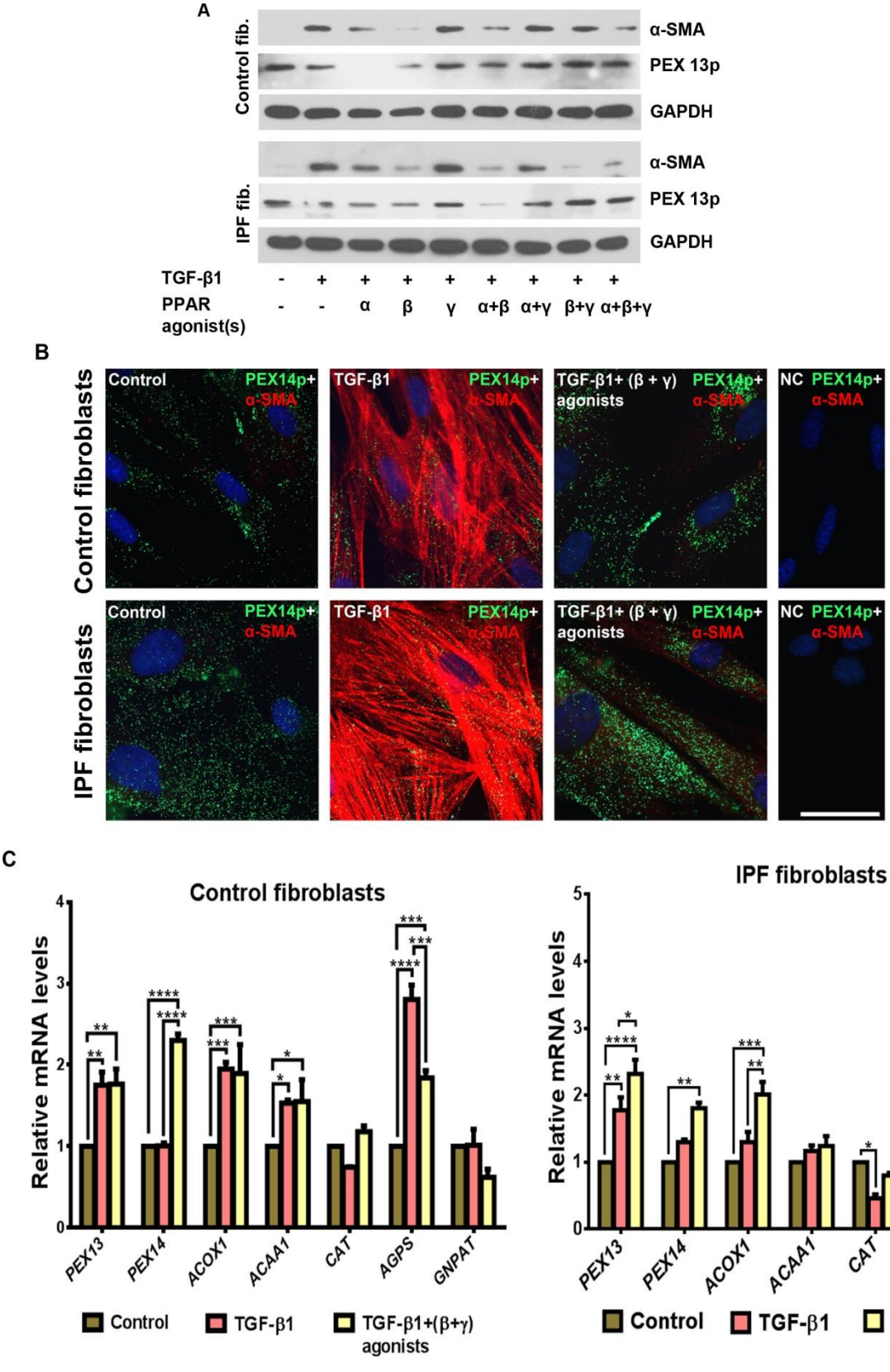
A
Control fib.
IPF fib.
α-SMA
PEX 13p
GAPDH
α-SMA
PEX 13p
GAPDH
TGF-β1 - + + + + + + + +
PPAR agonist(s) - - α β γ α+β α+γ β+γ α+β+γ
B
Control fibroblasts
IPF fibroblasts
Control PEX14p+ α-SMA
TGF-β1 PEX14p+ α-SMA
TGF-β1+ (β + γ) agonists PEX14p+ α-SMA
NC PEX14p+ α-SMA
C
Control fibroblasts
IPF fibroblasts
Relative mRNA levels
PEX13
PEX14
ACOX1
ACAA1
CAT
AGPS
GNPAT
Control
TGF-β1
TGF-β1+(β+γ) agonists

Figure 7. The synergistic effects of PPAR-γ on PPAR-β induced peroxisome biogenesis.

(A) and (B) Activation of PPAR-β in combination with PPAR-γ exhibited anti-fibrotic responses and simultaneously increased peroxisome biogenesis. Control and IPF primary human lung fibroblasts were seeded, the cultures serum-starved and challenged with TGF-β1 (5 ng/ml) for 24 h, followed by 24 h ligand activation of PPARs in the presence of TGF-β1. Total cell lysates were collected for Western blotting to detect α-SMA and PEX 13p proteins, using GAPDH as loading control. Immunofluorescence stainings for the analyses of the abundances of α-SMA and PEX14p were done after a similar treatment routine (see above) with cells cultured on cover slips (Scale bar: 10 μm). NC- negative control, data represent 3 experimental repeats (n = 3).

(C) PPAR-β in combination with PPAR-γ upregulated most mRNAs encoding peroxisomal proteins and TGF-β1 significantly downregulated catalase in IPF primary human lung fibroblasts. Control and IPF fibroblast cultures were challenged with TGF-β1 and drugs as indicated in the figure, followed by total RNA isolation for qRT-PCR analyses. Ct values of genes were normalized with HPRT1. Groups were analyzed by two-way ANOVA, using Tukey´s multiple comparisons test. *, **, *** and **** are defined as $p \leq 0.05$, $p \leq 0.01$, $p \leq 0.001$ and $p \leq 0.0001$ respectively, n = 3.

3.7. Only the simultaneous combined treatment with PPAR-γ and PPAR-β/δ activators elicited a strong anti-fibrotic response in IPF cell culture

IPF is a disease characterized by aberrant deposition of extracellular matrix into the interstitium for disruption of lung parenchyma. To investigate this aspect of the disease in vitro, the amounts of collagen released into media after treatment with the ligands were analyzed. It was interesting to note that combined simultaneous activation of PPAR-β/δ and PPAR-γ decreased endogenous and exogenous collagen compared to PPAR-γ treatment alone (Figure 8A and 8B). Nonetheless, it was not clear regarding the role of peroxisomes in pulmonary fibrosis albeit combined activation of PPAR-β/δ and PPAR-γ increased peroxisome biogenesis (Figure 8B) and most genes involved in peroxisomal fatty acid metabolism, and as well reversed the fibrosis phenotype. In contrast, TGF-β1 downregulated the peroxisomal antioxidative enzyme, catalase (Figure 7C). Interestingly, catalase is the most abundant enzyme in peroxisomes, implicating a functional role of the organelle in IPF which was further explored in this study.

Figure 8

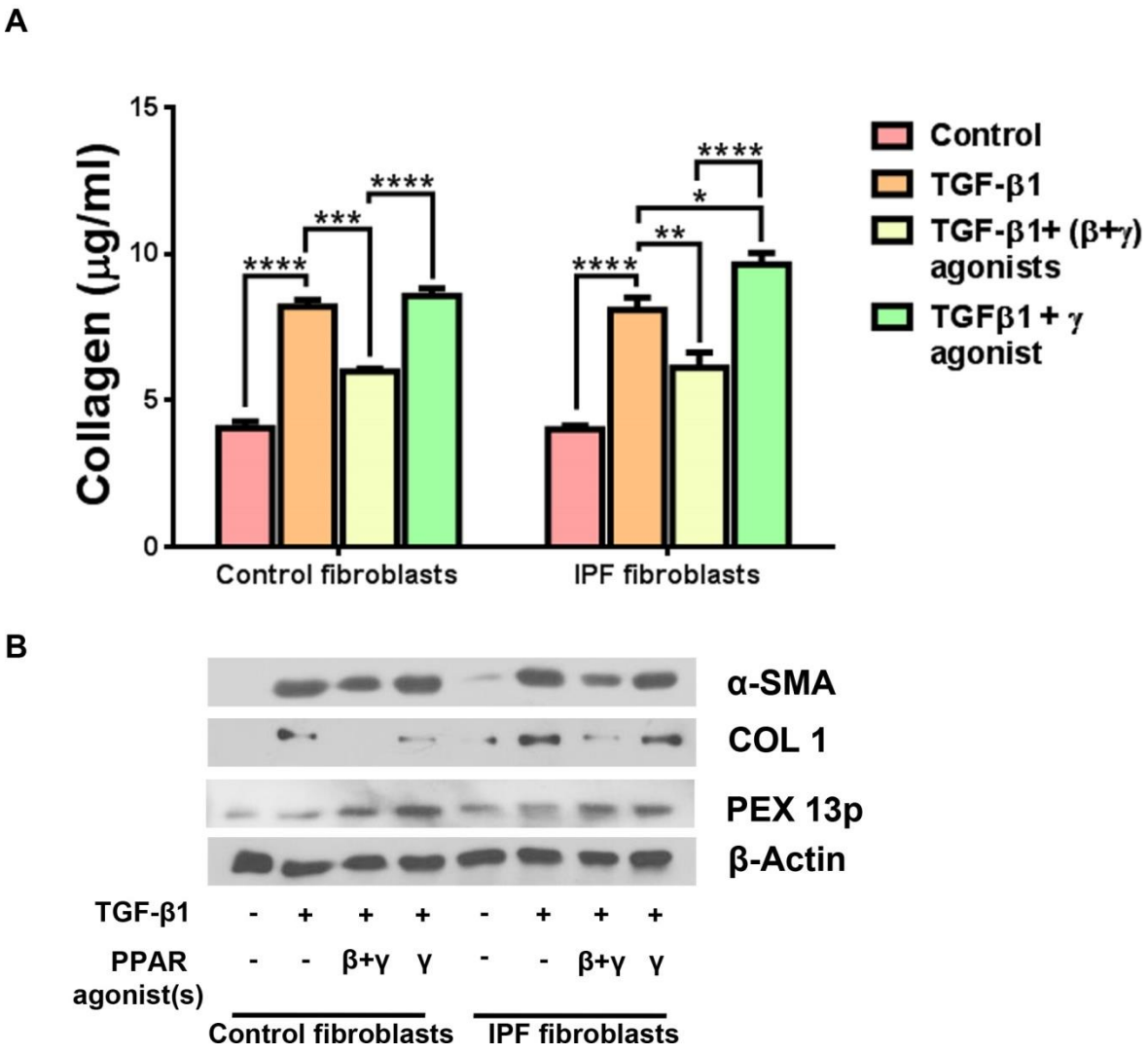

Figure 8. Only the simultaneous combined treatment with PPAR-γ and PPAR-β/δ activators elicited a strong anti-fibrotic response in IPF cell culture.

(A) and (B) Ligand activation of PPAR-β together with PPAR-γ strongly decreased the release of total collagen by TGF-β1-stimulated control and IPF primary human lung fibroblast cultures. Cells were seeded, the cultures serum-starved and treated with TGF-β1 (5 ng/ml) for 24 h before PPAR ligand treatment for another 24 h. Media were collected and analyzed for collagen content using the Sircol collagen assay (n = 4). In addition, fibroblasts were homogenized and total proteins isolated for Western blot analyses (n = 3) to detect intracellular protein levels of α-SMA, COL 1 and PEX 13p as well as β-actin as control.

(A) Groups of interest were analyzed by two-way ANOVA, using Tukey´s multiple comparisons test. *, **, *** and **** are defined as $p \leq 0.05$, $p \leq 0.01$, $p \leq 0.001$ and $p \leq 0.0001$ respectively.

3.8. The anti-fibrotic effect of activated PPAR-β/δ in combination with PPAR-γ is stable and inhibition of the receptors promoted abundance and release of collagen

Since coupled activation of PPAR-β/δ and PPAR-γ showed potential anti-fibrotic prospects under TGF-β1 stimulation and also induced peroxisome biogenesis, further experiments was done to explore whether this effect was stable over time or not. Indeed, in figure 9A a stable downregulation of collagen I and α-SMA is demonstrated in between 12 h and 48 h of treatments with PPAR-β/δ and PPAR-γ. PPAR-β/δ and PPAR-γ promote fatty acid metabolism possibly leading to peroxisome-derived endogenous activators of PPARs. It was therefore analyzed whether exogenous activation of PPAR-β/δ and PPAR-γ increased the metabolism of peroxisomal-derived lipids such as arachidonic acid (AA), docosahexaenoic acid (DHA), and eicosapentaenoic acid (EPA), which are potential endogenous activators of PPARs. Indeed, stimulation with PPAR agonists increased the synthesis of AA, DHA and EPA with PPAR-γ exhibiting strong effects on DHA (Figure 9B). The combination of both PPAR-β/δ and PPAR-γ receptor agonists in TGF-β1 treated fibroblasts induced a tremendous increase of AA, the precursor form of DHA and EPA. Additionally, AA, DHA and EPA were used to treat TGF-β1 stimulated control and IPF primary human lung fibroblasts. Interestingly, DHA downregulated collagen I and α-SMA in control and IPF primary human lung fibroblasts (Figure 9C). In a separate set of experiments, it was also discovered that, the activation of the two receptors repressed the promoter activity of COL1A2 (Figure 9D), indicating a putative PPRE (Peroxisome Proliferator-activated receptor Response Element) in this gene region, which explains the reason for the observed anti-fibrotic responses after treatments.

Figure 9

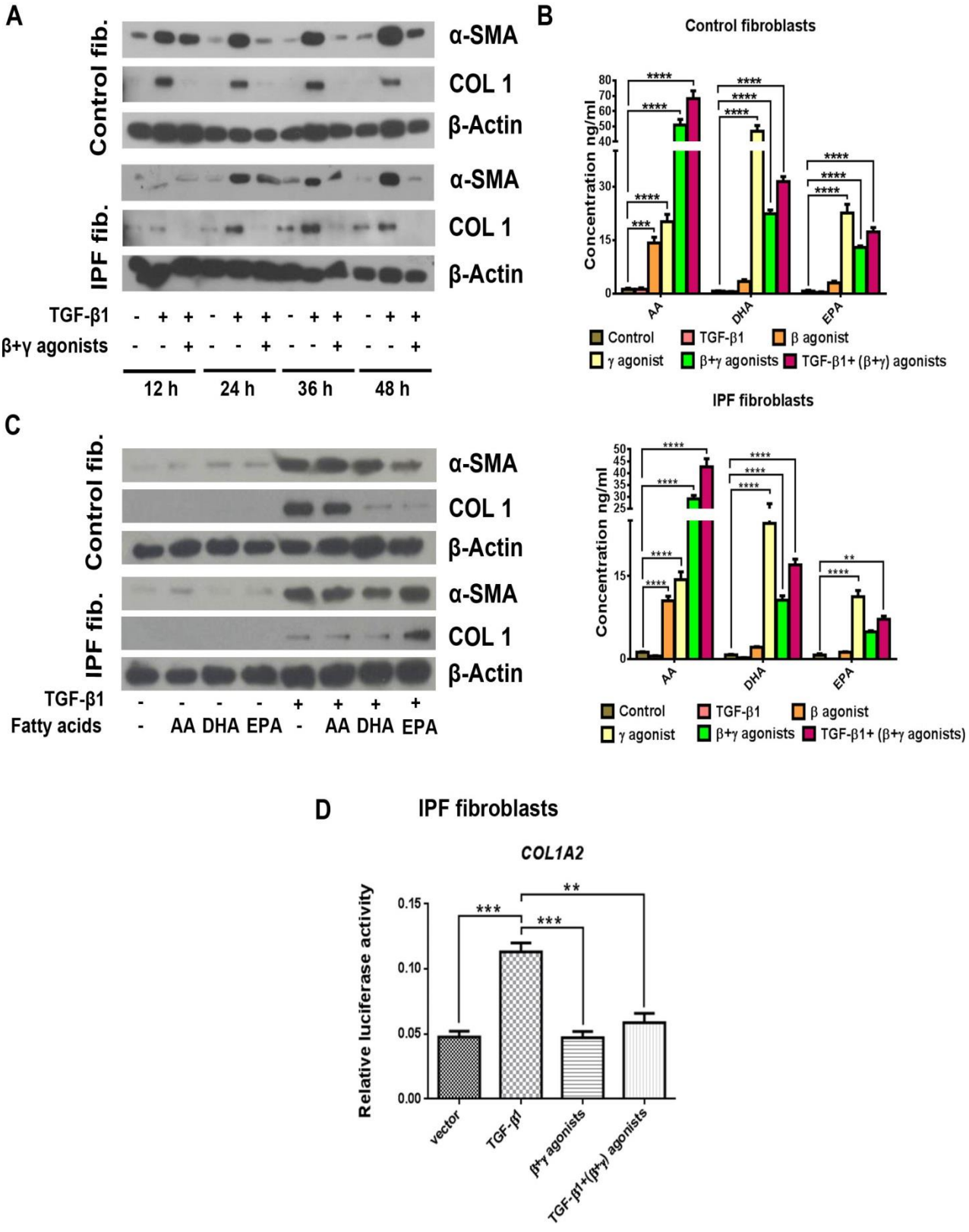
A
Control fib.
IPF fib.
α-SMA
COL 1
β-Actin
TGF-β1
β+γ agonists
12 h
24 h
36 h
48 h
B
Control fibroblasts
Concentration ng/ml
AA
DHA
EPA
Control
TGF-β1
β agonist
γ agonist
β+γ agonists
TGF-β1+ (β+γ) agonists
C
IPF fibroblasts
Fatty acids
D
IPF fibroblasts
COL1A2
Relative luciferase activity
vector
TGF-β1
β+γ agonists
TGF-β1+(β+γ) agonists

Figure 9. The anti-fibrotic effect of activated PPAR-β in combination with PPAR-γ is stable, and inhibitions of the receptors promoted abundance and release of collagen.

(A) Reversal of fibrosis phenotype by PPAR-β and PPAR-γ activation is stable. Control and IPF primary human lung fibroblast cultures were serum-starved after 80% confluency, treated with TGF-β1 (5 ng/ml) for 24 h, followed by simultaneous PPAR-β and -γ activation for 12 h – 48 h in the presence of TGF-β1. Total proteins were isolated for Western blotting and α-SMA, COL 1 and β-actin proteins detection (n = 3).

(B) Stability of anti-fibrotic properties of activated PPAR-β and PPAR-γ may be due to feedback response to synthesized lipids, which are natural activators of the receptors. Cells were serum-starved and treated with different PPAR ligands following 24 h stimulation with TGF-β1 or without TGF-β1 stimulation. Fibroblasts were also treated with TGF-β1 for 72 h. Media were collected after 48 h of different PPARs activation for fatty acid analyses of arachidonic (AA), docosahexaenoic (DHA), and eicosapentaenoic (EPA) acids. Groups of interest were analyzed by two-way ANOVA, using Tukey´s multiple comparisons test. **, *** and **** are defined as $p \leq 0.01$, $p \leq 0.001$ and $p \leq 0.0001$ respectively, n = 3.

(C) Docosahexaenoic acid (DHA) elicits anti-fibrotic responses in lung fibroblasts. Control and IPF fibroblast cultures were serum-starved and treated with or without TGF-β1 (5 ng/ml). AA, DHA and EPA were used for treatment following TGF-β1 stimulation and total cell lysates were collected for Western blotting and protein detections of α-SMA, COL 1 and β-actin as control (n = 3).

(D) Activated PPAR-β and PPAR-γ repressed the promoter of COL1A2 dual luciferase assays. IPF primary human lung fibroblasts were transfected with a COL1A2 promoter firefly luciferase reporter plasmid and a Renilla luciferase control plasmid for 72 h, serum-starved and treated with PPAR ligands alone or following TGF-β1 (5 ng/ml) stimulation for 24 h. Control and IPF fibroblast cultures were lysed and collected for luciferase activity measurements. Firefly luciferase values were normalized with values of Renilla luciferase activity plasmids. Groups were analyzed by one-way ANOVA, using Tukey´s multiple comparisons test. * and ** are defined as $p \leq 0.05$ and $p \leq 0.01$ respectively, n = 3.

3.9. Simultaneous combination of PPAR-β/δ and PPAR-γ inhibitors (antagonists) resulted in increased intracellular and extracellular collagen levels

Combined inhibitions of PPAR-β/δ and PPAR-γ were effective after 48 h of treatments and results showed remarkable increase in collagen I and α-SMA in IPF primary human lung fibroblasts at that point (Figure 10A, lanes 6). Further, re-activation of the inhibited receptors rescued the effects of the antagonists (Figure 10A and 10B). The pattern of extracellular collagen modulation after treatments conformed to the endogenous regulation of collagen I in the cells (Figure 10B). This is the first report that has explicitly explained the effects of the two receptors in pulmonary fibrosis. However, a dual agonist for PPAR-β/δ and PPAR-γ (V6) (Figure 10C) revealed only anti-fibrotic responses intracellularly (Figure 10D), but could not inhibit the release of extracellular collagen (Figure 10E). The results connote the importance of investigating the extracellular matrix in all in-vitro experimental IPF studies.

Figure 10

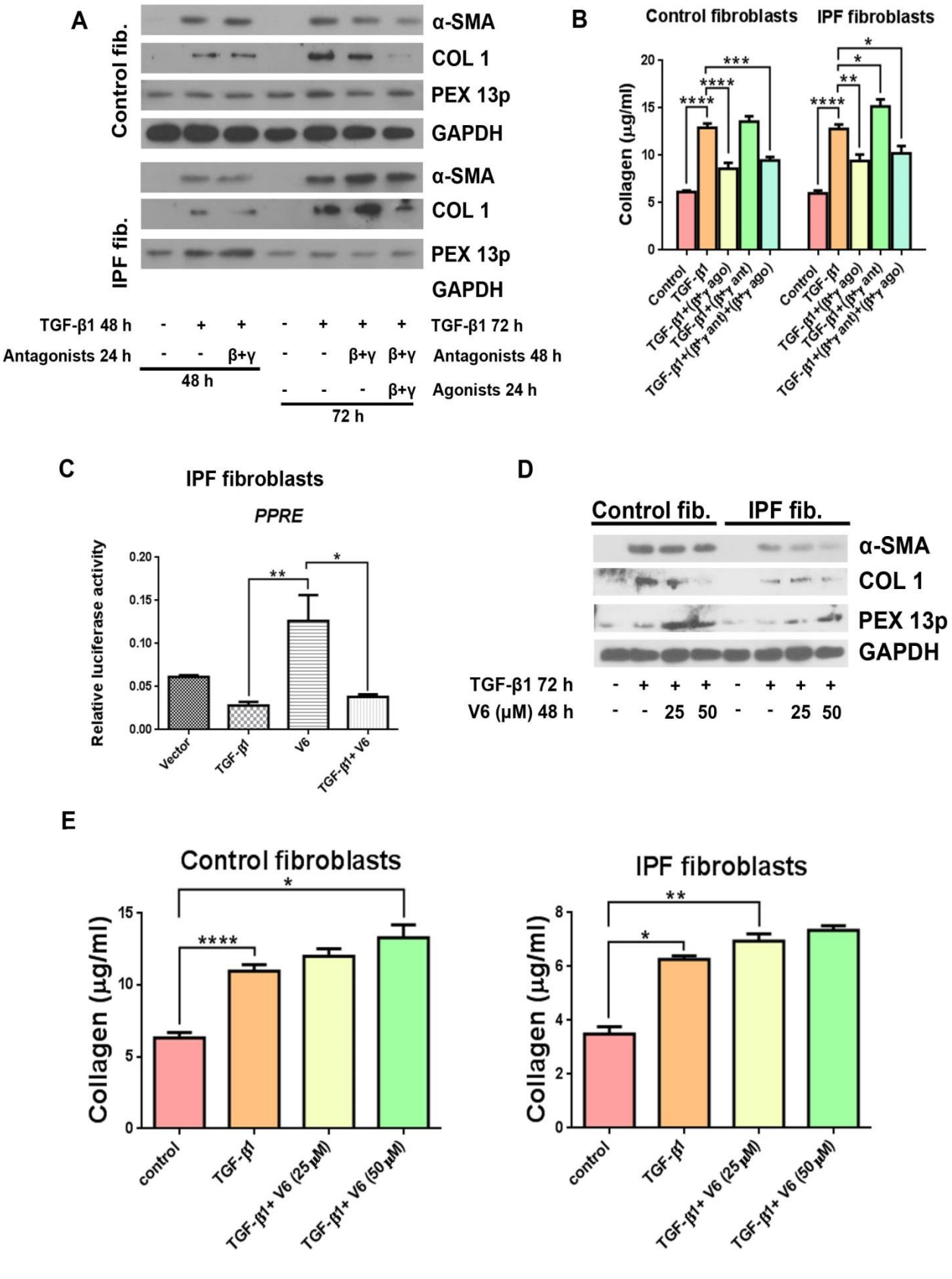
A
Control fib.
IPF fib.
α-SMA
COL 1
PEX 13p
GAPDH
TGF-β1 48 h
Antagonists 24 h
48 h
TGF-β1 72 h
Antagonists 48 h
Agonists 24 h
72 h
B
Control fibroblasts
IPF fibroblasts
Collagen (µg/ml)
Control
TGF-β1
TGF-β1+(β*γ ago)
TGF-β1+(β*γ ant)
TGF-β1+(β*γ ant)+(β*γ ago)
C
IPF fibroblasts
PPRE
Relative luciferase activity
Vector
TGF-β1
V6
TGF-β1+ V6
D
Control fib.
IPF fib.
α-SMA
COL 1
PEX 13p
GAPDH
TGF-β1 72 h
V6 (µM) 48 h
E
Control fibroblasts
IPF fibroblasts
Collagen (µg/ml)
control
TGF-β1
TGF-β1+ V6 (25µM)
TGF-β1+ V6 (50µM)

Figure 10. Simultaneous combination of PPAR-β/δ and PPAR-γ inhibitors (antagonists) resulted in increased intracellular and extracellular collagen levels.

(A) Inhibitions of PPAR-β and PPAR-γ increased the fibrosis phenotype in IPF primary cultures of human lung fibroblasts after 48 h and the effects were rescued in both cell types (control and IPF samples) following receptor reactivation. Control and IPF primary human lung fibroblast cultures were serum-starved and further challenged with TGF-β1. PPAR-β and PPAR-γ were first, simultaneously inhibited for 24 h and 48 h, and further activated for 24 h (lane 7) with specific ligands and inhibitors. Cell lysates were collected for Western blotting and protein detection (n = 3).

(B) PPAR-β and PPAR-γ antagonists stimulate the release of collagen from control and IPF primary human lung fibroblast cultures. Sircol assay analyses of collagen released into media after 72 h of TGF-β1 stimulation alone, 48 h of combined agonists and combined antagonist treatments following TGF-β1 stimulation for 24 h and, TGF-β1 stimulation for 24 h followed by 24 h antagonist treatments and combined further for 24 h with different agonist treatments. Groups of interest were analyzed by two-way ANOVA, using Tukey´s multiple comparisons test. *, **, *** and **** are defined as $p \leq 0.05$, $p \leq 0.01$, $p \leq 0.001$ and $p \leq 0.0001$ respectively, n = 4.

(C), (D) and (E) The putative commercially obtained dual PPAR-β and PPAR-γ agonist (V6, a synthetic molecule) enhances PPRE activity but is not anti-fibrotic. IPF primary human lung fibroblasts were transfected with the PPRE promoter firefly luciferase reporter plasmid and the Renilla luciferase plasmid for 72 h, serum-starved and treated with V6 and TGF-β1 or both. Cells were lysed and collected for luciferase activity measurements (C). Firefly luciferase values were normalized with values of Renilla luciferase. Similar treatment routines were followed for (D) and (E) as indicated in the figure and total cell lysates and media collected for immunoblotting and Sircol collagen assays respectively. Groups of interest for (C) and (E) were analyzed by one-way ANOVA, using Tukey´s multiple comparisons test. *, ** and **** are defined as $p \leq 0.05$, $p \leq 0.01$ and $p \leq 0.0001$ respectively. n = 3 (C) and n = 4 (E).

3.10. Combined activation of PPAR-β and PPAR-γ decreased the migration and invasion of IPF primary human lung fibroblasts

During the pathogenesis of fibrosis, fibroblasts are known to migrate from resident and other parts of the lungs to the wound healing site to contribute to the repair process. In view of this, inhibition of fibroblast migration could be beneficial as TGF-β1 induces fibroblast recruitment in fibrosis. Nevertheless, it is not known whether the migration process is progressive or limited at a certain stage of the disease only. IPF primary human lung fibroblasts were used in this part of the study and it was interesting that the simultaneous combined activation of PPAR-β and PPAR-γ decreased the migration of the cells after 24 h and 48 h (Figure 11A). Moreover, the combined activation of the receptors elicited a significant decrease in fibroblast invasion after 48 h (Figure 11B). Contrarily, the inhibition of

the receptors significantly increased invasion of IPF primary human lung fibroblasts after 48 h (Figure 11B).

Figure 11

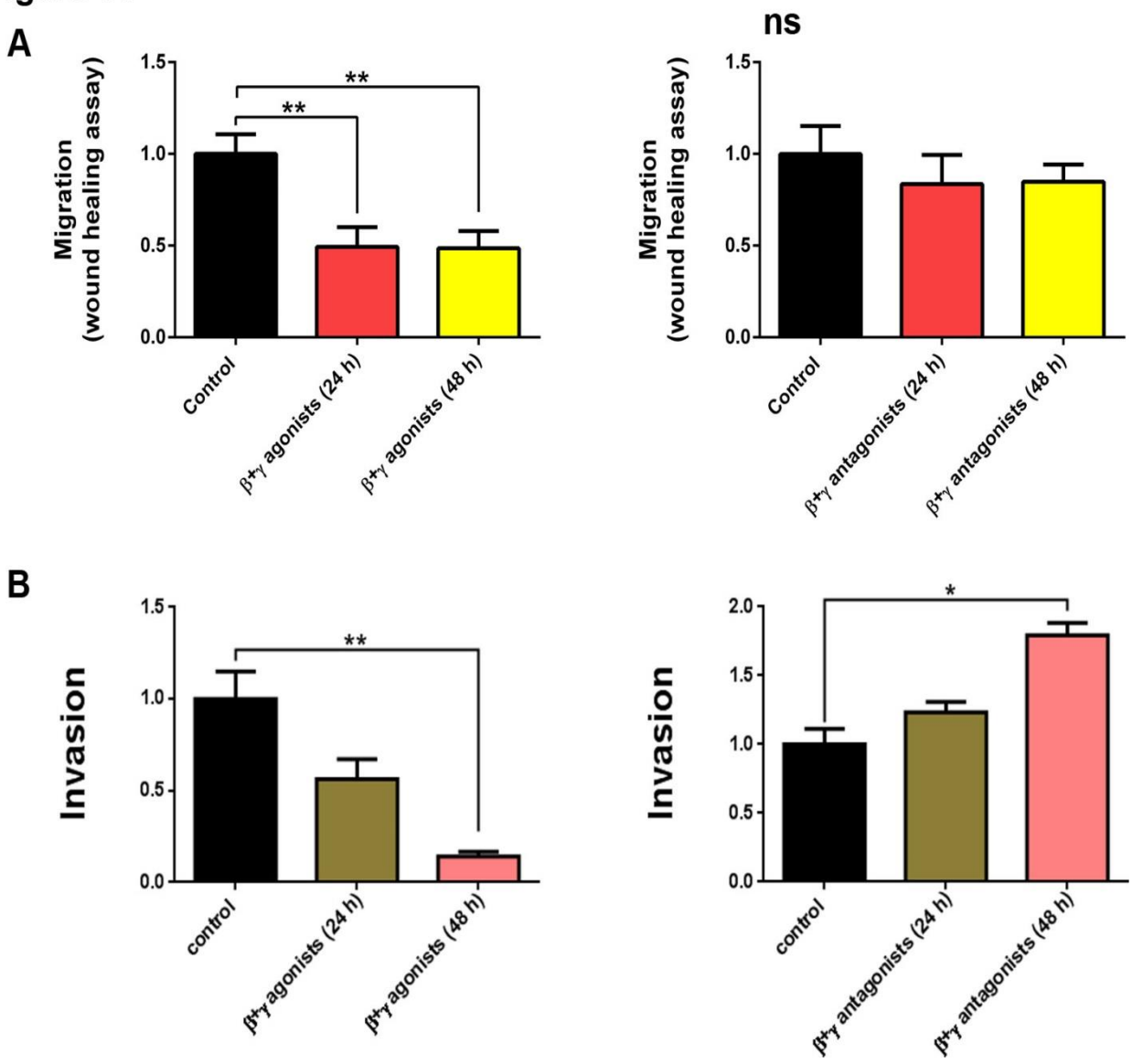

Figure 11. Combined activation of PPAR-β and PPAR-γ decreased the migration and invasion of IPF primary human lung fibroblasts.

(A) and (B) Migration and invasion assays of IPF primary human lung fibroblasts after treatments with PPAR agonists and antagonists. IPF cells were seeded, the cultures serum-starved and treated with ligands and inhibitors in 6-well plates. Cells in culture plates were directly used for migration assays and those for invasion assays were trypsinized and further assessed for invasion. Groups were analyzed by one-way ANOVA, using Tukey´s multiple comparisons test. * and ** are defined as $p \leq 0.05$ and $p \leq 0.01$ respectively, ns- not significant. Migration assay; PPAR agonists (n = 8) and PPAR antagonists (n = 6), Invasion assay; PPAR agonists (n = 4), PPAR antagonists (n = 3).

3.11. TGF-β1 downregulates catalase to trigger the progression of fibrosis

Since figure 7C showed that TGFβ1 downregulated catalase, we hypothesized that this decrease might lead to the progression of fibrosis. Time-point and concentration dependent treatments of control and IPF primary human lung fibroblasts with TGF-β1 supported this claim (Figure 12A and 12C). The modulation of collagen I protein in response to increasing concentrations of TGF-β1 was endogenously independent of the treatment groups (Figure 12C) however; the extracellular collagen analyzed from media was markedly increased but showed no significant differences between treatment groups (Figure 12C). The activity of catalase, after TGF-β1 stimulation of cells revealed gradual decreases with increasing concentrations of the recombinant cytokine, notably in IPF fibroblasts (Figure 12D). Former hypotheses directly linked increasing concentrations of TGF-β1 to collagen synthesis in fibrosis, notwithstanding the fact that the observed regulatory effects of TGF-β1 on catalase could also provide another paradigm in understanding the pathophysiology of fibrosis is essential.

3.12. Catalase was downregulated in human lungs and primary fibroblasts, and Bleomycin administration decreased catalase in mouse lungs

Furthermore, in this study, catalase was markedly decreased in IPF primary human lung fibroblasts and tissues compared to controls (Figure 13A and 13B, refer to page 72) with macrophages and alveolar epithelial type II cells expressing more of the protein. Bleomycin-induced mouse lungs also showed gradual decreases in catalase with a downregulation visible already at day 7 and more pronounced reduction between days 14 to 28 (Figure 13C). Glutathione peroxidase 1 and 2 compensated for catalase deficiency in human IPF lungs (Figure 13D) though the proteins were abundant in marcrophages and alveolar epithelial type II cells. Additionally, Figure 13E also showed a decrease in peroxisomal early biogenesis by reduced PEX 3p in IPF primary human lung fibroblasts.

Genes of peroxiredoxins 1, 4, 5 (*PRDX 1, 4, 5*) were significantly downregulated and the others (PRDX 2, 3 and 6) showed a tendency to decrease in IPF primary human lung fibroblasts (Figure 13F). The collected evidence suggests a dysregulation of catalase and other anti-oxidative proteins and genes for H_2O_2 degradation.

Figure 12

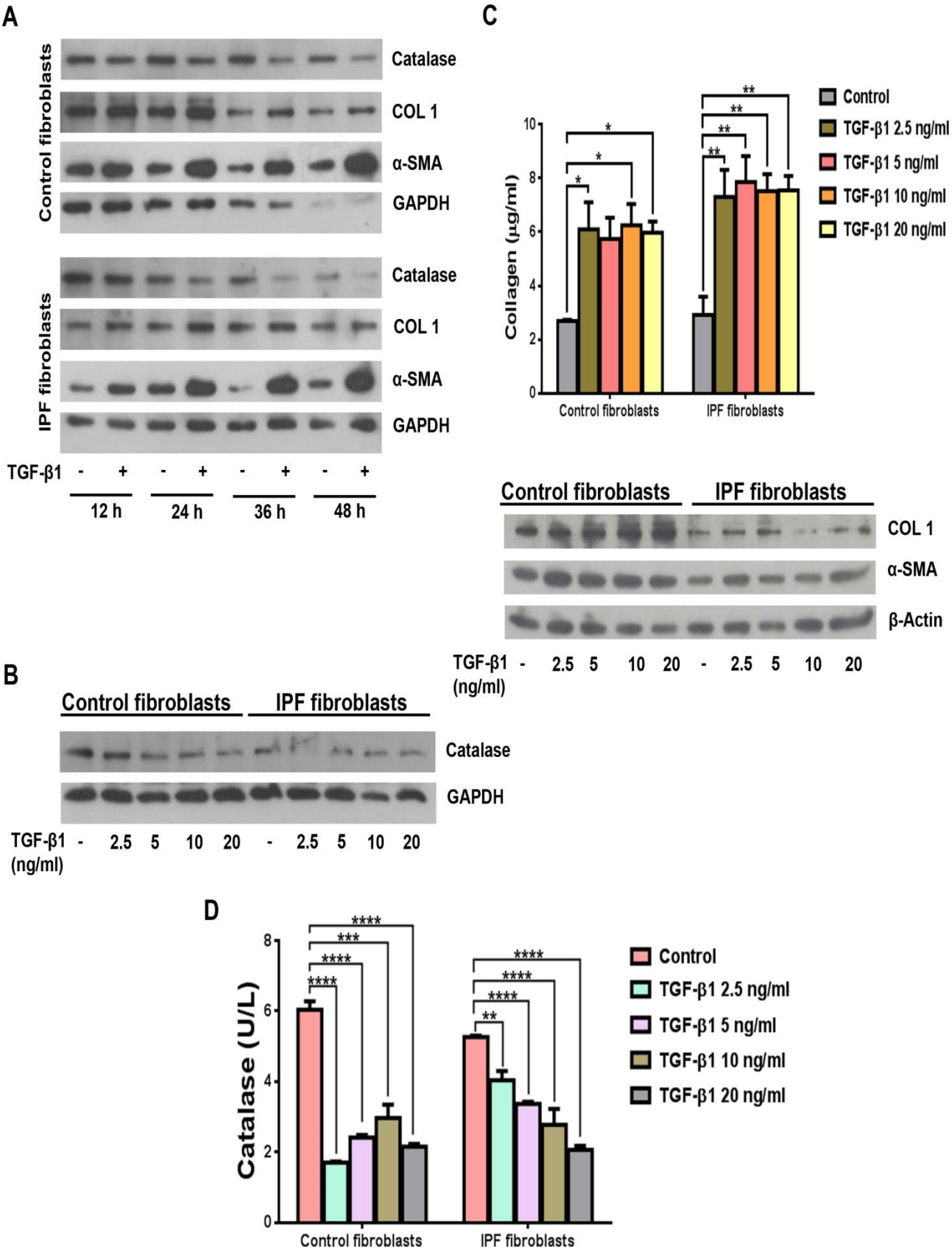
A
Control fibroblasts
Catalase
COL 1
α-SMA
GAPDH
IPF fibroblasts
Catalase
COL 1
α-SMA
GAPDH
TGF-β1 - + - + - + - +
12 h
24 h
36 h
48 h
C
Collagen (μg/ml)
Control
TGF-β1 2.5 ng/ml
TGF-β1 5 ng/ml
TGF-β1 10 ng/ml
TGF-β1 20 ng/ml
Control fibroblasts
IPF fibroblasts
Control fibroblasts
IPF fibroblasts
COL 1
α-SMA
β-Actin
TGF-β1 (ng/ml) - 2.5 5 10 20 - 2.5 5 10 20
B
Control fibroblasts
IPF fibroblasts
Catalase
GAPDH
TGF-β1 (ng/ml) - 2.5 5 10 20 - 2.5 5 10 20
D
Catalase (U/L)
Control
TGF-β1 2.5 ng/ml
TGF-β1 5 ng/ml
TGF-β1 10 ng/ml
TGF-β1 20 ng/ml
Control fibroblasts
IPF fibroblasts

Figure 12. TGF-β1 downregulates catalase to trigger the progression of fibrosis.

(A) and (B) TGF-β1 downregulates catalase in a time and concentration dependent manner. Control and IPF primary human lung fibroblasts were seeded, the cultures serum-starved and treated with 5 ng/ml TGF-β1 at different time points (A) and various concentrations for 48 h (B). Cell lysates were used for Western blotting. Data represent 3 experimental repeats (n = 3).

(C) The release of collagen into culture media by TGF-β1 stimulated primary human lung fibroblasts is independent of the concentration of the treatment compound. (n = 3).

(D) Catalase activity might be directly related to the regulation of collagen. Control and IPF primary fibroblast cultures were serum-starved and treated with various concentrations of TGF-β1. Cells were collected in 1X PBS, homogenized and measured for catalase activity, n = 3.

Groups of interest were analyzed by two-way ANOVA (C) and (D), using Tukey´s multiple comparisons test. *, **, *** and **** are defined as $p \leq 0.05$, $p \leq 0.01$, $p \leq 0.001$ and $p \leq 0.0001$ respectively.

Figure 13

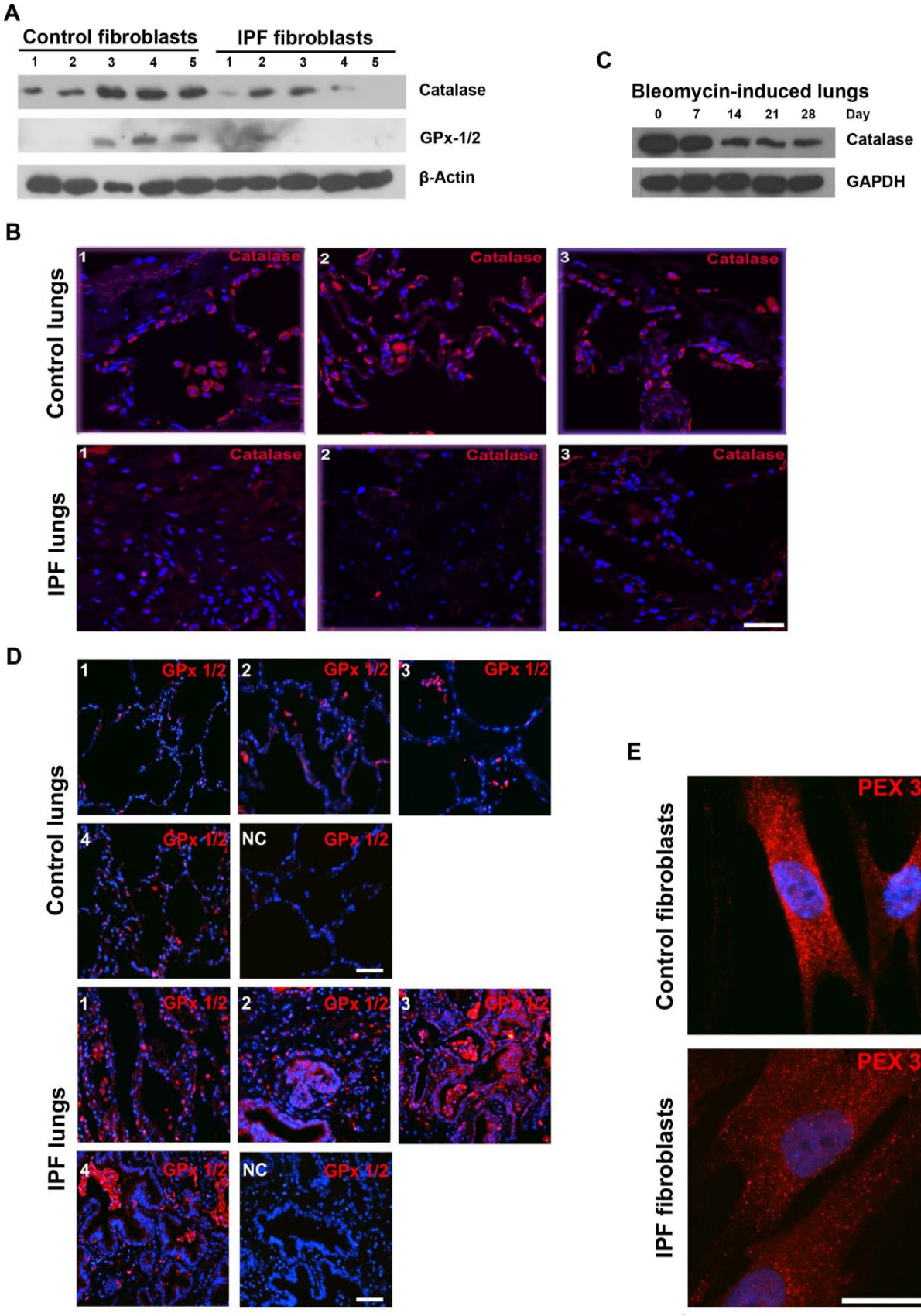
A
Control fibroblasts
IPF fibroblasts
1 2 3 4 5 1 2 3 4 5
Catalase
GPx-1/2
β-Actin
C
Bleomycin-induced lungs
0 7 14 21 28 Day
Catalase
GAPDH
B
Control lungs
IPF lungs
1 Catalase
2 Catalase
3 Catalase
D
GPx 1/2
4 GPx 1/2
NC GPx 1/2
E
PEX 3p
Control fibroblasts
IPF fibroblasts

F

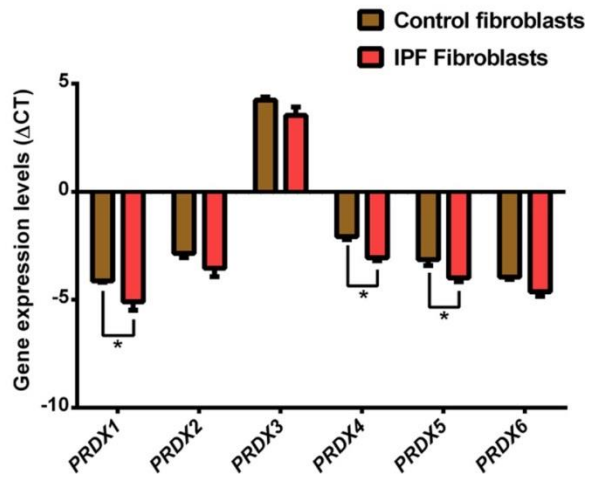

Figure 13. Catalase is downregulated in human lungs and primary fibroblasts, and Bleomycin administration decreased catalase in mouse lungs.

(A) and (B) Basal protein abundance of catalase are reduced in IPF primary human lung fibroblasts and IPF lung tissues compared to controls (Scale bar: 10 μm). Fibroblast cultures form 5 control (1-5) and 5 IPF (1-5) patients (A). Lung tissues form 3 control (1-3) and 3 IPF (1-3) patients (B).

(C) Bleomycin administration decreased catalase protein abundance in mouse lungs, n = 3.

(D) GPx 1/2 compensate for catalase deficiency in IPF human lungs. Lung tissues from 4 control (1-4) and 4 IPF (1-4) patients. NC – negative control, (Scale bar: 10 μm).

(E) PEX 3p is downregulated in IPF primary human lung fibroblasts (Scale bar: 10 μm).

(F) mRNA for PRDX1, 4 and 5 are more expressed in control compared to IPF primary human lung fibroblasts. Data was analyzed with the unpaired student's t-test. * is defined as $p \leq 0.05$, n = 5.

3.13. Overexpression of catalase elicited anti-fibrotic responses

The role of catalase in fibrosis was assessed after overexpressing the enzyme in control and IPF primary human lung fibroblasts. It was clearly evident that a decrease in fibrotic markers, collagen I and α-SMA (Figure 14A) occurred in catalase overexpression groups via an unidentified molecular mechanism directly or indirectly related to the biological function of the enzyme. Moreover, catalase overexpression elicited an additive effect to the anti-fibrotic properties of PPAR-β/δ and PPAR-γ as indicated in IPF primary human lung fibroblasts (Figure 14A, lane 6). The reduction in the production of ROS (Figure 14B) in cells overexpressing catalase strongly supports the importance of ROS in fibrosis progression.

Figure 14

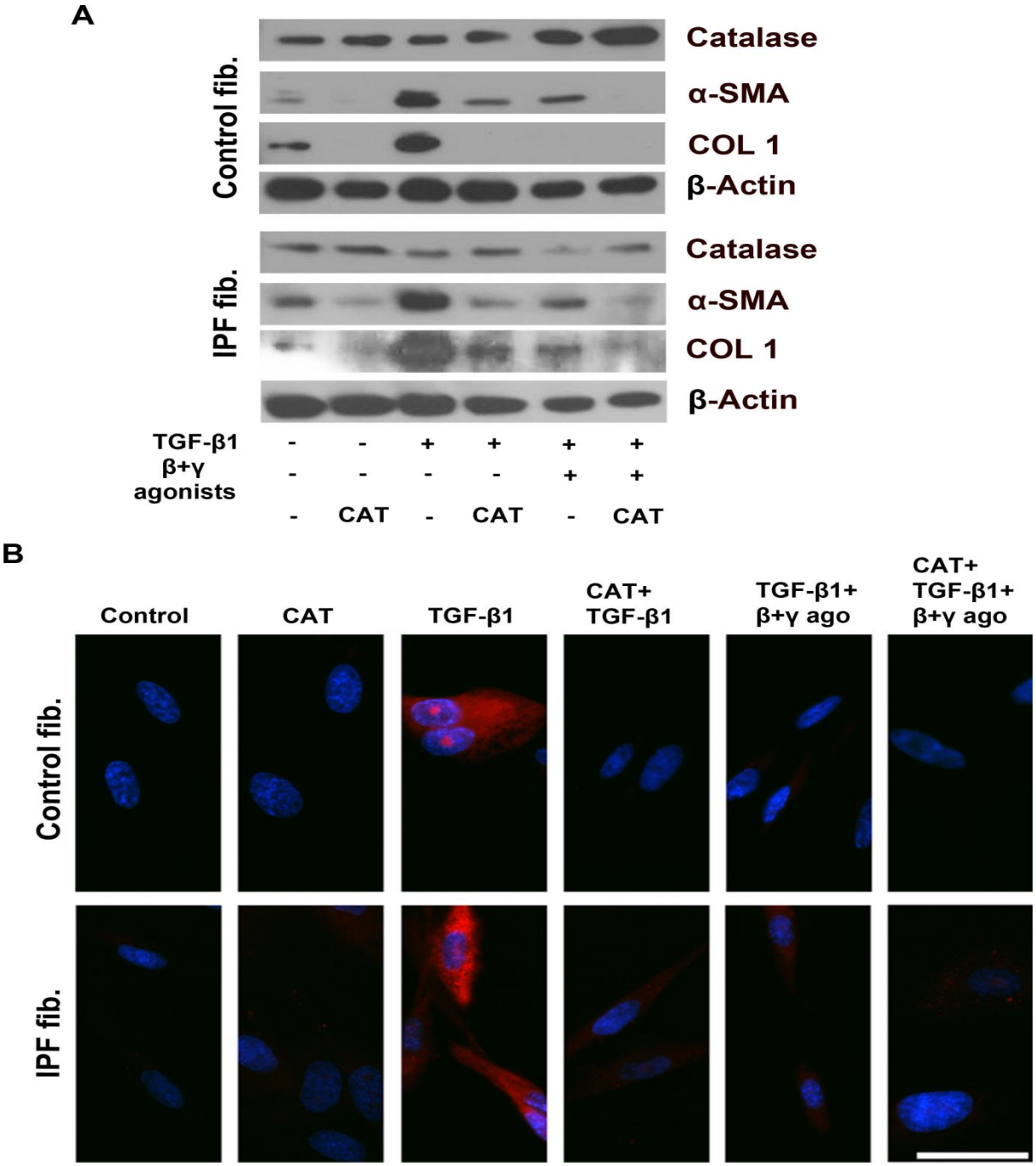

Figure 14. Overexpression of catalase elicited anti-fibrotic responses.

(A) and (B) Overexpression of catalase downregulated collagen and ROS production. Control and IPF primary human lung fibroblasts were transfected with a catalase overexpression vector for 72 h followed by 5 ng/ml TGF-β1 stimulation for 24 h. Combined GW0742 and Rosiglitazone treatment was done for 48 h. Dihydroethidium staining (B), CAT - catalase overexpression vector (Scale bar: 10 μm). Data represent 3 experimental repeats.

3.14. Inhibition of catalase with 3-amino-1, 2, 4-triazole enhanced fibrotic phenotype

Catalase appears to inhibit pulmonary fibrosis. To delineate its molecular role in the disease, 3-amino-1, 2, 4-triazole (AT), a compound known to block the activity of catalase selectively was first analyzed for its inhibitory effects in control and IPF primary human lung fibroblasts. Indeed, 3-amino-1, 2, 4-triazole treatment potentially inhibited the activity of catalase (Figure 15A). Additionally, intracellular collagen I and extracellular collagens increased strongly after AT treatment in combination with TGF-β1, even after combined activation of PPAR-β/δ and PPAR-γ in TGF-β1 stimulated cells, especially in IPF fibroblasts (Figure 15B and 15C). It is worthy to note that this effect occurs despite the strong anti-fibrotic properties of simultaneously activated PPAR-β/δ and PPAR-γ as already shown in Figure 9A and suggests: 1) that a decrease in catalase in IPF fibroblasts under TGF-β1 stimulation is detrimental, and 2) that catalase activity would be very beneficial in IPF fibroblasts under TGF-β1 stimulation. Additionally, inhibition of catalase increased ROS production, confirming oxidative imbalances during fibrosis progression (Figure 15D).

Figure 15

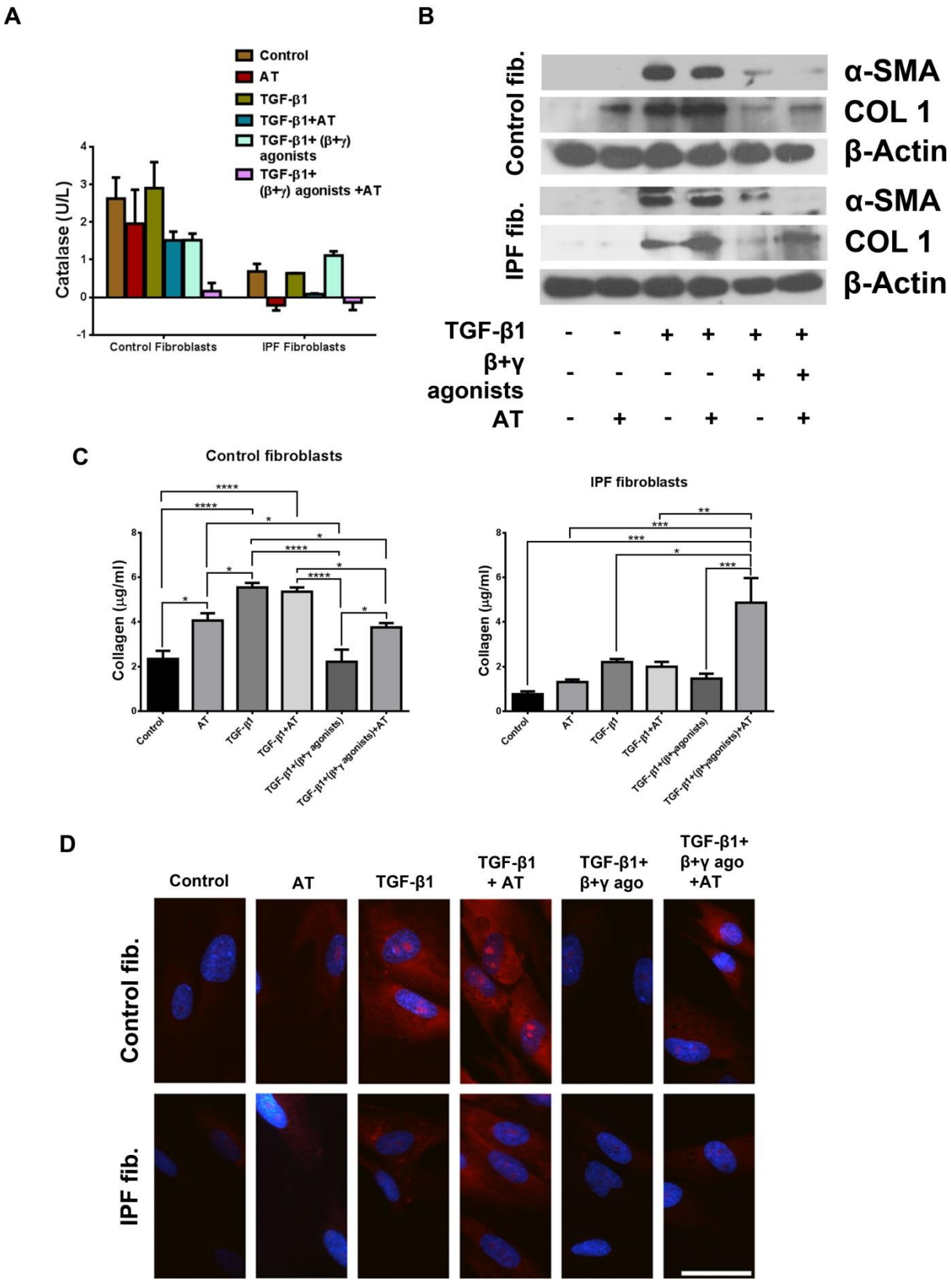
A
Control
AT
TGF-β1
TGF-β1+AT
TGF-β1+ (β+γ) agonists
TGF-β1+ (β+γ) agonists +AT
Catalase (U/L)
Control Fibroblasts
IPF Fibroblasts
B
Control fib.
IPF fib.
α-SMA
COL 1
β-Actin
α-SMA
COL 1
β-Actin
TGF-β1 - - + + + +
β+γ agonists - - - - + +
AT - + - + - +
C
Control fibroblasts
IPF fibroblasts
Collagen (µg/ml)
Control
AT
TGF-β1
TGF-β1+AT
TGF-β1+(β+γ agonists)
TGF-β1+(β+γ agonists)+AT
D
Control
AT
TGF-β1
TGF-β1 + AT
TGF-β1+ β+γ ago
TGF-β1+ β+γ ago +AT
Control fib.
IPF fib.

Figure 15. Inhibition of catalase with 3-amino-1, 2, 4-triazole enhanced fibrotic phenotype.
(A), (B), (C) and (D) 3-amino-1, 2, 4-triazole potentially blocks catalase activity and leads to increases in fibrosis markers and ROS production. Cells were serum-starved and treated with 5 ng/ml TGF-β1 for 24 h. GW0742, Rosiglitazone and 3-amino-1,2,4-triazole (AT) were simultaneously treated for 24 h. Catalase activity assay, n = 3 (A) Western blotting (B) Sircol collagen assays, n = 4 (C) Dihydroethidium staining, n = 3 (D) (Scale bar: 10 μm). Groups were analyzed by two-way ANOVA (A) and one-way ANOVA (C), using Tukey´s multiple comparisons test. *, **, *** and **** are defined as $p \leq 0.05$, $p \leq 0.01$, $p \leq 0.001$ and $p \leq 0.0001$ respectively.

3.15. Stable catalase knockdown cell lines produce H_2O_2 and enhanced fibrosis markers

It was observed that collagen I gene expression was upregulated in stable catalase knockdown cell lines (Figure 16A). In order to study the possible molecular mechanism regarding this phenomenon, a stable catalase knockdown cell line of control primary human lung fibroblasts were used for further experiments since IPF primary human lung fibroblasts (stable catalase knockdown cell line) could not survive in culture after few passages. It was however, unclear whether catalase is necessary for fibroblast survival since IPF primary human lung fibroblasts already had lower levels of the enzyme (see Figure 13A) and activity (see Figure 15A) compared to controls. Stable knockdown of catalase resulted in increased intracellular (Figure 16B) and extracellular collagens (Figure 16C) and decreased catalase activity (Figure 16E).
One of the main functional roles of catalase is the degradation of H_2O_2 into H_2O and O_2. Hydrogen peroxide effects have been well-studied in cell biology, wherefore its roles were also assessed in our model systems. Data from this thesis showed a reduction and increase in ROS in catalase overexpression and inhibition conditions respectively. That notwithstanding, H_2O_2 concentration increased at basal level and further, after treatment of stable catalase knockdown cell line with TGF-β1 (Figure 16D).

The production of H_2O_2 after TGF-β1 treatment of human lung fibroblasts has been well characterized but the accumulation of the molecule in cells devoid of catalase explains its metabolic function as a scavenging enzyme for the molecule. Also, stable catalase knockdown cell lines could not survive exogenous H_2O_2 treatments beyond 50 μM. Treatments at this concentration increased the expression of α-SMA and a relative elevation in collagen I in CAT sh1 (Figure 16F). The data opens discussions on whether H_2O_2 would be an intracellular signaling molecule for the transdifferentiation of fibroblasts into collagen-producing myofibroblasts at some stages of IPF development.

Figure 16

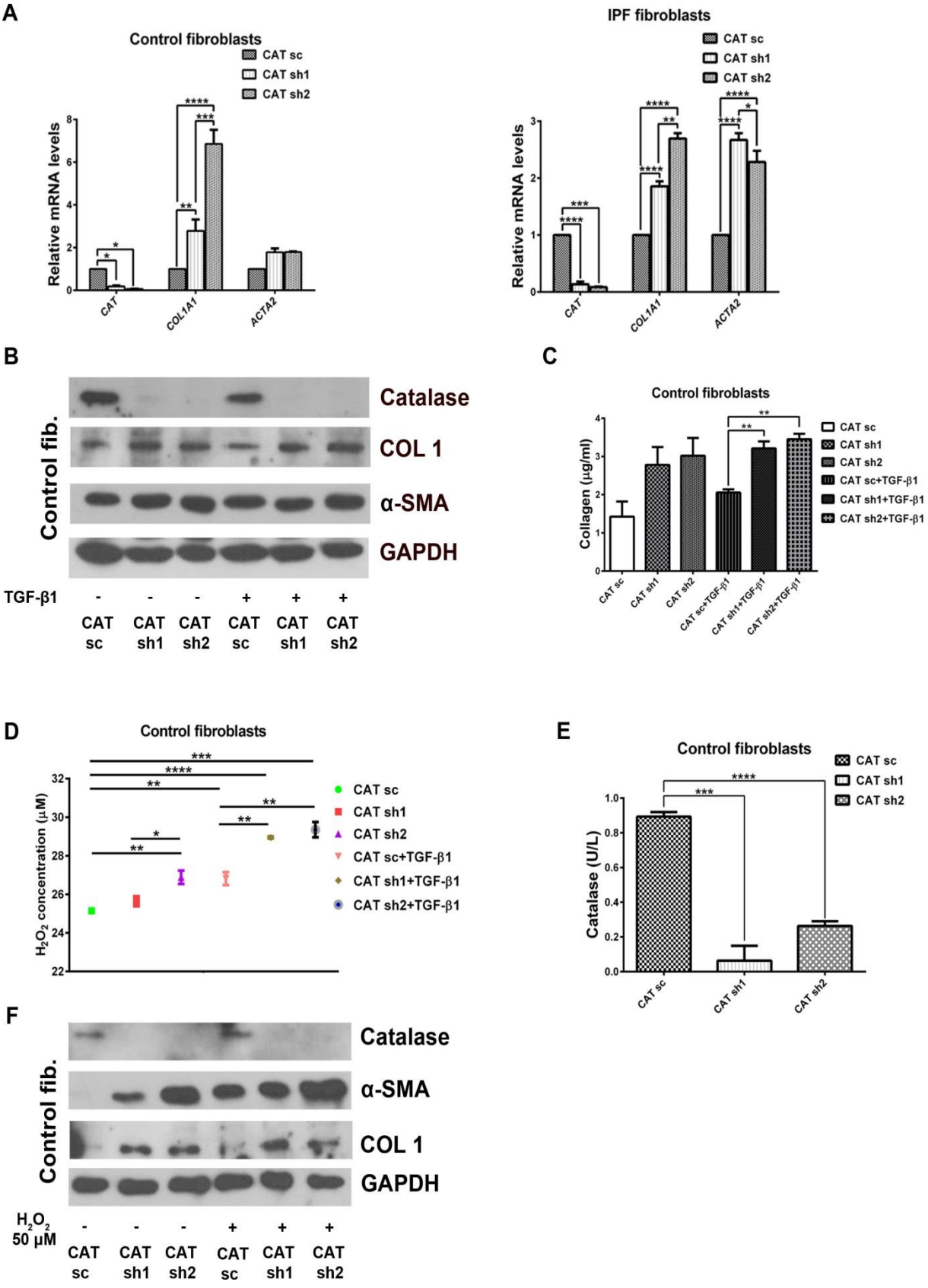
A
Control fibroblasts
CAT sc
CAT sh1
CAT sh2
Relative mRNA levels
CAT
COL1A1
ACTA2
IPF fibroblasts
B
Control fib.
Catalase
COL 1
α-SMA
GAPDH
TGF-β1
CAT sc
CAT sh1
CAT sh2
C
Control fibroblasts
Collagen (μg/ml)
CAT sc+TGF-β1
CAT sh1+TGF-β1
CAT sh2+TGF-β1
D
Control fibroblasts
H2O2 concentration (μM)
E
Control fibroblasts
Catalase (U/L)
F
Control fib.
Catalase
α-SMA
COL 1
GAPDH
H2O2 50 μM

Figure 16. Stable catalase knockdown cell lines produce H_2O_2 and enhanced fibrosis markers

(A), (B), (C) and (E) The stable knockdown of catalase decreased catalase activity, and remarkably upregulated collagen expression, abundance and release. Stable knockdown catalase cell lines were seeded, cell cultures serum-starved and total RNAs extracted for qRT-PCR analyses. Cells were also treated with 5 ng/ml TGF-β1 for 48 h, and total cell lysates and media collected for Western blotting and Sircol collagen assays respectively. Stable knockdown catalase cell lines were also seeded, serum-starved and homogenized in 1X PBS for catalase activity. Groups were analyzed by two-way ANOVA (A) and one-way ANOVA (C) and (E), using Tukey´s multiple comparisons test. *, **, *** and **** are defined as $p \leq 0.05$, $p \leq 0.01$, $p \leq 0.001$ and $p \leq 0.0001$ respectively. n = 3 (A) and (E), and n = 4 (C).

(D) H_2O_2 production increased in basal and TGF-β1 stimulated stable knockdown catalase cell lines. Data was analyzed with one-way ANOVA, using Tukey´s multiple comparisons test. *, **, *** and **** are defined as $p \leq 0.05$, $p \leq 0.01$, $p \leq 0.001$ and $p \leq 0.0001$ respectively, n = 3.

(F) Stable knockdown catalase cell lines were seeded, serum-starved and treated with H_2O_2 for 24 h. Whole cell lysates were collected for Western blotting and protein detections. Data represent 3 experimental repeats.

3.16. siRNA knockdown of catalase promoted release of extracellular collagen

Control and IPF primary human lung fibroblasts were transfected with catalase siRNA for 48 h and results indicated a decrease in intracellular collagen I (Figure 17A), significant increase in extracellular collagen released by IPF fibroblasts (Figure 17B) and upregulation of *COL1A1* gene (17C). The data supported the role of catalase in the modulation of IPF as already indicated.

3.17. Hydrogen peroxide induced profibrotic responses

To further explain the role of H_2O_2 in IPF, control and IPF primary human lung fibroblasts were challenged with increasing concentrations of H_2O_2. Interestingly, H_2O_2 promoted the increase of collagen abundance at 10 mM in control primary human lung fibroblasts, whereas in IPF fibroblasts there was already a consistent increased response to collagen production after treatments with higher concentrations of H_2O_2 (> 300 μM treatment (Figure 18A). The disparity in the two cell groups after H_2O_2 treatments may be consistent with the notion that higher levels of catalase suppress the development of fibrosis, or catalase is gradually depleted by TGF-β1 to enhance fibrosis progression.

Figure 17

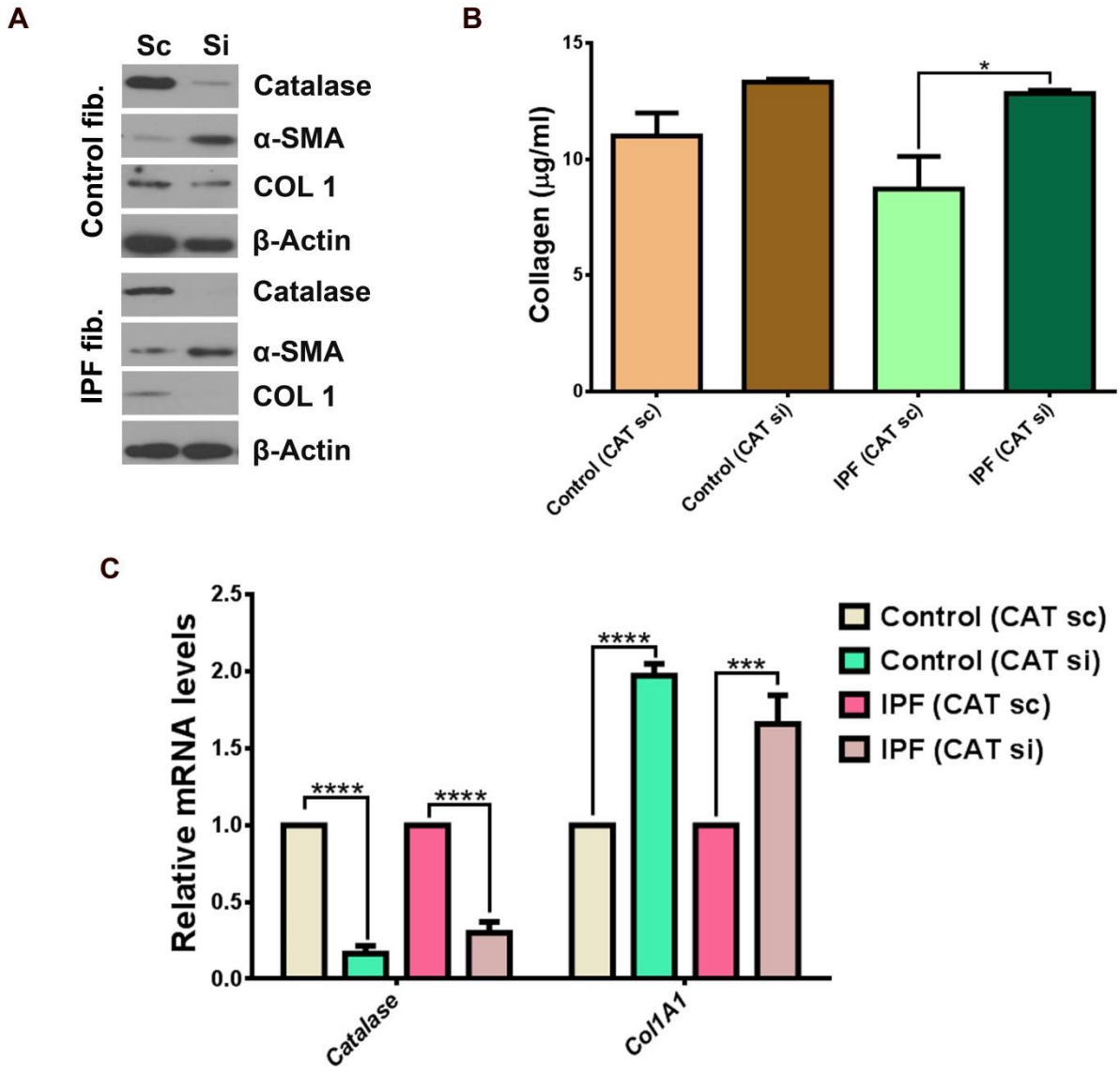

Figure 17. siRNA knockdown of catalase promoted release of extracellular collagen.

(A), (B) and (C) **C**ontrol and IPF primary human lung fibroblasts were seeded and transfected with catalase siRNA for 48 h. Total cell lysates were collected for Western blotting for catalase, α-SMA, COL 1 and β-actin detections. (A) Cell culture media for Sircol collagen assays (B) and total RNAs were extracted for qRT-PCR analyses (C). Groups were analyzed by two-way ANOVA (B) and (C), using Tukey´s multiple comparisons test. *, *** and **** are defined as $p \leq 0.05$, $p \leq 0.001$ and $p \leq 0.0001$ respectively, n = 5 (B) and n = 3 (C).

Figure 18

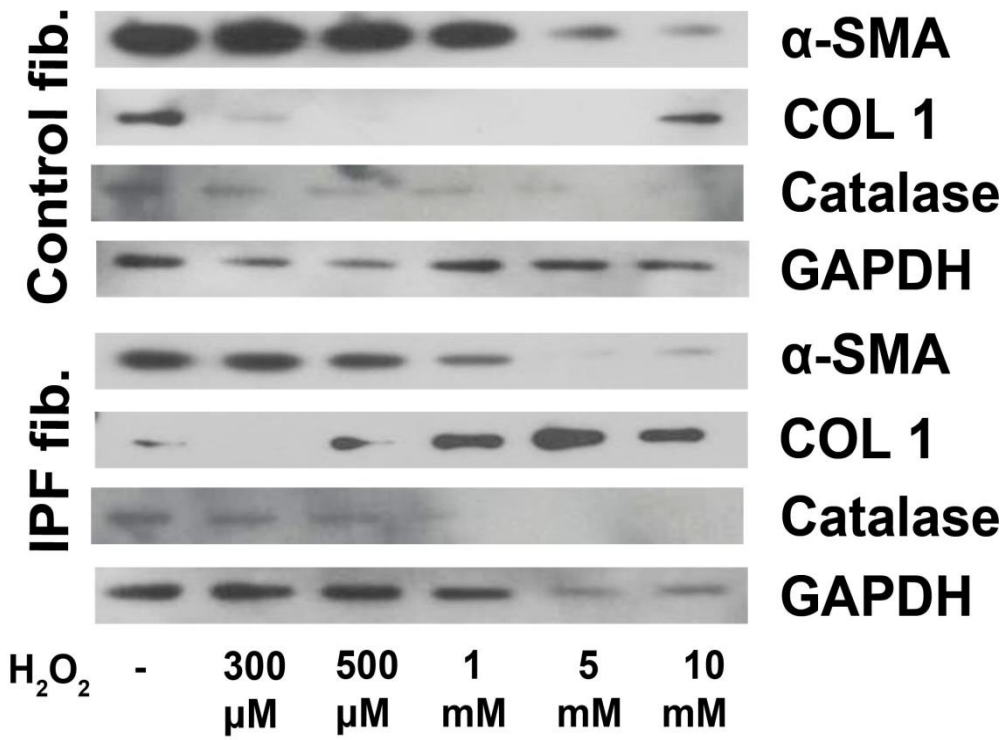

Figure 18. Hydrogen peroxide induces profibrotic responses.

H_2O_2 is a regulator of intracellular abundance of collagen. Control and IPF primary human lung fibroblasts were seeded, the cultures serum-starved and treated with various concentrations of H_2O_2 for 24 h. Whole cell lysates were collected for Western blotting and detections. Data represent 3 experimental repeats.

4. Discussion

Idiopathic pulmonary fibrosis is characterized by complex molecular mechanisms that interfere with the usual physiologic balance of the extracellular matrix (ECM) in the lungs [176]. Recent phase 3 clinical trials in IPF patients supported that the use of pirfenidone for one year decreased disease progression [326]. However, there is still the need to find other therapeutic regimens to support current ones.

In this dissertation, the regulation of collagen, a major structural component of interstitial ECM [327], and of ROS metabolism in IPF were of primary focus in contrast to studies which manipulated the cellular phenotype of fibroblasts and cell signaling pathways induced by pro-inflammatory and pro-fibrotic molecules in attempts to resolve IPF. Results in this thesis demonstrated that PPAR-β, peroxisome-derived docosahexaenoic acid and catalase are candidates for antifibrotic responses in IPF.

Before establishing the general finding in this study, the consistency of markers of pulmonary fibrosis, behaviour of primary human lung fibroblasts under TGF-β1 induction and MMPs in fibrosis, weas investigated.

4.1. α-smooth muscle actin is not a reliable IPF marker

Data from the experiments done for this dissertation demonstrated that the expression of α-SMA, a key marker used to study fibrosis, might correspond with collagen regulation in lung biopsies. Interestingly, α-SMA was not upregulated in IPF primary human lung fibroblasts compared to control fibroblasts. In the literature, the molecular characterization of fibrosis markers associates IPF extensively with collagen synthesis [328-330] and the use of α-SMA as a sole marker for studying fibrosis has been currently debated [331]. The latter publication revealed that co-staining of α-SMA and collagen in Bleomycin-induced fibrosis mouse models exhibited inconsistencies in different organs. The authors reported that all α-SMA-positive cells remarkably expressed collagen whereas only a small population of collagen-positive cells co-expressed α-SMA in the lung and kidney. This study also indicated that a population of fibroblasts that did not express α-SMA was able to secrete collagen during fibrogenesis. Data from this thesis provided insights on the restrictive use of α-SMA as single marker in fibrosis studies as control primary human lung fibroblasts expressed more α-SMA and TGFBRI and also secreted higher levels of active TGF-β1 than IPF groups in culture conditions under basal conditions. However, there were no differences between extracellular

collagen secreted by primary control and IPF human lung fibroblasts. This dissertation further delineates the irregularities of α-SMA as sole marker though during the past years many authors have suggested that the pathophysiology of fibrosis is characterized by excessive accumulation of collagen-rich ECM produced by α-SMA-positive myofibroblasts [332, 333]. This finding underscores the need to identify more specific markers that are solely relatable to cells that secrete collagen during the pathogenesis of pulmonary fibrosis, and to perform thorough investigation of ECM in all IPF studies. It is also therefore suggested, that metabolic markers, in addition to phenotype-associated ones be investigated in future studies.

4.2. TGF-β1 strongly induced the proliferation of IPF fibroblasts

It was reported that type I collagen forms a key component of the ECM during fibrosis [334], which provides enough evidence to focus on collagen degradation in IPF. Moreover, the production of collagen is mainly from fibroblasts in IPF [4, 197] and the proliferation of fibroblasts may plausibly promote the accumulation of interstitial proteins. Indeed, IPF primary human lung fibroblasts proliferated strongly in response to TGF-β1, providing a better understanding of the phenotypic heterogeneity between control and IPF primary human lung fibroblasts in this study. On the other hand, this result also justifies the importance of describing the metabolic differences between cells from healthy and IPF patients, to help develop standards and markers for IPF. The proliferative capacity of IPF primary human lung fibroblasts after TGF-β1 stimulation may add up to the complexities of this disease, suggesting molecular targeting of cell cycle pathways in addition to metabolic ones.

4.3. MMPs in lung fibrosis

Similar to this dissertation, different MMPs were variously regulated in control and IPF primary human lung fibroblasts as reported in another publication [335]. Interestingly, the inhibition of MMPs with a general blocker in this thesis was relevant in IPF and control fibroblasts. Moreover, basal levels of MMP1, MMP3 and MMP10 were lower in IPF primary human lung fibroblasts compared to controls however activated PPAR-β/δ increased their expressions. MMP1 knockdown cells also showed compensatory expressions of the genes (MMP3 and MMP10), suggesting their possible importance in regulating the pro-fibrotic phenotype in IPF which should be clarified in the future. Inhibitors for specific members of the MMP family are unfortunately not available and differential regulation of individual MMPs may either promote or inhibit the development of IPF [336]. However, it also has to be discussed that MMPs could be molecularly connected to some disease conditions which may

be associated to other cells in the lungs, hence local inhibition of specific MMPs may be detrimental to the normal biological functions of other cells in the lung cells.

4.4. PPARs in the resolution of IPF and inconsistencies of experimental models

A part of this dissertation focused on the use of PPARs in the resolution of fibrosis since earlier data have implicated PPARs, especially PPAR-γ, to elicit anti-fibrotic responses [251-254]. Interestingly, the experimental models used in those studies to simulate the disease process in vivo were inconsistent. In one of the studies, primary human lung fibroblasts were simultaneously treated with TGF-β1 and PPAR-γ agonists [254]. The results only indicated the interference of activated PPAR-γ in TGF-β1 pathways for the reverse of pro-fibrotic phenotype and ultimately, collagen production. Also in another study, human lung fibroblasts were pre-treated with PPAR-γ agonists followed by the stimulation of human lung fibroblasts with TGF-β1 in vitro, and in mice with Bleomycin sulfate [251]. Pre-treatment of PPAR-γ agonists in this model revealed the possible anti-inflammatory potential of the receptor. However, it is understandable that inflammation does not automatically lead to fibrosis [337] and this cellular process is also required for tissue homeostasis during wound healing. Additionally, some groups treated after Bleomycin instillation on day 11 with troglitazone to investigate the role of PPAR-γ in fibrosis resolution. However, the experiments lacked an essential control since they did not provide evidence of tissue remodeling and of fibrosis phenotype on day 11 after Bleomycin administration alone, compared to the troglitazone treated group. In light of the two studies, more scientists started investigating PPAR-γ in fibrosis. The studies of the following years delineated the anti-fibrotic potential of PPAR-γ by co-treating its agonists in parallel to TGF-β1. Profibrogenic effects mediated by TGF-β1 were reported to be inhibited by PPAR-γ agonists in human lung fibroblasts [253]. However, the study missed to document the effects of co-treatment of these compounds on exogenously secreted collagen, which is primarily related to ECM deposition in vivo. In fibrosis, aberrant deposition of ECM contributes to disease progression and studies that focus on inhibiting the differentiation of fibroblast to myofibroblasts might as well have to consider that some fibroblasts do not express α-SMA but are able to secret collagen into the ECM [331]. Another study that used the co-treatment model demonstrated that rosiglitazone suppressed myofibroblast differentiation, indicating a preventive role of PPAR-γ in fibrosis resolution [252]. However, α-SMA was used in the entire study as the sole marker for fibrosis, leaving much questions unanswered since collagen deposition should have been investigated as most appropriate marker for fibrosis.

4.5. PPAR-β/δ is a molecular target for collagen degradation in IPF

In reference to reports from earlier studies and their experimental approaches it is worth noting, that in order to understand the pathogenesis of fibrosis, experimental models should exactly simulate the disease process in vivo. In contrast to all other studies, in this dissertation, the experimental models used tried to mimic the disease process by stimulating primary human lung fibroblasts first with TGF-β1, followed by PPAR activation later. It is interesting that the regulatory effects of TGF-β1 on PPARs during the progression of IPF have not been published until now. Interestingly, the in vitro model used in this study demonstrated that PPAR-β/δ is upregulated in TGF-β1 stimulated control and IPF primary human lung fibroblasts. Furthermore, IPF human lung tissues expressed higher levels of PPAR-β/δ compared to controls. The reason for this effect is unclear but one explanation could be that PPAR-β/δ is possibly modulated for adaptive fibrosis response induced by TGF-β1. Thus, it was hypothesized that PPAR-β/δ might be a strong target for lung fibrosis resolution compared to PPAR-α and PPAR-γ. Indeed, subsequent results supported the hypothesis that activated PPAR-β/δ contributes to the reversal of fibrosis phenotype. The regulation of collagen synthesis 1) was paralleled by upregulation of specific activation of PPAR-β/δ 2) and members of the MMP family. The downregulation of collagen and upregulation of MMP is not clear and has to be analyzed in the future. The PPAR-β/δ-mediated molecular regulation was more pronounced on MMP1, 3 and 16 in control and IPF primary human lung fibroblasts, which are collagenase, stromelysin and membrane-type MMPs respectively. The observation highlights the potential involvements of MMPs in the degradation of collagen in ECM in fibrosis conditions.

4.6. Combined activation of PPAR-β/δ and PPAR-γ elicited stable anti-fibrotic properties

It was reported in this dissertation that combined activation of PPAR-β/δ and PPAR-γ exhibited strong anti-fibrotic responses and also proliferated peroxisomes. Before explaining the importance of peroxisome biogenesis and metabolism in fibrosis, the present study determined whether the anti-fibrotic properties of combined activations of PPAR-β/δ and PPAR-γ were relatively consistent in several aspects of the disease condition in vivo. Indeed, it was demonstrated that the anti-fibrotic response observed after activating both PPAR-β/δ and PPAR-γ was stable, reliable and repeatable and could modulate intra and extracellular collagens. One dimension essential for successful resolution of IPF is the reduction of excess ECM component secretion, especially collagen, since two-thirds of the dry weight of ECM is

made up of collagen fibres [184]. The findings from this dissertation also challenges earlier reports which suggested that activated PPAR-γ alone exerted anti-fibrotic potentials [251-254] as most of the collagen was released into culture media after treatment with PPAR-γ agonists (here, rosiglitazone) as shown in the study. This dissertation is the first report contrasting the potentials of sole treatment with PPAR-γ agonists in fibrosis as reported in the last two decades. It is suggested that differences in experimental models used might be the reason for this outcome; however, it is critical to exactly mimic the disease condition in vitro in order to provide reliable results for future in vivo studies or treatment strategies. The model used in this study may not be perfect but fibrosis was certainly simulated in vitro in a more appropriate way since the initial surge and high levels of TGF-β1 in the pathogenesis of IPF have been very well documented [79, 80, 82] and the involvement of TGF-β1 contributes to the progression of fibrosis.

4.7. Peroxisomes in IPF

Concerning the role of organelle involvement in this dissertation, it was demonstrated, that combined activation of PPAR-β/δ and PPAR-γ induced peroxisome biogenesis and also modulated other metabolic pathways of the organelle as well as the fibrosis phenotype. Additionally, the combined effect also elicited stronger anti-fibrotic effects than PPAR-β/δ alone. As a result, future studies can concentrate on finding potential dual agonists for PPAR-β/δ and PPAR-γ to enhance both peroxisome biogenesis and stronger anti-fibrotic effects. This dissertation also ascertained the importance of proliferating peroxisomes in fibrosis conditions with much focus on the functional compartments of the organelle, especially the antioxidative and β-oxidative systems. Moreover, ROS production in fibrosis has been already documented and the antioxidative enzymes of cells are known to be depleted in the IPF disease condition [108, 109].

4.8. Exogenous activation of PPARs increase peroxisome lipid metabolism

Fatty acid metabolism increased after combined activation of PPAR-β/δ and PPAR-γ and the products and derivatives are known endogenous activators of the receptors [338]. Arachidonic acid, docohexaenoic acid and eicosapentaenoic acid were increased after activation of PPAR-β/δ, PPAR-γ and both. Interestingly, all three PPAR isotypes are activated by arachidonic acid and docosahexanoic acid [339] and it is known that the activation of PPAR-β/δ and PPAR-γ promote fatty acid catabolism and lipid metabolism respectively [340, 341]. It is therefore hypothesized that the stability of the treatments may be due to the fact that exogenous

activation of both PPARs increase peroxisome fatty acid metabolism and the resulting metabolites further activated PPARs, establishing a stable activation loop on the receptors.

4.9. Combined inhibition of PPAR-β/δ and PPAR-γ progress fibrosis phenotype

The supportive role of PPAR-γ on PPAR-β/δ was not only limited to a single agonist of the former, and the inhibition of both receptors progressed fibrosis, emphasizing their importance in controlling fibrosis phenotype. Additionally, the inhibition of the receptors was effective after 48 hours of treatment as collagen was increased in control and IPF primary human lung fibroblasts. Also, the regulation of collagen in fibroblasts might not be the sole molecular responsibility of PPARs but might also be influenced by a complex interplay of different transcription factors or cofactors of the cells. Further, the differences between control and IPF primary human lung fibroblasts suggest that there may be some additional molecular pathways regulating collagen synthesis, release or degradation besides MMPs.

4.10. Combined activation of PPAR-β/δ and PPAR-γ inhibit migration and invasion of IPF primary human lung fibroblasts

In fibrosis, TGF-β1 induces fibroblast recruitment [342] and the interference of migration and invasion pathways of human lung fibroblasts may present a potential avenue to limit fibrogenesis at wound sites to enhance alveolar regeneration and restoration of the normal architectural components of the lungs. An earlier study has already acknowledged that PPAR-α and PPAR-γ inhibit proliferation and migration of smooth muscle cells [343]. Additionally, PPAR-γ agonist treatment of umbilical vein endothelial cells stimulated migration [344], making it convincing that systemic activation of PPARs might have variable effects on different cell types. Nevertheless, the results of this thesis collectively established, that combined activation of PPAR-β/δ and PPAR-γ does not only elicit anti-fibrotic responses but also influences migration and invasion of IPF primary human lung fibroblasts.

4.11. Balance in ECM is essential for fibrosis resolution

To expound further on what has been initially discussed, peroxisome proliferation by combined activation of PPAR-β/δ and PPAR-γ indicated a functional biological role of the organelle in inhibiting fibrosis progression or even having a potential role in fibrosis resolution. Fibrosis is marked by multiple levels of molecular regulations which contribute, in part and actively in the progression of the disease, and antioxidants are considerably depleted in fibrotic diseases [110-112]. Disruption in the antioxidant system relates to ROS metabolism

in the lungs and not directly to ECM homeostasis. However, the complexities in maintaining ECM balance during wound healing in the lungs require multiple approaches in studying IPF. In the past, many molecular connections between IPF and inflammation [151, 152] as well as ROS metabolism [101] focused on resolving the cellular processes rather than relating them to ECM balance. Consequently, interventions with antioxidants such as N-acetylcysteine as a form of clinical management did not improve the quality of life of patients and this outcome might have hindered further exploration of the antioxidant system in IPF. Similarly, modern clinical management compounds such as nintedanib [18] and pirfenidone [19] have prolonged patient's lifespan but could not prevent mortality. In as much as the molecular targeting of biological processes leading to IPF development is prudent, the association of these processes to ECM clearance is essential.

4.12. Catalase contributes to ECM balance in IPF

Metabolic profiling in IPF is important as TGF-β1 downregulated catalase and combined activation of PPAR-β/δ and PPAR-γ weakly upregulated the enzyme in primary human lung fibroblasts. To further explore reasons for this inconspicuous molecular effect, the functional metabolic roles of antioxidative enzymes in primary human lung fibroblasts were established in this study. Catalase, as well as other antioxidative enzymes, present in peroxisomes and the cytosol has protective effects in most of the cellular compartments. However, the link between catalase and collagen degradation remains unclear in this study and has to be elucidated in the future. It was reported that catalase protects the peroxisomal acyl-CoA β-oxidation system and thiolase from disruption and inactivation by H_2O_2 respectively [345]. A functional peroxisomal β-oxidation system, however, is necessary to prevent eicosanoid accumulation and is essential for the synthesis of DHA or other PUFA which are able to trap ROS, leading to less NF-kB activation. Nonetheless, it was reported in cardiac fibroblasts that increased ROS activates MMPs and decreased the synthesis of fibrillary collagen [346].

It was also interesting that TGF-β1 decreased catalase in a time and concentration dependent manner, while collagen was upregulated. This phenomenon has already been described in airway smooth muscle cells [114] albeit in fibrosis, catalase was only characterized in humans and a Bleomycin hydrochloride-induced lung fibrosis mouse model [347, 348] without delineating the fundamental molecular mechanisms associated with the pathogenesis of the disease. Besides, increasing concentrations of TGF-β1 downregulated catalase in smooth muscle cells [114] and Bleomycin administration caused the release of inflammatory and pro-fibrotic cytokines and in tend, reduced catalase activity in mice [347]. Data from this thesis

suggest that catalase activity may be essential for the resolution of fibrosis by essentially metabolizing ROS which are inducers of collagen synthesis [346] or by protecting the synthesis of DHA via peroxisomal β-oxidation and preventing oxidation of the lipid double bond, which has to be analysed in the future. Peroxisome-derived PUFAs are important components of cellular metabolism and they modulate NOX enzymes as well. For this reason, catalase might have an indirect effect by protecting peroxisomal lipid products against oxidation and function of other compartments.

Persistent ROS production is therefore suggested to be deterrent to collagen degradation and a homeostatic balance in ROS metabolism is probably required for normal healing in the lungs. Since ROS are generated by NOXs triggering oxidative stress in IPF fibroblasts, it is imperative that the activities of scavenging enzymes such as superoxide dismutase, catalase, glutathione peroxidases, thioredoxin, peroxiredoxins and glutathione transferase [108] are enhanced in IPF. In this study, it was indicative enough to expound the role of catalase in fibrosis since the enzyme was markedly decreased in IPF primary human lung fibroblasts compared to controls. This could be as a result of increased TGF-β1 production in IPF primary human lung fibroblasts as reported in our earlier paper [270]. Consequently, TGF-β1 stimulates ROS production and also disrupts the anti-oxidative compartments in cells [87]. This study raises concerns about the regulation of catalase and its activity after TGF-β1 stimulation of primary human lung fibroblasts.

4.13. The role of H_2O_2 in IPF

Results in this dissertation confirmed that higher concentrations of exogenous H_2O_2 increased intracellular collagen but α-SMA expression did not follow the regulatory pattern exhibited on collagen in the primary human lung fibroblasts used in this study. In view of this, fibroblasts expressing α-SMA do not necessarily produce collagen in IPF. Additionally, though TGF-β1 regulates the transdifferentiation of fibroblasts into α-SMA-positive myofibroblasts, synthesis of collagen may not be parallel with this molecular phenotype [331] as indicated by studies in the last two decades.

The modulatory effect of H_2O_2 on collagen questions whether the amount of the molecule in vivo is directly or indirectly related to the development of lung fibrosis. Even though smaller concentrations of H_2O_2 (5μM) were documented to downregulate procollagen α_1(I), α_2(I), α_1(III), α_1(IV) and α_2(IV) [346], excessive levels of the molecule increased collagen in this

thesis. This underscores the need to establish a standard range for H_2O_2 levels for normal and pathologic conditions to aid early diagnosis of IPF in patients.

Animal models for the study of pulmonary fibrosis do not present the histopathological phenotype of the disease as observed in humans [349]. It is arguable that the appearance of pathological features such as honeycomb, thick scars at the alveolar region and fibroblastic foci [209, 210], may take time to occur in humans and the predominantly used model for fibrosis induction in mice, that is Bleomycin treatment, might exhibit differential pathophysiological features compared to the natural development of fibrosis in humans. However, inferring from the possible potential of H_2O_2 in collagen regulation, it is proposed that the compound could be used to generate progressive lung fibrosis in animal model for IPF studies.

4.14. Conclusion

In summary, the study established that PPAR-β/δ elicits anti-fibrotic properties and is supported by PPAR-γ to suppress the promoter region of collagen. Thus, combined activation of PPAR-β/δ and PPAR-γ could serve as effective anti-fibrotic treatment model. TGF-β1 downregulated catalase and also induced ROS production which further promoted the development of fibrosis. H_2O_2 may be a key molecule that progresses collagen production in fibrosis, indicating that an imbalance in ROS metabolism should be a major molecular target for future studies in IPF. Results of the study therefore suggested that the induction of catalase in IPF patients may be appropriate for the regulation of collagen intracellularly and in ECM, hence the need for peroxisome proliferation to increase the abundance of the enzyme and of β-oxidation products. The biogenesis of peroxisomes is therefore essential to increase the compartmental store of catalase to remedy the aberrant synthesis of collagen during wound healing since at very high levels of ROS, catalase translocates into the cytoplasm. Peroxisome-derived docosahexaenoic acid also inhibited intracellular collagen synthesis thus supported the role of peroxisomes in IPF as well.

4.15. Graphical presentation of results

The scheme below explains the molecular mechanisms defined in this study.

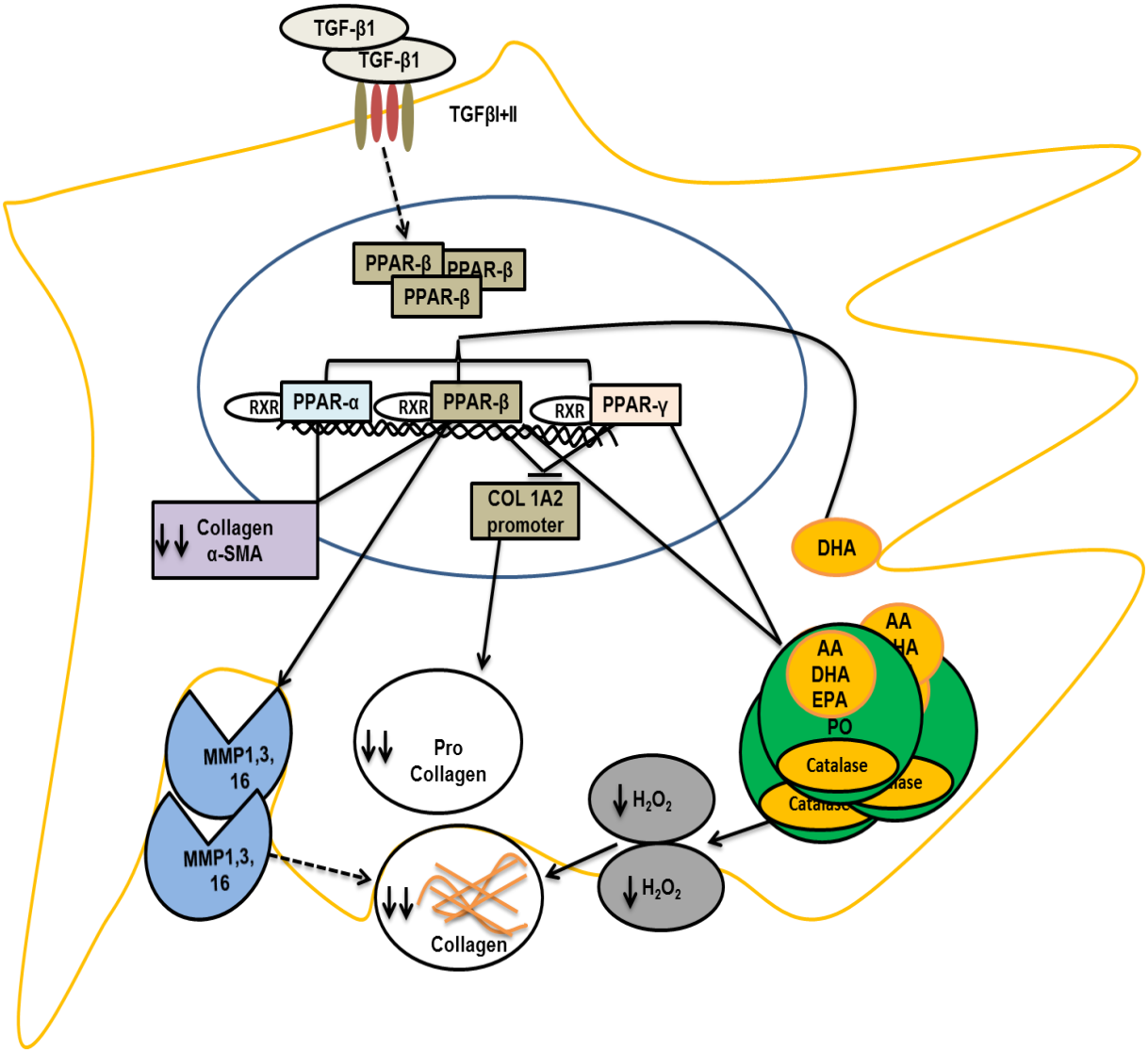

Figure 19. Schematic representation of the molecular involvement of PPARs and catalase in pulmonary fibrosis resolution.

TGF-β1 increases PPAR-β level and activation of PPAR-β upregulates MMP1, 3 and 16 which may degrade synthesized collagen. Collagen and α-SMA are downregulated following the activation of PPAR-α and PPAR-β. Activation of PPAR-β together with PPAR-γ proliferated peroxisomes (PO) and inhibited *COL1A2* promoter which further regulated collagen production. Catalase degraded H_2O_2 via redox-sensitive transcription factors to inhibit the induction of collagen production by the molecule. Coupled activation of PPAR-β and PPAR-γ regulated fatty acid metabolism and DHA stimulated the receptors, forming an activation-loop after induction of the receptors with synthetic drugs. [Arachidonic acid (AA), docosahexaenoic acid (DHA), and eicosapentaenoic acid (EPA) are synthesized in peroxisomes by β-oxidation].

4.16. Outlook

The investigating of the pathobiology of IPF is a broad research area and for that matter, some future experiments are recommended to progress knowledge in this field. There is the need to identify the sequence of PPRE at the promotor region of collagen 1A2 and also establish the protein-DNA interactions between PPARs and possible PPRE regions of all collagen promoters in various lung cell types involved in the pathogenesis of IPF. Future studies can also employ nucleotide deletion techniques to ascertain the most important sites necessary for the repression of the promoters.

It is also suggested that the initiation and progression of aberrant repair after lung injuries in individuals is principally dependent on differences in cellular response, cell components, and metabolism. As a result, the probability of developing lung fibrosis may relate to these processes which might be different in individuals. For instance, IPF is mainly diagnosed in adults after age 50, hence associates aging as risk factor in developing the disease. A comprehensive proteomics profiling of lung tissues from young healthy adults and individuals aged 50 and above, might reveal potential molecules that are deteriorated with age. The identified molecular targets can be assessed in IPF patients and then compared to established standards to inform future molecular targets in IPF studies.

Future studies in IPF are recommended to concentrate on proteins such as collagen I, III, V, IV and VIII including, elastin, fibronectin, tenascin, laminin, heparin sulfate and hyaluronan which are part of the ECM. Additionally, the modulation of collagen and ECM proteins in Bleomycin-induced lung fibrosis mouse model following local activation of PPAR-β/δ and PPAR-γ in the lung is suggested as well as treatment of explanted control and IPF lung biopsies in culture. Additionally, regarding the role of catalase in IPF, there is the need to establish the antifibrotic effects of catalase using Bleomycin-induced lung fibrosis model in acatalasemic mice and also elucidate whether H_2O_2 might be a potential profibrotic molecule for better phenotypic characterization of fibrosis in mouse.

Finally, the effect of combined activation of PPAR-β/δ and PPAR-γ on migration and invasion may be desirous in cancer research. Combined activation of PPAR-β/δ and PPAR-γ could be implicated in migration and invasion pathways to understand the metastasis of cells and tissues in cancer. However, this suggestion might be cell type dependent.

5. Summary

Idiopathic pulmonary fibrosis (IPF) is a devastating disease with median survival of patients of 2.5-3.5 years after diagnosis. The causes and molecular pathogenesis of persistent extracellular matrix production and collagen deposition in idiopathic pulmonary fibrosis still remains unclear. Novel treatments for this restrictive lung disease are limited, and available ones, e.g. nintedanib and pirfenidone, only delay the further progression of IPF. Molecular targets for the treatment of IPF have delineated the anti-fibrotic properties of a family of nuclear hormone receptors known as peroxisome proliferator-activated receptors (PPARs), amongst which mainly the PPAR-γ isotype was investigated. Only limited information is available on the roles of PPAR-α in IPF and no studies are yet available on PPAR-δ/β in pulmonary fibrosis. Additionally, oxidative stress, caused by an increase of reactive oxygen species (ROS), is an important triggering factor influencing the molecular pathogenesis of IPF. The prospects of antioxidants as combined therapy with other treatment regimens for IPF and the regulatory roles of PPARs on peroxisomal genes call for the exploration of catalase function, the major antioxidative enzyme in peroxisomes, in IPF fibroblasts. Also the influence of metabolites of peroxisomal β-oxidation in the molecular pathogenesis of IPF is completely unknown. In view of this, in the present study the potential roles of PPAR-mediated peroxisomal anti-oxidative function and β-oxidation products in IPF were explored.

Using primary human lung fibroblasts from control and IPF patients as well as lung biopsies from patients and bleomycin-treated mice, the beneficial anti-fibrotic properties of PPAR-β (and its combination with PPAR-γ), peroxisomal β-oxidation products and catalase were demonstrated. Control human lung fibroblasts in primary cell culture exhibited higher α-SMA, collagen I and TGFBR1 abundance than IPF primary human lung fibroblasts, whereas the extracellular abundance of secreted collagen I exhibited no significant differences between the two cell groups under basal cell culture conditions. The levels of active TGF-β1 released into culture media by control fibroblasts were comparatively higher than the amounts released by IPF fibroblasts under these conditions. Lung tissue of different IPF patients showed increased PPAR-β/δ abundance and IPF fibroblasts exhibited higher levels and expressions of PPAR-α and PPAR-γ than control fibroblasts under basal conditions. Moreover, after TGF-β1 stimulation PPAR-β/δ was induced in control and IPF primary human lung fibroblasts. Without TGF-β1 treatment all groups of control primary human lung fibroblasts proliferated more than IPF fibroblasts. TGF-β1 stimulation led to a highly significant increase of IPF fibroblast proliferation (1.91 fold higher OD values) than in control fibroblasts (1.4 fold OD

increase). Moreover, mRNA expression values for matrix metalloproteinases (1/2/3/8/10/12) were significantly lower in IPF fibroblasts compared to controls.
Interestingly, remarkably lower abundance levels of α-SMA and collagen I were observed when PPAR-β/δ was activated in TGF-β1 stimulated control and IPF fibroblasts and the combined activation of all three PPARs elicited stronger anti-fibrotic effects. Sole PPAR-α or PPAR-γ activation showed similar, but weaker effects as PPAR-β/δ activation.
Active MMP1 was strongly increased in Western blots after PPAR-β/δ activation as well as after its combined stimulation with PPAR-α or PPAR-γ in control and IPF primary human lung fibroblasts. PPAR-β/δ activation strongly upregulated MMP 1, 3 and 16-mRNAs in both cell groups. Unexpectedly, the MMP1-siRNA knockdown decreased collagen I abundance due to a strong compensatory upregulation of MMPs 3, 10, 12 and 16 in control and IPF primary human lung fibroblasts. Additionally, MMPs 7, 11, 13, 14 and 19 were strongly upregulated in control primary human lung fibroblasts.

Simultaneous parallel activation of PPAR-β/δ and PPAR-γ increased peroxisome biogenesis and proliferation, exhibited stable decreases in α-SMA and collagen I, and increased the extracellular levels of peroxisome-derived arachidonic acid (AA), docosahexaenoic acid (DHA), eicosapentaenoic acid (EPA) and in TGF-β1 stimulated control and IPF human lung fibroblasts. Combined activation of PPAR-β and PPAR-γ also decreased the migration of IPF primary human lung fibroblasts, as well as their invasion into the lower chamber of a modified Boyden chamber. Docosahexaenoic acid (DHA), an endogenous ligand of PPAR-α, PPAR-β/δ and PPAR-γ, downregulated α-SMA and collagen I in both cell groups, suggesting an activation loop after combined stimulation of PPAR-β/δ and PPAR-γ with synthetic compounds. Combined inhibitions of PPAR-β/δ and PPAR-γ were effective after 48 h of treatments and resulted in a remarkable increase in collagen I and α-SMA in IPF primary human lung fibroblasts. A synthetic dual agonist for PPAR-β/δ and PPAR-γ (V6) revealed anti-fibrotic responses intracellularly but could not lower extracellular collagen levels.

Interestingly, TGFβ1 downregulated catalase abundance and activity enhancing the progression into a fibrotic phenotype in control and IPF primary human lung fibroblasts. Furthermore, peroxisomal catalase and the mRNA for peroxiredoxins 1, 5 were markedly decreased in IPF primary human lung fibroblasts. Moreover, catalase was also decreased in IPF human lung biopsies. In contrast, glutathione peroxidases 1 and 2 detected with an antibody against both proteins were increased, possibly compensated for this deficiency

though it is understandable that only glutathione peroxidase 1 is in peroxisomes. Also in the Bleomycin-induced lung fibrosis mouse model catalase gradually decreased in the lung tissue starting from the seventh day after Bleomycin administration. In control and IPF primary human lung fibroblasts catalase overexpression elicited an additive effect to the anti-fibrotic properties of PPAR-β/δ and PPAR-γ and also reduced ROS production. In contrast, inhibition of catalase increased collagen I and ROS production. Additionally, stable catalase knockdown cells showed increased expression of the collagen I mRNA and protein abundance. Moreover, catalase siRNA knockdown in control and IPF primary human lung fibroblasts resulted in increased secretion of extracellular collagen and *COL1A1* gene expression.

Hydrogen peroxide concentrations increased in catalase knockdown cell lines (control primary human lung fibroblast) compared to experimental controls. Moreover, TGF-β1 treatment of catalase knockdown cell line further increased H_2O_2 released into the culture medium. Hydrogen peroxide promoted an increase of abundance of collagen only at 10 mM (highest concentration used in experiment) in control primary human lung fibroblasts, whereas in IPF fibroblasts, there was a consistent increased response to collagen production after treatments with lower concentrations of H_2O_2 (500 μM, 1 mM and 5 mM).

In summary, PPAR-β in combination with PPAR-γ reversed the fibrotic phenotype, increased peroxisomal biogenesis and peroxisomal β-oxidation. Peroxisome-derived docosahexaenoic acid is involved in the regulation of intracellular collagen I levels and peroxisomal catalase plays important role in the regulation of intra- and extracellular collagen. The study therefore underscores potential therapeutic roles of peroxisomes in prevention of IPF progression.

6. Zusammenfassung

Idiopathische Lungenfibrose (IPF) ist eine verheerende Krankheit mit medianer Überlebenszeit von Patienten von 2,5 bis 3,5 Jahren nach der Diagnose. Die Ursachen und molekulare Pathogenese der persistierenden extrazellulären Matrixproduktion und Kollagenablagerung bei idiopathischer Lungenfibrose sind noch unklar. Neuartige Behandlungsstrategien für diese restriktive Lungenerkrankung sind begrenzt und verfügbare, z.B. Nintedanib und Perfirnidon, verzögern nur die weitere Progression von IPF. Molekulare Ziele für die Behandlung von IPF haben die antifibrotischen Eigenschaften einer Familie von nukleären Hormonrezeptoren, den Peroxisomen-Proliferator-aktivierte Rezeptoren (PPARs), aufgezeigt, von denen hauptsächlich der PPAR-γ-Isotyp untersucht wurde. Über die Rolle von PPAR-α in IPF sind nur begrenzte Informationen verfügbar, und es liegen noch keine Studien zu PPAR-δ/β bei Lungenfibrose vor. Darüber hinaus ist oxidativer Stress ein wichtiger auslösender Faktor, der die molekulare Pathogenese von IPF beeinflusst. Das Potential von Antioxidantien in Kombinationstherapie mit anderen Behandlungsmöglichkeiten für IPF und die regulatorische Wirkung von PPARs auf peroxisomale Gene, weisen auf die notwendige Erforschung der Katalase-Funktion- dem wichtigsten antioxidativen Enzym in Peroxisomen - in IPF-Fibroblasten hin. Darüber hinaus ist auch der Einfluss von Metaboliten der peroxisomalen β-Oxidation auf die molekulare Pathogenese von IPF völlig unbekannt. Vor diesem Hintergrund wurden in der vorliegenden Doktorarbeit die möglichen Rollen von PPAR-vermittelter peroxisomaler antioxidativer Funktion und β-Oxidationsprodukten in IPF untersucht.

Unter Verwendung von primären humanen Lungenfibroblasten von Kontroll- und IPF-Patienten sowie Lungenbiopsien von Patienten und Bleomycin-behandelten Mäusen, wurden in dieser Dissertation die günstigen anti-fibrotischen Eigenschaften von PPAR-β (und seine Kombination mit PPAR-γ), peroxisomalen β-Oxidationsprodukten sowie Katalase gezeigt. Erste Ergebnisse erbrachten, dass einige Lungenbereiche, die für α-SMA - einem Marker, der häufig in der Literatur für aktivierte Myofibroblasten verwendet wird - angefärbt wurden, keine Kollagen-I-Färbungen zeigten. Darüber hinaus besaßen menschliche Lungenfibroblasten der Kontrollgruppen in primärer Zellkultur höhere α-SMA-, Kollagen I- und TGFBR1-Proteinmengen als IPF-primäre menschliche Lungenfibroblasten, wohingegen die extrazelluläre Menge sekretierten Kollagens I keine signifikanten Unterschiede zwischen den zwei Zellgruppen unter basalen Zellkulturbedingungen aufwies. Die Mengen an aktivem TGF-β1, die von Kontrollfibroblasten in Kulturmedien freigesetzt wurden, waren vergleichsweise höher als die Mengen, die von IPF-Fibroblasten unter den gleichen

Bedingungen freigesetzt wurden. Lungengewebe von verschiedenen IPF-Patienten wies erhöhte PPAR-β/δ-Abundanz auf und IPF-Fibroblasten zeigten eine erhöhte Expression von PPAR-α und PPAR-γ als Kontroll-Fibroblasten unter basalen Bedingungen. Darüber hinaus wurde PPAR-β/δ nach TGF-β1-Stimulation in primären humanen Lungen-Fibroblasten der Kontrolle und IPF induziert. Ohne TGF-β1-Behandlung proliferierten alle Gruppen von primären menschlichen Lungenfibroblasten der Kontrollgruppen stärker als IPF-Fibroblasten. TGF-β1-Stimulation führte zu einer hochsignifikanten Zunahme der IPF-Fibroblasten-proliferation (1,91-fach höhere OD-Werte) als bei Kontrollfibroblasten (1,4-fache Zunahme). Darüber hinaus waren die mRNA-Expressionswerte für Matrixmetalloproteinasen (1/2/3/8/10/12) in IPF-Fibroblasten signifikant niedriger. Interessanterweise wurden stark erniedrigte Mengen an α-SMA und Kollagen I beobachtet, wenn PPAR-β/δ in TGF-β1-stimulierten Kontroll- und IPF-Fibroblasten aktiviert wurde. Die Aktivierung aller drei PPARs rief noch stärkere anti-fibrotische Wirkungen hervor. PPAR-α- oder PPAR-γ-Aktivierung zeigte ähnliche, jedoch schwächere Wirkungen wie PPAR-β / δ-Aktivierung.

Aktives MMP1 war nach PPAR-β/δ-Aktivierung sowie nach kombinierter Behandlung mit PPAR-α oder PPAR-γ in Western-Blots stark erhöht. Die PPAR-β/δ-Aktivierung führte in beiden Zellgruppen zu einer stark erhöhten mRNA-Expression für MMPs 1, 3 und 16. Unerwarteterweise verringerte der MMP1-siRNA-Knockdown den Kollagen I-Gehalt aufgrund einer starken kompensatorischen Hochregulierung der MMPs 3, 10, 12 und 16 in beiden Fibroblastengruppen (Kontrolle und IPF). Zusätzlich waren die mRNAs der MMPs 7, 11, 13, 14 und 19 in der Kontrollgruppe stark hochreguliert.

Die gleichzeitige parallele Aktivierung von PPAR-β/δ und PPAR-γ induzierte die Biogenese und Proliferation von Peroxisomen, führte zur eindeutigen Verminderung von α-SMA und Kollagen I und steigerte den Metabolismus von Arachidonsäure (AA), Docosahexaensäure (DHA) und Eicosapentaensäure (EPA) in TGF-β1-stimulierten humanen Lungenfibroblasten der Kontroll- und IPF-Gruppen. Die kombinierte Aktivierung von PPAR-β und PPAR-γ verminderte auch die Migration von IPF-Lungenfibroblasten sowie ihre Invasion in zerkratzte Räume in Scratch-Assays. Behandlung mit Docosahexaensäure (DHA) verringerte die Mengen an α-SMA und Kollagen I beiden Zellgruppen, was auf eine Aktivierungsschleife nach kombinierter Stimulation von PPAR-β/δ und PPAR-γ hindeutet. Die kombinierte Inhibition von PPAR-β/δ und PPAR-γ war nach 48 h Behandlung wirksam und führte zu einer starken Zunahme von Kollagen I und α-SMA in IPF-Lungenfibroblasten. Ein kommerziell erhältlicher, dualer synthetischer Einzelmolekular Agonist für PPAR-β/δ und

PPAR-γ (V6) zeigte zwar intrazelluläre antifibrotische Reaktionen, konnte jedoch die extrazellulären Kollagenspiegel nicht absenken.

Interessanterweise senkte TGF-β1 die Katalase-Abundanz und –Aktivität und führte damit zu einer Verstärkung des Fibrose-phänotyps in primären Kontroll- und IPF-Lungenfibroblasten. Darüber hinaus waren in dieser Studie die Katalase und die mRNA für peroxisomalen Peroxiredoxine 1 und 5 in primären IPF-Lungenfibroblasten deutlich verringert. Ferner war auch die Katalase-Proteinenge in menschlichen Lungenbiopsien von IPF-Patienten verringert, während die Glutathionperoxidasen 1 und 2 induziert warer, mösglicherweise um den Katalasemangel zu kompensieren. Gewebeproben von Mauslungen eines Bleomycin-induzierten Lungenfibrosemodells zeigten ebenfalls eine allmähliche Abnahme der Katalase bereits nach dem siebten Tag der Bleomycin Verabreichung. Katalase-Überexpression rief einen additiven Effekt auf die antifibrotischen Eigenschaften von PPAR-β/δ und PPAR-γ hervor und reduzierte auch die ROS-Produktion in primären Lungenfibroblasten der Kontroll- und IPF- Gruppen. Dagegen führte die Hemmung der Katalaseaktivität zur erhöhten Produktion von Kollagen I und ROS. Zusätzlich zeigten stabile Katalase-Knockdown-Zellen erhöhte Expression des Kollagen-I-Gens und eine vermehrte Kollagen I-Protein-Abundanz. Der Katalase-siRNA-Knockdown in Kontroll- und IPF-Lungenfibroblasten führte auch zu einer erhöhten Freisetzung von extrazellulärem Kollagen und *COL1A1*-Genexpression. Die Wasserstoffperoxidkonzentration stieg in der Katalase-Knockdown-Zelllinie im Vergleich zur experimentellen Kontrollgruppe an. Darüber hinaus verstärkte die TGF-β1-Behandlung der Katalase-Knockdown-Zelllinie die Erhöhung des freigesetzten H_2O_2 ins Kulturmedium. In Kontroll-Lungenfibroblasten erhöhte nur die höchste Konzentration von H_2O_2 (10 mM) die Kollagenfreisetzung, während in IPF-Fibroblasten bereits geringe H_2O_2 Konzentrationen von 500 μM, 1 mM und 5 mM die Kollagenmengen steigerten.

Zusammenfassend vermindert die Behandlung mit einer Kombination von PPAR-β- und PPAR-γ-Aktivatoren den fibrotischen Phänotyp, erhöht die peroxisomale Biogenese und peroxisomale β-Oxidation. Docosahexaensäure und peroxisomale Katalase sind an der Regulation des fibrotischen Phänotyps von IPF-Fibroblasten und der intrazellulären Kollagen I-Menge beteiligt, was die mögliche therapeutische Rolle von Peroxisomen zur Verbinderung der IPF-Progression.

7. References

1. Tomasek, J.J., et al., *Myofibroblasts and mechano-regulation of connective tissue remodelling.* Nat Rev Mol Cell Biol, 2002. **3**(5): p. 349-63.
2. Borthwick, L.A., T.A. Wynn, and A.J. Fisher, *Cytokine mediated tissue fibrosis.* Biochim Biophys Acta, 2013. **1832**(7): p. 1049-60.
3. Scadding, J.G. and K.F. Hinson, *Diffuse fibrosing alveolitis (diffuse interstitial fibrosis of the lungs). Correlation of histology at biopsy with prognosis.* Thorax, 1967. **22**(4): p. 291-304.
4. Scotton, C.J. and R.C. Chambers, *Molecular targets in pulmonary fibrosis: the myofibroblast in focus.* Chest, 2007. **132**(4): p. 1311-21.
5. Raghu, G., et al., *Incidence and prevalence of idiopathic pulmonary fibrosis.* Am J Respir Crit Care Med, 2006. **174**(7): p. 810-6.
6. Behr, J., et al., *Management of patients with idiopathic pulmonary fibrosis in clinical practice: the INSIGHTS-IPF registry.* Eur Respir J, 2015. **46**(1): p. 186-96.
7. Kaunisto, J., et al., *Idiopathic pulmonary fibrosis--a systematic review on methodology for the collection of epidemiological data.* BMC Pulm Med, 2013. **13**: p. 53.
8. Trawinska, M.A., R.D. Rupesinghe, and S.P. Hart, *Patient considerations and drug selection in the treatment of idiopathic pulmonary fibrosis.* Ther Clin Risk Manag, 2016. **12**: p. 563-74.
9. Agabiti, N., et al., *Idiopathic Pulmonary Fibrosis (IPF) incidence and prevalence in Italy.* Sarcoidosis Vasc Diffuse Lung Dis, 2014. **31**(3): p. 191-7.
10. Ley, B. and H.R. Collard, *Epidemiology of idiopathic pulmonary fibrosis.* Clin Epidemiol, 2013. **5**: p. 483-92.
11. Nakamura, Y. and T. Suda, *Idiopathic Pulmonary Fibrosis: Diagnosis and Clinical Manifestations.* Clin Med Insights Circ Respir Pulm Med, 2015. **9**(Suppl 1): p. 163-71.
12. Denham, J.W. and M. Hauer-Jensen, *The radiotherapeutic injury--a complex 'wound'.* Radiother Oncol, 2002. **63**(2): p. 129-45.
13. Chen, J. and J. Stubbe, *Bleomycins: towards better therapeutics.* Nat Rev Cancer, 2005. **5**(2): p. 102-12.
14. Kelly, B.G., et al., *A rearranged form of Epstein-Barr virus DNA is associated with idiopathic pulmonary fibrosis.* Am J Respir Crit Care Med, 2002. **166**(4): p. 510-3.
15. Tang, Y.W., et al., *Herpesvirus DNA is consistently detected in lungs of patients with idiopathic pulmonary fibrosis.* J Clin Microbiol, 2003. **41**(6): p. 2633-40.
16. Kishaba, T., *Practical management of Idiopathic Pulmonary Fibrosis.* Sarcoidosis Vasc Diffuse Lung Dis, 2015. **32**(2): p. 90-8.
17. Collard, H.R., et al., *Acute exacerbations of idiopathic pulmonary fibrosis.* Am J Respir Crit Care Med, 2007. **176**(7): p. 636-43.
18. Richeldi, L., et al., *Efficacy and safety of nintedanib in idiopathic pulmonary fibrosis.* N Engl J Med, 2014. **370**(22): p. 2071-82.
19. King, T.E., Jr., et al., *A phase 3 trial of pirfenidone in patients with idiopathic pulmonary fibrosis.* N Engl J Med, 2014. **370**(22): p. 2083-92.
20. Swigris, J.J., et al., *Idiopathic pulmonary fibrosis: challenges and opportunities for the clinician and investigator.* Chest, 2005. **127**(1): p. 275-83.
21. Kistler, K.D., et al., *Lung transplantation in idiopathic pulmonary fibrosis: a systematic review of the literature.* BMC Pulm Med, 2014. **14**: p. 139.
22. Simionescu, M., *Cellular components of the air-blood barrier.* J Cell Mol Med, 2001. **5**(3): p. 320-1.
23. Timpl, R. and J.C. Brown, *Supramolecular assembly of basement membranes.* Bioessays, 1996. **18**(2): p. 123-32.

24. Wynn, T.A., *Common and unique mechanisms regulate fibrosis in various fibroproliferative diseases.* J Clin Invest, 2007. **117**(3): p. 524-9.
25. Clark, R.A., *Basics of cutaneous wound repair.* J Dermatol Surg Oncol, 1993. **19**(8): p. 693-706.
26. Wynn, T.A., *Cellular and molecular mechanisms of fibrosis.* J Pathol, 2008. **214**(2): p. 199-210.
27. McDonald, J.A., *Idiopathic pulmonary fibrosis. A paradigm for lung injury and repair.* Chest, 1991. **99**(3 Suppl): p. 87S-93S.
28. Strieter, R.M., *Pathogenesis and natural history of usual interstitial pneumonia: the whole story or the last chapter of a long novel.* Chest, 2005. **128**(5 Suppl 1): p. 526S-532S.
29. Sisson, T.H., et al., *Targeted injury of type II alveolar epithelial cells induces pulmonary fibrosis.* Am J Respir Crit Care Med, 2010. **181**(3): p. 254-63.
30. Rahman, I. and W. MacNee, *Oxidative stress and regulation of glutathione in lung inflammation.* Eur Respir J, 2000. **16**(3): p. 534-54.
31. Rahman, I. and W. MacNee, *Role of oxidants/antioxidants in smoking-induced lung diseases.* Free Radic Biol Med, 1996. **21**(5): p. 669-81.
32. Winterbourn, C.C., *Reconciling the chemistry and biology of reactive oxygen species.* Nat Chem Biol, 2008. **4**(5): p. 278-86.
33. Brennan, F.M., R.N. Maini, and M. Feldmann, *Cytokine expression in chronic inflammatory disease.* Br Med Bull, 1995. **51**(2): p. 368-84.
34. Rahman, I. and W. MacNee, *Role of transcription factors in inflammatory lung diseases.* Thorax, 1998. **53**(7): p. 601-12.
35. Kliment, C.R. and T.D. Oury, *Oxidative stress, extracellular matrix targets, and idiopathic pulmonary fibrosis.* Free Radic Biol Med, 2010. **49**(5): p. 707-17.
36. Cheresh, P., et al., *Oxidative stress and pulmonary fibrosis.* Biochim Biophys Acta, 2013. **1832**(7): p. 1028-40.
37. Gharaee-Kermani, M., et al., *Recent advances in molecular targets and treatment of idiopathic pulmonary fibrosis: focus on TGFbeta signaling and the myofibroblast.* Curr Med Chem, 2009. **16**(11): p. 1400-17.
38. Davies, H.R., L. Richeldi, and E.H. Walters, *Immunomodulatory agents for idiopathic pulmonary fibrosis.* Cochrane Database Syst Rev, 2003(3): p. CD003134.
39. Lawrence, D.A., *Transforming growth factor-beta: a general review.* Eur Cytokine Netw, 1996. **7**(3): p. 363-74.
40. Border, W.A. and N.A. Noble, *Transforming growth factor beta in tissue fibrosis.* N Engl J Med, 1994. **331**(19): p. 1286-92.
41. Gentry, L.E. and B.W. Nash, *The pro domain of pre-pro-transforming growth factor beta 1 when independently expressed is a functional binding protein for the mature growth factor.* Biochemistry, 1990. **29**(29): p. 6851-7.
42. Miyazono, K., et al., *Latent high molecular weight complex of transforming growth factor beta 1. Purification from human platelets and structural characterization.* J Biol Chem, 1988. **263**(13): p. 6407-15.
43. Taipale, J., et al., *Latent transforming growth factor-beta 1 associates to fibroblast extracellular matrix via latent TGF-beta binding protein.* J Cell Biol, 1994. **124**(1-2): p. 171-81.
44. Oklu, R. and R. Hesketh, *The latent transforming growth factor beta binding protein (LTBP) family.* Biochem J, 2000. **352 Pt 3**: p. 601-10.

45. Flaumenhaft, R., et al., *Basic fibroblast growth factor-induced activation of latent transforming growth factor beta in endothelial cells: regulation of plasminogen activator activity.* J Cell Biol, 1992. **118**(4): p. 901-9.
46. Sato, Y. and D.B. Rifkin, *Inhibition of endothelial cell movement by pericytes and smooth muscle cells: activation of a latent transforming growth factor-beta 1-like molecule by plasmin during co-culture.* J Cell Biol, 1989. **109**(1): p. 309-15.
47. Yu, Q. and I. Stamenkovic, *Cell surface-localized matrix metalloproteinase-9 proteolytically activates TGF-beta and promotes tumor invasion and angiogenesis.* Genes Dev, 2000. **14**(2): p. 163-76.
48. Schultz-Cherry, S. and J.E. Murphy-Ullrich, *Thrombospondin causes activation of latent transforming growth factor-beta secreted by endothelial cells by a novel mechanism.* J Cell Biol, 1993. **122**(4): p. 923-32.
49. Mu, D., et al., *The integrin alpha(v)beta8 mediates epithelial homeostasis through MT1-MMP-dependent activation of TGF-beta1.* J Cell Biol, 2002. **157**(3): p. 493-507.
50. Assoian, R.K., et al., *Transforming growth factor-beta in human platelets. Identification of a major storage site, purification, and characterization.* J Biol Chem, 1983. **258**(11): p. 7155-60.
51. Cheifetz, S., B. Like, and J. Massague, *Cellular distribution of type I and type II receptors for transforming growth factor-beta.* J Biol Chem, 1986. **261**(21): p. 9972-8.
52. Cheifetz, S., et al., *The transforming growth factor-beta system, a complex pattern of cross-reactive ligands and receptors.* Cell, 1987. **48**(3): p. 409-15.
53. Kubiczkova, L., et al., *TGF-beta - an excellent servant but a bad master.* J Transl Med, 2012. **10**: p. 183.
54. Rahimi, R.A. and E.B. Leof, *TGF-beta signaling: a tale of two responses.* J Cell Biochem, 2007. **102**(3): p. 593-608.
55. Huang, F. and Y.G. Chen, *Regulation of TGF-beta receptor activity.* Cell Biosci, 2012. **2**: p. 9.
56. Esparza-Lopez, J., et al., *Ligand binding and functional properties of betaglycan, a co-receptor of the transforming growth factor-beta superfamily. Specialized binding regions for transforming growth factor-beta and inhibin A.* J Biol Chem, 2001. **276**(18): p. 14588-96.
57. Souchelnytskyi, S., et al., *Phosphorylation of Ser165 in TGF-beta type I receptor modulates TGF-beta1-induced cellular responses.* EMBO J, 1996. **15**(22): p. 6231-40.
58. Wrana, J.L., et al., *Mechanism of activation of the TGF-beta receptor.* Nature, 1994. **370**(6488): p. 341-7.
59. Huse, M., et al., *The TGF beta receptor activation process: an inhibitor- to substrate-binding switch.* Mol Cell, 2001. **8**(3): p. 671-82.
60. Shi, Y. and J. Massague, *Mechanisms of TGF-beta signaling from cell membrane to the nucleus.* Cell, 2003. **113**(6): p. 685-700.
61. Hata, A. and B.N. Davis, *Control of microRNA biogenesis by TGFbeta signaling pathway-A novel role of Smads in the nucleus.* Cytokine Growth Factor Rev, 2009. **20**(5-6): p. 517-21.
62. Mu, Y., S.K. Gudey, and M. Landstrom, *Non-Smad signaling pathways.* Cell Tissue Res, 2012. **347**(1): p. 11-20.
63. Morikawa, M., et al., *Genome-wide mechanisms of Smad binding.* Oncogene, 2013. **32**(13): p. 1609-15.
64. Massague, J., J. Seoane, and D. Wotton, *Smad transcription factors.* Genes Dev, 2005. **19**(23): p. 2783-810.
65. Derynck, R. and Y.E. Zhang, *Smad-dependent and Smad-independent pathways in TGF-beta family signalling.* Nature, 2003. **425**(6958): p. 577-84.

66. Kang, J.S., C. Liu, and R. Derynck, *New regulatory mechanisms of TGF-beta receptor function.* Trends Cell Biol, 2009. **19**(8): p. 385-94.
67. Hartsough, M.T. and K.M. Mulder, *Transforming growth factor beta activation of p44mapk in proliferating cultures of epithelial cells.* J Biol Chem, 1995. **270**(13): p. 7117-24.
68. Park, S.S., et al., *Involvement of c-Src kinase in the regulation of TGF-beta1-induced apoptosis.* Oncogene, 2004. **23**(37): p. 6272-81.
69. Yu, L., M.C. Hebert, and Y.E. Zhang, *TGF-beta receptor-activated p38 MAP kinase mediates Smad-independent TGF-beta responses.* EMBO J, 2002. **21**(14): p. 3749-59.
70. Yu, N., et al., *Overexpression of transforming growth factor beta1 in malignant prostate cells is partly caused by a runaway of TGF-beta1 auto-induction mediated through a defective recruitment of protein phosphatase 2A by TGF-beta type I receptor.* Urology, 2010. **76**(6): p. 1519 e8-13.
71. Watanabe, Y., et al., *TMEPAI, a transmembrane TGF-beta-inducible protein, sequesters Smad proteins from active participation in TGF-beta signaling.* Mol Cell, 2010. **37**(1): p. 123-34.
72. Gomis, R.R., et al., *A FoxO-Smad synexpression group in human keratinocytes.* Proc Natl Acad Sci U S A, 2006. **103**(34): p. 12747-52.
73. Gomis, R.R., et al., *C/EBPbeta at the core of the TGFbeta cytostatic response and its evasion in metastatic breast cancer cells.* Cancer Cell, 2006. **10**(3): p. 203-14.
74. Koinuma, D., et al., *Chromatin immunoprecipitation on microarray analysis of Smad2/3 binding sites reveals roles of ETS1 and TFAP2A in transforming growth factor beta signaling.* Mol Cell Biol, 2009. **29**(1): p. 172-86.
75. Silvestri, C., et al., *Genome-wide identification of Smad/Foxh1 targets reveals a role for Foxh1 in retinoic acid regulation and forebrain development.* Dev Cell, 2008. **14**(3): p. 411-23.
76. Feng, X.H., et al., *The tumor suppressor Smad4/DPC4 and transcriptional adaptor CBP/p300 are coactivators for smad3 in TGF-beta-induced transcriptional activation.* Genes Dev, 1998. **12**(14): p. 2153-63.
77. Janknecht, R., N.J. Wells, and T. Hunter, *TGF-beta-stimulated cooperation of smad proteins with the coactivators CBP/p300.* Genes Dev, 1998. **12**(14): p. 2114-9.
78. Bataller, R. and D.A. Brenner, *Liver fibrosis.* J Clin Invest, 2005. **115**(2): p. 209-18.
79. Bergeron, A., et al., *Cytokine profiles in idiopathic pulmonary fibrosis suggest an important role for TGF-beta and IL-10.* Eur Respir J, 2003. **22**(1): p. 69-76.
80. Coker, R.K., et al., *Transforming growth factors-beta 1, -beta 2, and -beta 3 stimulate fibroblast procollagen production in vitro but are differentially expressed during bleomycin-induced lung fibrosis.* Am J Pathol, 1997. **150**(3): p. 981-91.
81. Ellmers, L.J., et al., *Transforming growth factor-beta blockade down-regulates the renin-angiotensin system and modifies cardiac remodeling after myocardial infarction.* Endocrinology, 2008. **149**(11): p. 5828-34.
82. Tzortzaki, E.G., et al., *Effects of antifibrotic agents on TGF-beta1, CTGF and IFN-gamma expression in patients with idiopathic pulmonary fibrosis.* Respir Med, 2007. **101**(8): p. 1821-9.
83. Kolb, M., et al., *Differences in the fibrogenic response after transfer of active transforming growth factor-beta1 gene to lungs of "fibrosis-prone" and "fibrosis-resistant" mouse strains.* Am J Respir Cell Mol Biol, 2002. **27**(2): p. 141-50.
84. Liu, R.M., et al., *Transforming growth factor beta suppresses glutamate-cysteine ligase gene expression and induces oxidative stress in a lung fibrosis model.* Free Radic Biol Med, 2012. **53**(3): p. 554-63.

85. Giri, S.N., D.M. Hyde, and M.A. Hollinger, *Effect of antibody to transforming growth factor beta on bleomycin induced accumulation of lung collagen in mice.* Thorax, 1993. **48**(10): p. 959-66.
86. Higashiyama, H., et al., *Inhibition of activin receptor-like kinase 5 attenuates bleomycin-induced pulmonary fibrosis.* Exp Mol Pathol, 2007. **83**(1): p. 39-46.
87. Liu, R.M. and L.P. Desai, *Reciprocal regulation of TGF-beta and reactive oxygen species: A perverse cycle for fibrosis.* Redox Biol, 2015. **6**: p. 565-77.
88. Serini, G., et al., *The fibronectin domain ED-A is crucial for myofibroblastic phenotype induction by transforming growth factor-beta1.* J Cell Biol, 1998. **142**(3): p. 873-81.
89. Kuhn, C. and J.A. McDonald, *The roles of the myofibroblast in idiopathic pulmonary fibrosis. Ultrastructural and immunohistochemical features of sites of active extracellular matrix synthesis.* Am J Pathol, 1991. **138**(5): p. 1257-65.
90. Desmouliere, A., I.A. Darby, and G. Gabbiani, *Normal and pathologic soft tissue remodeling: role of the myofibroblast, with special emphasis on liver and kidney fibrosis.* Lab Invest, 2003. **83**(12): p. 1689-707.
91. Evans, R.A., et al., *TGF-beta1-mediated fibroblast-myofibroblast terminal differentiation-the role of Smad proteins.* Exp Cell Res, 2003. **282**(2): p. 90-100.
92. Cai, G.Q., et al., *Neuronal Wiskott-Aldrich syndrome protein (N-WASP) is critical for formation of alpha-smooth muscle actin filaments during myofibroblast differentiation.* Am J Physiol Lung Cell Mol Physiol, 2012. **303**(8): p. L692-702.
93. Zhang, K., et al., *In situ hybridization analysis of rat lung alpha 1(I) and alpha 2(I) collagen gene expression in pulmonary fibrosis induced by endotracheal bleomycin injection.* Lab Invest, 1994. **70**(2): p. 192-202.
94. Samarakoon, R., J.M. Overstreet, and P.J. Higgins, *TGF-beta signaling in tissue fibrosis: redox controls, target genes and therapeutic opportunities.* Cell Signal, 2013. **25**(1): p. 264-8.
95. Harvey, K.A., et al., *Diverse signaling pathways regulate fibroblast differentiation and transformation through Rho kinase activation.* J Cell Physiol, 2007. **211**(2): p. 353-63.
96. Ward, P.A. and G.W. Hunninghake, *Lung inflammation and fibrosis.* Am J Respir Crit Care Med, 1998. **157**(4 Pt 2): p. S123-9.
97. Balaban, R.S., S. Nemoto, and T. Finkel, *Mitochondria, oxidants, and aging.* Cell, 2005. **120**(4): p. 483-95.
98. Gonzalez, F.J., *Role of cytochromes P450 in chemical toxicity and oxidative stress: studies with CYP2E1.* Mutat Res, 2005. **569**(1-2): p. 101-10.
99. Schrader, M. and H.D. Fahimi, *Mammalian peroxisomes and reactive oxygen species.* Histochem Cell Biol, 2004. **122**(4): p. 383-93.
100. Ishikawa, F., et al., *A mitochondrial thioredoxin-sensitive mechanism regulates TGF-beta-mediated gene expression associated with epithelial-mesenchymal transition.* Biochem Biophys Res Commun, 2014. **443**(3): p. 821-7.
101. Bracey, N.A., et al., *Mitochondrial NLRP3 protein induces reactive oxygen species to promote Smad protein signaling and fibrosis independent from the inflammasome.* J Biol Chem, 2014. **289**(28): p. 19571-84.
102. Church, D.F. and W.A. Pryor, *Free-radical chemistry of cigarette smoke and its toxicological implications.* Environ Health Perspect, 1985. **64**: p. 111-26.
103. Cho, A.K., et al., *Redox activity of airborne particulate matter at different sites in the Los Angeles Basin.* Environ Res, 2005. **99**(1): p. 40-7.
104. Comhair, S.A., M.J. Thomassen, and S.C. Erzurum, *Differential induction of extracellular glutathione peroxidase and nitric oxide synthase 2 in airways of healthy individuals exposed to 100% O(2) or cigarette smoke.* Am J Respir Cell Mol Biol, 2000. **23**(3): p. 350-4.

105. Chiu, S.M., et al., *Copper ion-mediated sensitization of nuclear matrix attachment sites to ionizing radiation.* Biochemistry, 1993. **32**(24): p. 6214-9.
106. Stohs, S.J. and D. Bagchi, *Oxidative mechanisms in the toxicity of metal ions.* Free Radic Biol Med, 1995. **18**(2): p. 321-36.
107. Stadtman, E.R., *Role of oxidant species in aging.* Curr Med Chem, 2004. **11**(9): p. 1105-12.
108. Birben, E., et al., *Oxidative stress and antioxidant defense.* World Allergy Organ J, 2012. **5**(1): p. 9-19.
109. Asami, S., et al., *Cigarette smoking induces an increase in oxidative DNA damage, 8-hydroxydeoxyguanosine, in a central site of the human lung.* Carcinogenesis, 1997. **18**(9): p. 1763-6.
110. Roum, J.H., et al., *Systemic deficiency of glutathione in cystic fibrosis.* J Appl Physiol (1985), 1993. **75**(6): p. 2419-24.
111. Tirouvanziam, R., et al., *High-dose oral N-acetylcysteine, a glutathione prodrug, modulates inflammation in cystic fibrosis.* Proc Natl Acad Sci U S A, 2006. **103**(12): p. 4628-33.
112. Boots, A.W., et al., *Antioxidant status associated with inflammation in sarcoidosis: a potential role for antioxidants.* Respir Med, 2009. **103**(3): p. 364-72.
113. Islam, K.N., et al., *TGF-beta1 triggers oxidative modifications and enhances apoptosis in HIT cells through accumulation of reactive oxygen species by suppression of catalase and glutathione peroxidase.* Free Radic Biol Med, 1997. **22**(6): p. 1007-17.
114. Michaeloudes, C., et al., *TGF-beta regulates Nox4, MnSOD and catalase expression, and IL-6 release in airway smooth muscle cells.* Am J Physiol Lung Cell Mol Physiol, 2011. **300**(2): p. L295-304.
115. Peltoniemi, M., et al., *Expression of glutaredoxin is highly cell specific in human lung and is decreased by transforming growth factor-beta in vitro and in interstitial lung diseases in vivo.* Hum Pathol, 2004. **35**(8): p. 1000-7.
116. Gao, F., et al., *Extracellular superoxide dismutase in pulmonary fibrosis.* Antioxid Redox Signal, 2008. **10**(2): p. 343-54.
117. Cui, Y., et al., *Oxidative stress contributes to the induction and persistence of TGF-beta1 induced pulmonary fibrosis.* Int J Biochem Cell Biol, 2011. **43**(8): p. 1122-33.
118. Oshino, N., et al., *The role of H 2 O 2 generation in perfused rat liver and the reaction of catalase compound I and hydrogen donors.* Arch Biochem Biophys, 1973. **154**(1): p. 117-31.
119. Kirkman, H.N., G.F. Gaetani, and E.H. Clemons, *NADP-binding proteins causing reduced availability and sigmoid release of NADP+ in human erythrocytes.* J Biol Chem, 1986. **261**(9): p. 4039-45.
120. White, E., J.S. Shannon, and R.E. Patterson, *Relationship between vitamin and calcium supplement use and colon cancer.* Cancer Epidemiol Biomarkers Prev, 1997. **6**(10): p. 769-74.
121. El-Agamey, A., et al., *Carotenoid radical chemistry and antioxidant/pro-oxidant properties.* Arch Biochem Biophys, 2004. **430**(1): p. 37-48.
122. Masella, R., et al., *Novel mechanisms of natural antioxidant compounds in biological systems: involvement of glutathione and glutathione-related enzymes.* J Nutr Biochem, 2005. **16**(10): p. 577-86.
123. French, C.S., *Temperature Characteristics for the Metabolism of Chlorella : Iii. The Catalytic Decomposition of Hydrogen Peroxide by Chlorella Pyrenoidosa.* J Gen Physiol, 1934. **18**(2): p. 209-13.
124. Koppenol, W.H., *The centennial of the Fenton reaction.* Free Radic Biol Med, 1993. **15**(6): p. 645-51.
125. Weidinger, A. and A.V. Kozlov, *Biological Activities of Reactive Oxygen and Nitrogen Species: Oxidative Stress versus Signal Transduction.* Biomolecules, 2015. **5**(2): p. 472-84.

126. Cadet, J. and J.R. Wagner, *Oxidatively generated base damage to cellular DNA by hydroxyl radical and one-electron oxidants: similarities and differences.* Arch Biochem Biophys, 2014. **557**: p. 47-54.
127. Salgo, M.G., G.L. Squadrito, and W.A. Pryor, *Peroxynitrite causes apoptosis in rat thymocytes.* Biochem Biophys Res Commun, 1995. **215**(3): p. 1111-8.
128. Panasenko, O.M., et al., *Hypochlorite induces lipid peroxidation in blood lipoproteins and phospholipid liposomes.* Free Radic Biol Med, 1995. **19**(2): p. 133-40.
129. Schrader, M. and H.D. Fahimi, *Peroxisomes and oxidative stress.* Biochim Biophys Acta, 2006. **1763**(12): p. 1755-66.
130. Dhaunsi, G.S., et al., *NADPH oxidase in human lung fibroblasts.* J Biomed Sci, 2004. **11**(5): p. 617-22.
131. Hecker, L., et al., *NADPH oxidase-4 mediates myofibroblast activation and fibrogenic responses to lung injury.* Nat Med, 2009. **15**(9): p. 1077-81.
132. Mueller, C.F., et al., *ATVB in focus: redox mechanisms in blood vessels.* Arterioscler Thromb Vasc Biol, 2005. **25**(2): p. 274-8.
133. Jenkins, R.H., et al., *Myofibroblastic differentiation leads to hyaluronan accumulation through reduced hyaluronan turnover.* J Biol Chem, 2004. **279**(40): p. 41453-60.
134. Ito, T., et al., *Hyaluronan regulates transforming growth factor-beta1 receptor compartmentalization.* J Biol Chem, 2004. **279**(24): p. 25326-32.
135. Meran, S., et al., *Hyaluronan facilitates transforming growth factor-beta1-mediated fibroblast proliferation.* J Biol Chem, 2008. **283**(10): p. 6530-45.
136. Meran, S., et al., *Hyaluronan facilitates transforming growth factor-beta1-dependent proliferation via CD44 and epidermal growth factor receptor interaction.* J Biol Chem, 2011. **286**(20): p. 17618-30.
137. Simpson, R.M., et al., *Aging fibroblasts resist phenotypic maturation because of impaired hyaluronan-dependent CD44/epidermal growth factor receptor signaling.* Am J Pathol, 2010. **176**(3): p. 1215-28.
138. Midgley, A.C., et al., *Transforming growth factor-beta1 (TGF-beta1)-stimulated fibroblast to myofibroblast differentiation is mediated by hyaluronan (HA)-facilitated epidermal growth factor receptor (EGFR) and CD44 co-localization in lipid rafts.* J Biol Chem, 2013. **288**(21): p. 14824-38.
139. Maltseva, O., et al., *Fibroblast growth factor reversal of the corneal myofibroblast phenotype.* Invest Ophthalmol Vis Sci, 2001. **42**(11): p. 2490-5.
140. Wettlaufer, S.H., et al., *Reversal of the Transcriptome by Prostaglandin E2 during Myofibroblast Dedifferentiation.* Am J Respir Cell Mol Biol, 2016. **54**(1): p. 114-27.
141. Bringardner, B.D., et al., *The role of inflammation in the pathogenesis of idiopathic pulmonary fibrosis.* Antioxid Redox Signal, 2008. **10**(2): p. 287-301.
142. Standiford, T.J., et al., *Macrophage inflammatory protein-1 alpha expression in interstitial lung disease.* J Immunol, 1993. **151**(5): p. 2852-63.
143. Car, B.D., et al., *Elevated IL-8 and MCP-1 in the bronchoalveolar lavage fluid of patients with idiopathic pulmonary fibrosis and pulmonary sarcoidosis.* Am J Respir Crit Care Med, 1994. **149**(3 Pt 1): p. 655-9.
144. Antoniou, K.M., et al., *Different angiogenic activity in pulmonary sarcoidosis and idiopathic pulmonary fibrosis.* Chest, 2006. **130**(4): p. 982-8.
145. Fowlkes, J.L. and M.K. Winkler, *Exploring the interface between metallo-proteinase activity and growth factor and cytokine bioavailability.* Cytokine Growth Factor Rev, 2002. **13**(3): p. 277-87.

146. Taipale, J. and J. Keski-Oja, *Growth factors in the extracellular matrix.* FASEB J, 1997. **11**(1): p. 51-9.
147. Hasegawa, M., et al., *Elevated serum tumor necrosis factor-alpha levels in patients with systemic sclerosis: association with pulmonary fibrosis.* J Rheumatol, 1997. **24**(4): p. 663-5.
148. Piguet, P.F., et al., *Expression and localization of tumor necrosis factor-alpha and its mRNA in idiopathic pulmonary fibrosis.* Am J Pathol, 1993. **143**(3): p. 651-5.
149. Miyazaki, Y., et al., *Expression of a tumor necrosis factor-alpha transgene in murine lung causes lymphocytic and fibrosing alveolitis. A mouse model of progressive pulmonary fibrosis.* J Clin Invest, 1995. **96**(1): p. 250-9.
150. Siwik, D.A., D.L. Chang, and W.S. Colucci, *Interleukin-1beta and tumor necrosis factor-alpha decrease collagen synthesis and increase matrix metalloproteinase activity in cardiac fibroblasts in vitro.* Circ Res, 2000. **86**(12): p. 1259-65.
151. Thavarajah, K., et al., *Pulmonary complications of tumor necrosis factor-targeted therapy.* Respir Med, 2009. **103**(5): p. 661-9.
152. Kolb, M., et al., *Transient expression of IL-1beta induces acute lung injury and chronic repair leading to pulmonary fibrosis.* J Clin Invest, 2001. **107**(12): p. 1529-36.
153. Wynn, T.A., *Integrating mechanisms of pulmonary fibrosis.* J Exp Med, 2011. **208**(7): p. 1339-50.
154. Lappalainen, U., et al., *Interleukin-1beta causes pulmonary inflammation, emphysema, and airway remodeling in the adult murine lung.* Am J Respir Cell Mol Biol, 2005. **32**(4): p. 311-8.
155. Wilson, M.S., et al., *Bleomycin and IL-1beta-mediated pulmonary fibrosis is IL-17A dependent.* J Exp Med, 2010. **207**(3): p. 535-52.
156. Kinder, B.W., et al., *Baseline BAL neutrophilia predicts early mortality in idiopathic pulmonary fibrosis.* Chest, 2008. **133**(1): p. 226-32.
157. Nuovo, G.J., et al., *The distribution of immunomodulatory cells in the lungs of patients with idiopathic pulmonary fibrosis.* Mod Pathol, 2012. **25**(3): p. 416-33.
158. Feghali-Bostwick, C.A., et al., *Cellular and humoral autoreactivity in idiopathic pulmonary fibrosis.* J Immunol, 2007. **179**(4): p. 2592-9.
159. Pene, J., et al., *Chronically inflamed human tissues are infiltrated by highly differentiated Th17 lymphocytes.* J Immunol, 2008. **180**(11): p. 7423-30.
160. Kuwabara, T., et al., *The Role of IL-17 and Related Cytokines in Inflammatory Autoimmune Diseases.* Mediators Inflamm, 2017. **2017**: p. 3908061.
161. Furuie, H., et al., *Altered accessory cell function of alveolar macrophages: a possible mechanism for induction of Th2 secretory profile in idiopathic pulmonary fibrosis.* Eur Respir J, 1997. **10**(4): p. 787-94.
162. Jakubzick, C., et al., *Augmented pulmonary IL-4 and IL-13 receptor subunit expression in idiopathic interstitial pneumonia.* J Clin Pathol, 2004. **57**(5): p. 477-86.
163. Keane, M.P., et al., *IL-12 attenuates bleomycin-induced pulmonary fibrosis.* Am J Physiol Lung Cell Mol Physiol, 2001. **281**(1): p. L92-7.
164. Kuwano, K., et al., *P21Waf1/Cip1/Sdi1 and p53 expression in association with DNA strand breaks in idiopathic pulmonary fibrosis.* Am J Respir Crit Care Med, 1996. **154**(2 Pt 1): p. 477-83.
165. Plataki, M., et al., *Expression of apoptotic and antiapoptotic markers in epithelial cells in idiopathic pulmonary fibrosis.* Chest, 2005. **127**(1): p. 266-74.
166. Sakai, N. and A.M. Tager, *Fibrosis of two: Epithelial cell-fibroblast interactions in pulmonary fibrosis.* Biochim Biophys Acta, 2013. **1832**(7): p. 911-21.

167. Cool, C.D., et al., *Fibroblast foci are not discrete sites of lung injury or repair: the fibroblast reticulum.* Am J Respir Crit Care Med, 2006. **174**(6): p. 654-8.
168. Yamada, M., et al., *Dual-immunohistochemistry provides little evidence for epithelial-mesenchymal transition in pulmonary fibrosis.* Histochem Cell Biol, 2008. **129**(4): p. 453-62.
169. Kalluri, R. and E.G. Neilson, *Epithelial-mesenchymal transition and its implications for fibrosis.* J Clin Invest, 2003. **112**(12): p. 1776-84.
170. Pan, L.H., et al., *Type II alveolar epithelial cells and interstitial fibroblasts express connective tissue growth factor in IPF.* Eur Respir J, 2001. **17**(6): p. 1220-7.
171. Andersson-Sjoland, A., et al., *Fibrocytes are a potential source of lung fibroblasts in idiopathic pulmonary fibrosis.* Int J Biochem Cell Biol, 2008. **40**(10): p. 2129-40.
172. Mehrad, B., et al., *Circulating peripheral blood fibrocytes in human fibrotic interstitial lung disease.* Biochem Biophys Res Commun, 2007. **353**(1): p. 104-8.
173. Mercer, P.F., et al., *Pulmonary epithelium is a prominent source of proteinase-activated receptor-1-inducible CCL2 in pulmonary fibrosis.* Am J Respir Crit Care Med, 2009. **179**(5): p. 414-25.
174. Strieter, R.M., et al., *The role of circulating mesenchymal progenitor cells (fibrocytes) in the pathogenesis of pulmonary fibrosis.* J Leukoc Biol, 2009. **86**(5): p. 1111-8.
175. Ekert, J.E., et al., *Chemokine (C-C motif) ligand 2 mediates direct and indirect fibrotic responses in human and murine cultured fibrocytes.* Fibrogenesis Tissue Repair, 2011. **4**(1): p. 23.
176. Todd, N.W., I.G. Luzina, and S.P. Atamas, *Molecular and cellular mechanisms of pulmonary fibrosis.* Fibrogenesis Tissue Repair, 2012. **5**(1): p. 11.
177. Taille, C., et al., *Identification of periplakin as a new target for autoreactivity in idiopathic pulmonary fibrosis.* Am J Respir Crit Care Med, 2011. **183**(6): p. 759-66.
178. Arras, M., et al., *Interleukin-9 reduces lung fibrosis and type 2 immune polarization induced by silica particles in a murine model.* Am J Respir Cell Mol Biol, 2001. **24**(4): p. 368-75.
179. Arras, M., et al., *B lymphocytes are critical for lung fibrosis control and prostaglandin E2 regulation in IL-9 transgenic mice.* Am J Respir Cell Mol Biol, 2006. **34**(5): p. 573-80.
180. Schultz, G.S. and A. Wysocki, *Interactions between extracellular matrix and growth factors in wound healing.* Wound Repair Regen, 2009. **17**(2): p. 153-62.
181. Lu, P., V.M. Weaver, and Z. Werb, *The extracellular matrix: a dynamic niche in cancer progression.* J Cell Biol, 2012. **196**(4): p. 395-406.
182. Olczyk, P., L. Mencner, and K. Komosinska-Vassev, *The role of the extracellular matrix components in cutaneous wound healing.* Biomed Res Int, 2014. **2014**: p. 747584.
183. Akram, K.M., et al., *Lung Regeneration: Endogenous and Exogenous Stem Cell Mediated Therapeutic Approaches.* Int J Mol Sci, 2016. **17**(1).
184. Liang, J., et al., *Role of hyaluronan and hyaluronan-binding proteins in human asthma.* J Allergy Clin Immunol, 2011. **128**(2): p. 403-411 e3.
185. Dunsmore, S.E. and D.E. Rannels, *Extracellular matrix biology in the lung.* Am J Physiol, 1996. **270**(1 Pt 1): p. L3-27.
186. Suki, B., et al., *Biomechanics of the lung parenchyma: critical roles of collagen and mechanical forces.* J Appl Physiol (1985), 2005. **98**(5): p. 1892-9.
187. Montes, G.S., *Structural biology of the fibres of the collagenous and elastic systems.* Cell Biol Int, 1996. **20**(1): p. 15-27.
188. Santos, F.B., et al., *Time course of lung parenchyma remodeling in pulmonary and extrapulmonary acute lung injury.* J Appl Physiol (1985), 2006. **100**(1): p. 98-106.
189. Rocco, P.R., et al., *Lung tissue mechanics and extracellular matrix remodeling in acute lung injury.* Am J Respir Crit Care Med, 2001. **164**(6): p. 1067-71.

190. Miserocchi, G., et al., *Pulmonary interstitial pressure in intact in situ lung: transition to interstitial edema.* J Appl Physiol (1985), 1993. **74**(3): p. 1171-7.
191. Johnson, Z., A.E. Proudfoot, and T.M. Handel, *Interaction of chemokines and glycosaminoglycans: a new twist in the regulation of chemokine function with opportunities for therapeutic intervention.* Cytokine Growth Factor Rev, 2005. **16**(6): p. 625-36.
192. Hynes, R.O., *The extracellular matrix: not just pretty fibrils.* Science, 2009. **326**(5957): p. 1216-9.
193. Page-McCaw, A., A.J. Ewald, and Z. Werb, *Matrix metalloproteinases and the regulation of tissue remodelling.* Nat Rev Mol Cell Biol, 2007. **8**(3): p. 221-33.
194. Cox, T.R. and J.T. Erler, *Remodeling and homeostasis of the extracellular matrix: implications for fibrotic diseases and cancer.* Dis Model Mech, 2011. **4**(2): p. 165-78.
195. Liu, F., et al., *Feedback amplification of fibrosis through matrix stiffening and COX-2 suppression.* J Cell Biol, 2010. **190**(4): p. 693-706.
196. Tschumperlin, D.J., *Matrix, mesenchyme, and mechanotransduction.* Ann Am Thorac Soc, 2015. **12 Suppl 1**: p. S24-9.
197. Klingberg, F., B. Hinz, and E.S. White, *The myofibroblast matrix: implications for tissue repair and fibrosis.* J Pathol, 2013. **229**(2): p. 298-309.
198. Moeller, A., et al., *Circulating fibrocytes are an indicator of poor prognosis in idiopathic pulmonary fibrosis.* Am J Respir Crit Care Med, 2009. **179**(7): p. 588-94.
199. Maharaj, S.S., et al., *Fibrocytes in chronic lung disease--facts and controversies.* Pulm Pharmacol Ther, 2012. **25**(4): p. 263-7.
200. Li, Y., et al., *Severe lung fibrosis requires an invasive fibroblast phenotype regulated by hyaluronan and CD44.* J Exp Med, 2011. **208**(7): p. 1459-71.
201. White, E.S., et al., *Integrin alpha4beta1 regulates migration across basement membranes by lung fibroblasts: a role for phosphatase and tensin homologue deleted on chromosome 10.* Am J Respir Crit Care Med, 2003. **168**(4): p. 436-42.
202. Sisson, T.H., et al., *Increased survivin expression contributes to apoptosis-resistance in IPF fibroblasts.* Adv Biosci Biotechnol, 2012. **3**(6A): p. 657-664.
203. Chang, W., et al., *SPARC suppresses apoptosis of idiopathic pulmonary fibrosis fibroblasts through constitutive activation of beta-catenin.* J Biol Chem, 2010. **285**(11): p. 8196-206.
204. Moodley, Y.P., et al., *Fibroblasts isolated from normal lungs and those with idiopathic pulmonary fibrosis differ in interleukin-6/gp130-mediated cell signaling and proliferation.* Am J Pathol, 2003. **163**(1): p. 345-54.
205. Wilborn, J., et al., *Cultured lung fibroblasts isolated from patients with idiopathic pulmonary fibrosis have a diminished capacity to synthesize prostaglandin E2 and to express cyclooxygenase-2.* J Clin Invest, 1995. **95**(4): p. 1861-8.
206. Nho, R.S., et al., *Pathological alteration of FoxO3a activity promotes idiopathic pulmonary fibrosis fibroblast proliferation on type i collagen matrix.* Am J Pathol, 2011. **179**(5): p. 2420-30.
207. *American Thoracic Society. Idiopathic pulmonary fibrosis: diagnosis and treatment. International consensus statement. American Thoracic Society (ATS), and the European Respiratory Society (ERS).* Am J Respir Crit Care Med, 2000. **161**(2 Pt 1): p. 646-64.
208. Raghu, G., et al., *An official ATS/ERS/JRS/ALAT statement: idiopathic pulmonary fibrosis: evidence-based guidelines for diagnosis and management.* Am J Respir Crit Care Med, 2011. **183**(6): p. 788-824.
209. Cavazza, A., et al., *The role of histology in idiopathic pulmonary fibrosis: an update.* Respir Med, 2010. **104 Suppl 1**: p. S11-22.

210. Fukuda, Y., et al., *Significance of early intra-alveolar fibrotic lesions and integrin expression in lung biopsy specimens from patients with idiopathic pulmonary fibrosis.* Hum Pathol, 1995. **26**(1): p. 53-61.
211. Katzenstein, A.L., et al., *Usual interstitial pneumonia: histologic study of biopsy and explant specimens.* Am J Surg Pathol, 2002. **26**(12): p. 1567-77.
212. Katzenstein, A.L., S. Mukhopadhyay, and J.L. Myers, *Diagnosis of usual interstitial pneumonia and distinction from other fibrosing interstitial lung diseases.* Hum Pathol, 2008. **39**(9): p. 1275-94.
213. Hanak, V., et al., *Profusion of fibroblast foci in patients with idiopathic pulmonary fibrosis does not predict outcome.* Respir Med, 2008. **102**(6): p. 852-6.
214. Nishimura, K., et al., *Usual interstitial pneumonia: histologic correlation with high-resolution CT.* Radiology, 1992. **182**(2): p. 337-42.
215. Johkoh, T., et al., *Idiopathic interstitial pneumonias: diagnostic accuracy of thin-section CT in 129 patients.* Radiology, 1999. **211**(2): p. 555-60.
216. Strieter, R.M. and B. Mehrad, *New mechanisms of pulmonary fibrosis.* Chest, 2009. **136**(5): p. 1364-70.
217. Macias-Barragan, J., et al., *The multifaceted role of pirfenidone and its novel targets.* Fibrogenesis Tissue Repair, 2010. **3**: p. 16.
218. Conte, E., et al., *Effect of pirfenidone on proliferation, TGF-beta-induced myofibroblast differentiation and fibrogenic activity of primary human lung fibroblasts.* Eur J Pharm Sci, 2014. **58**: p. 13-9.
219. Hilberg, F., et al., *BIBF 1120: triple angiokinase inhibitor with sustained receptor blockade and good antitumor efficacy.* Cancer Res, 2008. **68**(12): p. 4774-82.
220. Chaudhary, N.I., et al., *Inhibition of PDGF, VEGF and FGF signalling attenuates fibrosis.* Eur Respir J, 2007. **29**(5): p. 976-85.
221. Tobin, R.W., et al., *Increased prevalence of gastroesophageal reflux in patients with idiopathic pulmonary fibrosis.* Am J Respir Crit Care Med, 1998. **158**(6): p. 1804-8.
222. Lee, J.S., et al., *Anti-acid treatment and disease progression in idiopathic pulmonary fibrosis: an analysis of data from three randomised controlled trials.* Lancet Respir Med, 2013. **1**(5): p. 369-76.
223. *Unilateral lung transplantation for pulmonary fibrosis. Toronto Lung Transplant Group.* N Engl J Med, 1986. **314**(18): p. 1140-5.
224. Nishiyama, O., et al., *Effects of pulmonary rehabilitation in patients with idiopathic pulmonary fibrosis.* Respirology, 2008. **13**(3): p. 394-9.
225. Tzouvelekis, A., F. Bonella, and P. Spagnolo, *Update on therapeutic management of idiopathic pulmonary fibrosis.* Ther Clin Risk Manag, 2015. **11**: p. 359-70.
226. Lee, C.H., P. Olson, and R.M. Evans, *Minireview: lipid metabolism, metabolic diseases, and peroxisome proliferator-activated receptors.* Endocrinology, 2003. **144**(6): p. 2201-7.
227. Desvergne, B. and W. Wahli, *Peroxisome proliferator-activated receptors: nuclear control of metabolism.* Endocr Rev, 1999. **20**(5): p. 649-88.
228. Wahli, W., *Peroxisome proliferator-activated receptors (PPARs): from metabolic control to epidermal wound healing.* Swiss Med Wkly, 2002. **132**(7-8): p. 83-91.
229. Fajas, L., J.C. Fruchart, and J. Auwerx, *PPARgamma3 mRNA: a distinct PPARgamma mRNA subtype transcribed from an independent promoter.* FEBS Lett, 1998. **438**(1-2): p. 55-60.
230. Fajas, L., et al., *The organization, promoter analysis, and expression of the human PPARgamma gene.* J Biol Chem, 1997. **272**(30): p. 18779-89.
231. Evans, R.M., G.D. Barish, and Y.X. Wang, *PPARs and the complex journey to obesity.* Nat Med, 2004. **10**(4): p. 355-61.

232. Berger, J. and D.E. Moller, *The mechanisms of action of PPARs.* Annu Rev Med, 2002. **53**: p. 409-35.
233. Lalloyer, F. and B. Staels, *Fibrates, glitazones, and peroxisome proliferator-activated receptors.* Arterioscler Thromb Vasc Biol, 2010. **30**(5): p. 894-9.
234. Feige, J.N., et al., *From molecular action to physiological outputs: peroxisome proliferator-activated receptors are nuclear receptors at the crossroads of key cellular functions.* Prog Lipid Res, 2006. **45**(2): p. 120-59.
235. Willson, T.M., M.H. Lambert, and S.A. Kliewer, *Peroxisome proliferator-activated receptor gamma and metabolic disease.* Annu Rev Biochem, 2001. **70**: p. 341-67.
236. Guan, Y. and M.D. Breyer, *Peroxisome proliferator-activated receptors (PPARs): novel therapeutic targets in renal disease.* Kidney Int, 2001. **60**(1): p. 14-30.
237. Fajas, L., M.B. Debril, and J. Auwerx, *Peroxisome proliferator-activated receptor-gamma: from adipogenesis to carcinogenesis.* J Mol Endocrinol, 2001. **27**(1): p. 1-9.
238. Guri, A.J., et al., *The role of T cell PPAR gamma in mice with experimental inflammatory bowel disease.* BMC Gastroenterol, 2010. **10**: p. 60.
239. Delerive, P., J.C. Fruchart, and B. Staels, *Peroxisome proliferator-activated receptors in inflammation control.* J Endocrinol, 2001. **169**(3): p. 453-9.
240. Chinetti, G., J.C. Fruchart, and B. Staels, *Peroxisome proliferator-activated receptors (PPARs): nuclear receptors at the crossroads between lipid metabolism and inflammation.* Inflamm Res, 2000. **49**(10): p. 497-505.
241. Werman, A., et al., *Ligand-independent activation domain in the N terminus of peroxisome proliferator-activated receptor gamma (PPARgamma). Differential activity of PPARgamma1 and -2 isoforms and influence of insulin.* J Biol Chem, 1997. **272**(32): p. 20230-5.
242. Kliewer, S.A., et al., *Convergence of 9-cis retinoic acid and peroxisome proliferator signalling pathways through heterodimer formation of their receptors.* Nature, 1992. **358**(6389): p. 771-4.
243. Monsalve, F.A., et al., *Peroxisome proliferator-activated receptor targets for the treatment of metabolic diseases.* Mediators Inflamm, 2013. **2013**: p. 549627.
244. Juge-Aubry, C., et al., *DNA binding properties of peroxisome proliferator-activated receptor subtypes on various natural peroxisome proliferator response elements. Importance of the 5'-flanking region.* J Biol Chem, 1997. **272**(40): p. 25252-9.
245. Horlein, A.J., et al., *Ligand-independent repression by the thyroid hormone receptor mediated by a nuclear receptor co-repressor.* Nature, 1995. **377**(6548): p. 397-404.
246. Chen, J.D. and R.M. Evans, *A transcriptional co-repressor that interacts with nuclear hormone receptors.* Nature, 1995. **377**(6548): p. 454-7.
247. Toyama, T., et al., *PPARalpha ligands activate antioxidant enzymes and suppress hepatic fibrosis in rats.* Biochem Biophys Res Commun, 2004. **324**(2): p. 697-704.
248. Ogata, T., et al., *Stimulation of peroxisome-proliferator-activated receptor alpha (PPAR alpha) attenuates cardiac fibrosis and endothelin-1 production in pressure-overloaded rat hearts.* Clin Sci (Lond), 2002. **103 Suppl 48**: p. 284S-288S.
249. Genovese, T., et al., *Role of endogenous and exogenous ligands for the peroxisome proliferator-activated receptor alpha in the development of bleomycin-induced lung injury.* Shock, 2005. **24**(6): p. 547-55.
250. Lakatos, H.F., et al., *The Role of PPARs in Lung Fibrosis.* PPAR Res, 2007. **2007**: p. 71323.
251. Milam, J.E., et al., *PPAR-gamma agonists inhibit profibrotic phenotypes in human lung fibroblasts and bleomycin-induced pulmonary fibrosis.* Am J Physiol Lung Cell Mol Physiol, 2008. **294**(5): p. L891-901.

252. Lin, Q., et al., *Rosiglitazone inhibits migration, proliferation, and phenotypic differentiation in cultured human lung fibroblasts.* Exp Lung Res, 2010. **36**(2): p. 120-8.
253. Ferguson, H.E., et al., *Electrophilic peroxisome proliferator-activated receptor-gamma ligands have potent antifibrotic effects in human lung fibroblasts.* Am J Respir Cell Mol Biol, 2009. **41**(6): p. 722-30.
254. Burgess, H.A., et al., *PPARgamma agonists inhibit TGF-beta induced pulmonary myofibroblast differentiation and collagen production: implications for therapy of lung fibrosis.* Am J Physiol Lung Cell Mol Physiol, 2005. **288**(6): p. L1146-53.
255. Chen, L., et al., *Oleoylethanolamide, an endogenous PPAR-alpha ligand, attenuates liver fibrosis targeting hepatic stellate cells.* Oncotarget, 2015. **6**(40): p. 42530-40.
256. Reynders, V., et al., *Peroxisome proliferator-activated receptor alpha (PPAR alpha) down-regulation in cystic fibrosis lymphocytes.* Respir Res, 2006. **7**: p. 104.
257. Qin, Y.W., et al., *Simvastatin inhibited cardiac hypertrophy and fibrosis in apolipoprotein E-deficient mice fed a "Western-style diet" by increasing PPAR alpha and gamma expression and reducing TC, MMP-9, and Cat S levels.* Acta Pharmacol Sin, 2010. **31**(10): p. 1350-8.
258. Li, S., et al., *Proximal tubule PPARalpha attenuates renal fibrosis and inflammation caused by unilateral ureteral obstruction.* Am J Physiol Renal Physiol, 2013. **305**(5): p. F618-27.
259. Kostadinova, R., et al., *GW501516-activated PPARbeta/delta promotes liver fibrosis via p38-JNK MAPK-induced hepatic stellate cell proliferation.* Cell Biosci, 2012. **2**(1): p. 34.
260. Stockert, J., et al., *Reverse crosstalk of TGFbeta and PPARbeta/delta signaling identified by transcriptional profiling.* Nucleic Acids Res, 2011. **39**(1): p. 119-31.
261. Gao, F., et al., *TRPV1 Activation Attenuates High-Salt Diet-Induced Cardiac Hypertrophy and Fibrosis through PPAR-delta Upregulation.* PPAR Res, 2014. **2014**: p. 491963.
262. Chang, W.T., J.T. Cheng, and Z.C. Chen, *Telmisartan improves cardiac fibrosis in diabetes through peroxisome proliferator activated receptor delta (PPARdelta): from bedside to bench.* Cardiovasc Diabetol, 2016. **15**(1): p. 113.
263. Ramirez, A., E.N. Ballard, and J. Roman, *TGFbeta1 Controls PPARgamma Expression, Transcriptional Potential, and Activity, in Part, through Smad3 Signaling in Murine Lung Fibroblasts.* PPAR Res, 2012. **2012**: p. 375876.
264. Kulkarni, A.A., et al., *PPAR-gamma ligands repress TGFbeta-induced myofibroblast differentiation by targeting the PI3K/Akt pathway: implications for therapy of fibrosis.* PLoS One, 2011. **6**(1): p. e15909.
265. Ghosh, A.K., et al., *Constitutive Smad signaling and Smad-dependent collagen gene expression in mouse embryonic fibroblasts lacking peroxisome proliferator-activated receptor-gamma.* Biochem Biophys Res Commun, 2008. **374**(2): p. 231-6.
266. Hao, G.H., et al., *Agonists at PPAR-gamma suppress angiotensin II-induced production of plasminogen activator inhibitor-1 and extracellular matrix in rat cardiac fibroblasts.* Br J Pharmacol, 2008. **153**(7): p. 1409-19.
267. Hou, X., et al., *MicroRNA-27a promotes renal tubulointerstitial fibrosis via suppressing PPARgamma pathway in diabetic nephropathy.* Oncotarget, 2016. **7**(30): p. 47760-47776.
268. Zhu, H.Y., et al., *Peroxisome proliferator-activated receptor-gamma agonist troglitazone suppresses transforming growth factor-beta1 signalling through miR-92b upregulation-inhibited Axl expression in human keloid fibroblasts in vitro.* Am J Transl Res, 2016. **8**(8): p. 3460-70.
269. Scirpo, R., et al., *Stimulation of nuclear receptor peroxisome proliferator-activated receptor-gamma limits NF-kappaB-dependent inflammation in mouse cystic fibrosis biliary epithelium.* Hepatology, 2015. **62**(5): p. 1551-62.

270. Oruqaj, G., et al., *Compromised peroxisomes in idiopathic pulmonary fibrosis, a vicious cycle inducing a higher fibrotic response via TGF-beta signaling.* Proc Natl Acad Sci U S A, 2015. **112**(16): p. E2048-57.
271. Smith, J.J. and J.D. Aitchison, *Peroxisomes take shape.* Nat Rev Mol Cell Biol, 2013. **14**(12): p. 803-17.
272. Grabenbauer, M., et al., *Three-dimensional ultrastructural analysis of peroxisomes in HepG2 cells. Absence of peroxisomal reticulum but evidence of close spatial association with the endoplasmic reticulum.* Cell Biochem Biophys, 2000. **32 Spring**: p. 37-49.
273. Hruban, Z., et al., *Microbodies: constituent organelles of animal cells.* Lab Invest, 1972. **27**(2): p. 184-91.
274. De Duve, C. and P. Baudhuin, *Peroxisomes (microbodies and related particles).* Physiol Rev, 1966. **46**(2): p. 323-57.
275. Islinger, M., et al., *The peroxisome: an update on mysteries.* Histochem Cell Biol, 2012. **137**(5): p. 547-74.
276. Yamamoto, K. and H.D. Fahimi, *Three-dimensional reconstruction of a peroxisomal reticulum in regenerating rat liver: evidence of interconnections between heterogeneous segments.* J Cell Biol, 1987. **105**(2): p. 713-22.
277. Schrader, M., R. Wodopia, and H.D. Fahimi, *Induction of tubular peroxisomes by UV irradiation and reactive oxygen species in HepG2 cells.* J Histochem Cytochem, 1999. **47**(9): p. 1141-8.
278. Ishizuka, M., et al., *Overexpression of human acyl-CoA thioesterase upregulates peroxisome biogenesis.* Exp Cell Res, 2004. **297**(1): p. 127-41.
279. Hoivik, D.J., et al., *Fibrates induce hepatic peroxisome and mitochondrial proliferation without overt evidence of cellular proliferation and oxidative stress in cynomolgus monkeys.* Carcinogenesis, 2004. **25**(9): p. 1757-69.
280. Girzalsky, W., D. Saffian, and R. Erdmann, *Peroxisomal protein translocation.* Biochim Biophys Acta, 2010. **1803**(6): p. 724-31.
281. Smith, J.J., et al., *Transcriptional responses to fatty acid are coordinated by combinatorial control.* Mol Syst Biol, 2007. **3**: p. 115.
282. van Zutphen, T. and I.J. van der Klei, *Quantitative analysis of organelle abundance, morphology and dynamics.* Curr Opin Biotechnol, 2011. **22**: p. 127-32.
283. Rakhshandehroo, M., et al., *Peroxisome proliferator-activated receptor alpha target genes.* PPAR Res, 2010. **2010**.
284. Qian, G., et al., *Peroxisomes in Different Skeletal Cell Types during Intramembranous and Endochondral Ossification and Their Regulation during Osteoblast Differentiation by Distinct Peroxisome Proliferator-Activated Receptors.* PLoS One, 2015. **10**(12): p. e0143439.
285. Gould, S.J. and D. Valle, *Peroxisome biogenesis disorders: genetics and cell biology.* Trends Genet, 2000. **16**(8): p. 340-5.
286. Wanders, R.J. and H.R. Waterham, *Peroxisomal disorders: the single peroxisomal enzyme deficiencies.* Biochim Biophys Acta, 2006. **1763**(12): p. 1707-20.
287. van Roermund, C.W., et al., *The human peroxisomal ABC half transporter ALDP functions as a homodimer and accepts acyl-CoA esters.* FASEB J, 2008. **22**(12): p. 4201-8.
288. Ferdinandusse, S. and S.M. Houten, *Peroxisomes and bile acid biosynthesis.* Biochim Biophys Acta, 2006. **1763**(12): p. 1427-40.
289. Keane, M.H., et al., *Bile acid treatment alters hepatic disease and bile acid transport in peroxisome-deficient PEX2 Zellweger mice.* Hepatology, 2007. **45**(4): p. 982-97.

290. Baumgart, E., et al., *Mitochondrial alterations caused by defective peroxisomal biogenesis in a mouse model for Zellweger syndrome (PEX5 knockout mouse).* Am J Pathol, 2001. **159**(4): p. 1477-94.
291. Pieuchot, L. and G. Jedd, *Peroxisome assembly and functional diversity in eukaryotic microorganisms.* Annu Rev Microbiol, 2012. **66**: p. 237-63.
292. Tam, Y.Y., et al., *Pex3p initiates the formation of a preperoxisomal compartment from a subdomain of the endoplasmic reticulum in Saccharomyces cerevisiae.* J Biol Chem, 2005. **280**(41): p. 34933-9.
293. Hoepfner, D., et al., *Contribution of the endoplasmic reticulum to peroxisome formation.* Cell, 2005. **122**(1): p. 85-95.
294. van der Zand, A., et al., *Biochemically distinct vesicles from the endoplasmic reticulum fuse to form peroxisomes.* Cell, 2012. **149**(2): p. 397-409.
295. Motley, A.M. and E.H. Hettema, *Yeast peroxisomes multiply by growth and division.* J Cell Biol, 2007. **178**(3): p. 399-410.
296. Schrader, M., et al., *Expression of PEX11beta mediates peroxisome proliferation in the absence of extracellular stimuli.* J Biol Chem, 1998. **273**(45): p. 29607-14.
297. Opalinski, L., et al., *Membrane curvature during peroxisome fission requires Pex11.* EMBO J, 2011. **30**(1): p. 5-16.
298. Levak-Frank, S., et al., *Muscle-specific overexpression of lipoprotein lipase causes a severe myopathy characterized by proliferation of mitochondria and peroxisomes in transgenic mice.* J Clin Invest, 1995. **96**(2): p. 976-86.
299. Schrader, M., N.A. Bonekamp, and M. Islinger, *Fission and proliferation of peroxisomes.* Biochim Biophys Acta, 2012. **1822**(9): p. 1343-57.
300. Karnati, S. and E. Baumgart-Vogt, *Peroxisomes in airway epithelia and future prospects of these organelles for pulmonary cell biology.* Histochem Cell Biol, 2009. **131**(4): p. 447-54.
301. Colasante, C., et al., *Peroxisomes in cardiomyocytes and the peroxisome / peroxisome proliferator-activated receptor-loop.* Thromb Haemost, 2015. **113**(3): p. 452-63.
302. Theodoulou, F.L., et al., *Peroxisome membrane proteins: multiple trafficking routes and multiple functions?* Biochem J, 2013. **451**(3): p. 345-52.
303. Jones, J.M., J.C. Morrell, and S.J. Gould, *PEX19 is a predominantly cytosolic chaperone and import receptor for class 1 peroxisomal membrane proteins.* J Cell Biol, 2004. **164**(1): p. 57-67.
304. Matsuzaki, T. and Y. Fujiki, *The peroxisomal membrane protein import receptor Pex3p is directly transported to peroxisomes by a novel Pex19p- and Pex16p-dependent pathway.* J Cell Biol, 2008. **183**(7): p. 1275-86.
305. Walton, P.A., P.E. Hill, and S. Subramani, *Import of stably folded proteins into peroxisomes.* Mol Biol Cell, 1995. **6**(6): p. 675-83.
306. Liu, X., C. Ma, and S. Subramani, *Recent advances in peroxisomal matrix protein import.* Curr Opin Cell Biol, 2012. **24**(4): p. 484-9.
307. Platta, H.W., S. Hagen, and R. Erdmann, *The exportomer: the peroxisomal receptor export machinery.* Cell Mol Life Sci, 2013. **70**(8): p. 1393-411.
308. Platta, H.W., et al., *Ubiquitination of the peroxisomal import receptor Pex5p is required for its recycling.* J Cell Biol, 2007. **177**(2): p. 197-204.
309. Smith, J.J. and J.D. Aitchison, *Regulation of peroxisome dynamics.* Curr Opin Cell Biol, 2009. **21**(1): p. 119-26.
310. Antonenkov, V.D., R.T. Sormunen, and J.K. Hiltunen, *The rat liver peroxisomal membrane forms a permeability barrier for cofactors but not for small metabolites in vitro.* J Cell Sci, 2004. **117**(Pt 23): p. 5633-42.

311. Fransen, M., et al., *Role of peroxisomes in ROS/RNS-metabolism: implications for human disease.* Biochim Biophys Acta, 2012. **1822**(9): p. 1363-73.
312. Wanders, R.J., *Metabolic functions of peroxisomes in health and disease.* Biochimie, 2014. **98**: p. 36-44.
313. Dixit, E., et al., *Peroxisomes are signaling platforms for antiviral innate immunity.* Cell, 2010. **141**(4): p. 668-81.
314. Singh, I., et al., *Lignoceric acid is oxidized in the peroxisome: implications for the Zellweger cerebro-hepato-renal syndrome and adrenoleukodystrophy.* Proc Natl Acad Sci U S A, 1984. **81**(13): p. 4203-7.
315. Wanders, R.J., et al., *Peroxisomal fatty acid alpha- and beta-oxidation in humans: enzymology, peroxisomal metabolite transporters and peroxisomal diseases.* Biochem Soc Trans, 2001. **29**(Pt 2): p. 250-67.
316. Reddy, J.K. and T. Hashimoto, *Peroxisomal beta-oxidation and peroxisome proliferator-activated receptor alpha: an adaptive metabolic system.* Annu Rev Nutr, 2001. **21**: p. 193-230.
317. Wanders, R.J. and H.R. Waterham, *Biochemistry of mammalian peroxisomes revisited.* Annu Rev Biochem, 2006. **75**: p. 295-332.
318. Pedersen, J.I., et al., *Molecular cloning and expression of cDNA encoding 3alpha,7alpha,12alpha-trihydroxy-5beta-chole stanoyl-CoA oxidase from rabbit liver.* J Biol Chem, 1997. **272**(29): p. 18481-9.
319. Van Veldhoven, P.P., *Biochemistry and genetics of inherited disorders of peroxisomal fatty acid metabolism.* J Lipid Res, 2010. **51**(10): p. 2863-95.
320. Singh, I., *Mammalian peroxisomes: metabolism of oxygen and reactive oxygen species.* Ann N Y Acad Sci, 1996. **804**: p. 612-27.
321. Bonekamp, N.A., et al., *Reactive oxygen species and peroxisomes: struggling for balance.* Biofactors, 2009. **35**(4): p. 346-55.
322. Singh, A.K., et al., *Demonstration of glutathione peroxidase in rat liver peroxisomes and its intraorganellar distribution.* Arch Biochem Biophys, 1994. **315**(2): p. 331-8.
323. Yamashita, H., et al., *Characterization of human and murine PMP20 peroxisomal proteins that exhibit antioxidant activity in vitro.* J Biol Chem, 1999. **274**(42): p. 29897-904.
324. Ferdinandusse, S., et al., *Toxicity of peroxisomal C27-bile acid intermediates.* Mol Genet Metab, 2009. **96**(3): p. 121-8.
325. Filatova, A., et al., *Acidosis Acts through HSP90 in a PHD/VHL-Independent Manner to Promote HIF Function and Stem Cell Maintenance in Glioma.* Cancer Res, 2016. **76**(19): p. 5845-5856.
326. Noble, P.W., et al., *Pirfenidone for idiopathic pulmonary fibrosis: analysis of pooled data from three multinational phase 3 trials.* Eur Respir J, 2016. **47**(1): p. 243-53.
327. Frantz, C., K.M. Stewart, and V.M. Weaver, *The extracellular matrix at a glance.* J Cell Sci, 2010. **123**(Pt 24): p. 4195-200.
328. Nakos, G., A. Adams, and N. Andriopoulos, *Antibodies to collagen in patients with idiopathic pulmonary fibrosis.* Chest, 1993. **103**(4): p. 1051-8.
329. Ramos, C., et al., *Fibroblasts from idiopathic pulmonary fibrosis and normal lungs differ in growth rate, apoptosis, and tissue inhibitor of metalloproteinases expression.* Am J Respir Cell Mol Biol, 2001. **24**(5): p. 591-8.
330. Su, Y., et al., *Association of serum levels of laminin, type IV collagen, procollagen III N-terminal peptide, and hyaluronic acid with the progression of interstitial lung disease.* Medicine (Baltimore), 2017. **96**(18): p. e6617.

331. Sun, K.H., et al., *alpha-Smooth muscle actin is an inconsistent marker of fibroblasts responsible for force-dependent TGFbeta activation or collagen production across multiple models of organ fibrosis.* Am J Physiol Lung Cell Mol Physiol, 2016. **310**(9): p. L824-36.
332. Zhang, H.Y., et al., *Lung fibroblast alpha-smooth muscle actin expression and contractile phenotype in bleomycin-induced pulmonary fibrosis.* Am J Pathol, 1996. **148**(2): p. 527-37.
333. Zhang, K., et al., *Myofibroblasts and their role in lung collagen gene expression during pulmonary fibrosis. A combined immunohistochemical and in situ hybridization study.* Am J Pathol, 1994. **145**(1): p. 114-25.
334. Rossert, J., C. Terraz, and S. Dupont, *Regulation of type I collagen genes expression.* Nephrol Dial Transplant, 2000. **15 Suppl 6**: p. 66-8.
335. Nkyimbeng, T., et al., *Pivotal role of matrix metalloproteinase 13 in extracellular matrix turnover in idiopathic pulmonary fibrosis.* PLoS One, 2013. **8**(9): p. e73279.
336. Craig, V.J., et al., *Matrix metalloproteinases as therapeutic targets for idiopathic pulmonary fibrosis.* Am J Respir Cell Mol Biol, 2015. **53**(5): p. 585-600.
337. Zhou, C., et al., *Differentiating Glomerular Inflammation from Fibrosis in a Bone Marrow Chimera for Rat Anti-Glomerular Basement Membrane Glomerulonephritis.* Am J Nephrol, 2015. **42**(1): p. 42-53.
338. Varga, T., Z. Czimmerer, and L. Nagy, *PPARs are a unique set of fatty acid regulated transcription factors controlling both lipid metabolism and inflammation.* Biochim Biophys Acta, 2011. **1812**(8): p. 1007-22.
339. Bishop-Bailey, D., *Peroxisome proliferator-activated receptors in the cardiovascular system.* Br J Pharmacol, 2000. **129**(5): p. 823-34.
340. Barish, G.D., V.A. Narkar, and R.M. Evans, *PPAR delta: a dagger in the heart of the metabolic syndrome.* J Clin Invest, 2006. **116**(3): p. 590-7.
341. Ferre, P., *The biology of peroxisome proliferator-activated receptors: relationship with lipid metabolism and insulin sensitivity.* Diabetes, 2004. **53 Suppl 1**: p. S43-50.
342. Postlethwaite, A.E., et al., *Stimulation of the chemotactic migration of human fibroblasts by transforming growth factor beta.* J Exp Med, 1987. **165**(1): p. 251-6.
343. Zahradka, P., et al., *Peroxisome proliferator-activated receptor alpha and gamma ligands differentially affect smooth muscle cell proliferation and migration.* J Pharmacol Exp Ther, 2006. **317**(2): p. 651-9.
344. Liu, W., et al., *PPAR-gamma promotes endothelial cell migration by inducing the expression of Sema3g.* J Cell Biochem, 2015. **116**(4): p. 514-23.
345. Hashimoto, F. and H. Hayashi, *Significance of catalase in peroxisomal fatty acyl-CoA beta-oxidation: NADH oxidation by acetoacetyl-CoA and H2O2.* J Biochem, 1990. **108**(3): p. 426-31.
346. Siwik, D.A., P.J. Pagano, and W.S. Colucci, *Oxidative stress regulates collagen synthesis and matrix metalloproteinase activity in cardiac fibroblasts.* Am J Physiol Cell Physiol, 2001. **280**(1): p. C53-60.
347. Odajima, N., et al., *The role of catalase in pulmonary fibrosis.* Respir Res, 2010. **11**: p. 183.
348. Deger, Y., et al., *Protective effect of alpha-tocopherol on oxidative stress in experimental pulmonary fibrosis in rats.* Cell Biochem Funct, 2007. **25**(6): p. 633-7.
349. B, B.M., et al., *Animal models of fibrotic lung disease.* Am J Respir Cell Mol Biol, 2013. **49**(2): p. 167-79.

8. Acknowledgements

I am heavily-laden with appreciations to several individuals and organizations for their kind gestures and roles during my study.

I express my warmest gratitude to Prof. Dr. Eveline Baumgart-Vogt for giving me the rare opportunity to undertake this study in her laboratory at the Institute for Anatomy and Cell Biology, Justus Liebig University, Giessen, Germany and above all, express my sincere thanks for her immerse support and uttermost guidance throughout this study. I am indebted to Prof. Dr. Martin Diener for his co-supervisory role during this project. Many thanks to Dr. Srikanth Karnati for his patience and support during my PhD study.

My profound gratitude goes to Dr. Omelyan Trompak, Dr. Natalia El-Merhie, Dr. Wang Shan, Dr. Claudia Colasante, PD Dr. Barbara Ahlemeyer, Vannuruswamy Garikapati, Dr. Vijith Vijayan and Harsha Harshavardhan for their excellent support.

I value the genuine technical supports of Petra Hahn-Kohlberger, Andrea Textor, Bianca Pfeiffer, Susanne Pfreimer, and Elke Richter. Many thanks to Prof. Marc Fransen of Université catholique de Louvain, Belgium, for the catalase overexpression plasmid.

I would like to express my heartfelt gratitude to DAAD (Der Deutsche Akademische Austauschdienst) and Government of Ghana for the financial support during my study. Special thanks to the former Dean of School of Veterinary Medicine, University of Ghana, Prof. George Aning, for his fatherly and mentorship role in my life.

I am thankful to the MBML committee, Prof. Dr. Werner Seeger, Dr. Rory Morty, Dr. Elie El Agha and Dr. Ivana Mizikova, not forgetting the MBML class of 2017. Special thanks to my core friends for the memories we made and most importantly, the invaluable encouragements during my PhD studies.

To my family, especially Ms. Irene Mintah and my daughter, Ms. Paige Boateng, I sincerely thank you for your patience and understanding while I was away from home to do my PhD study.